TRAIL:

Optimizing trail locations by terrain conditions and other considerations, at high resolution

by

David Matthew Howley Campbell

BSc. Forestry, UNB, 2008

A Thesis, Dissertation or Report Submitted in Partial Fulfilment of the Requirements for the Degree of:

Masters of Science in Forestry

in the Graduate Academic Unit of Forestry and Environmental Management

This thesis, dissertation or report is accepted by the

Dean of Graduate Studies

THE UNIVERSITY OF NEW BRUNSWICK

January 2012

Abstract

This thesis informs about a new GIS-based extension tool to delineate and evaluate trail routes through already accessed or non-accessed terrain, with the purpose of avoiding trouble spots, minimizing construction costs and reducing ecological damage. The process refers to the Trail Routing, Analysis, and Investigative Layout tool (TRAIL), and works as an extension on the ESRI ArcMap platform. Once uploaded and engaged, TRAIL guides the user:

1. to upload the data layers needed for the route-layout and evaluation purpose, e.g., local digital elevation model (DEM), DEM-derived slope and wet-areas map (WAM) with its cartographic depth-to-water layer, and the WAM-generated as well as machine-specific soil–rutting map;
2. to set the conditions for trail-related risk tolerances pertaining to, e.g., crossing stream channels, wet areas, rugged terrain, steep slopes, etc.
3. to select the beginning and end locations for the proposed route(s),
4. to analyze alternative multi-criteria trail route options.

Designed specifically for developing recreational trails, TRAIL allows for a wide range of applications. TRAIL provides a platform for designing ecologically sensitive and cost effective hiking trails and can be applied within a forest operations context. Case studies are explored to demonstrate the merit of TRAIL as a general linear feature planning model. The case studies refer to a TRAIL evaluation of a proposed forest operations road and a proposed recreational trail through non-accessed terrain.

Scientifically, the TRAIL tool is based on a detailed assessment of soil trafficability, as governed by type of usage (type of vehicle and seasonality) and its physical characteristics (management practices, landscape position, vegetation, and mechanical soil properties such as the resistance to penetration). To a large extent, physical characteristics vary from trafficable when dry to non-trafficable when too wet, as (i) they exist in the field and as mapped from LiDAR-generated bare-ground digital elevation data and (ii) as mapped using the UNB-generated and field-verified wet-areas mapping protocol. Field verification involved determining soil penetrability - measured as cone penetration index (CI) using a soil penetrometer - and the CI determining variables referring to such soil texture (sand%, silt%, clay%), bulk density, organic matter content, coarse fragment content, and moisture condition along ridge-to-depression transects. Acquisition of these data allowed for high-resolution moisture-dependent soil trafficability mapping, with texture, density, organic matter and coarse fragment contents as additional CI predictors. In turn, CI was used to map potential single to multiple rutting depth as described by Vega et al. (2008).

Table of Contents

List of Tables

List of Figures

Chapter 1 : Introduction to Thesis

This thesis is focused upon trail and road planning and related risk assessments within forested landscapes. A tool incorporating the scientific assessment of soil trafficability is presented that includes routing considerations related to topography, vegetation, hydrology, vehicle type, existing transportation networks, and management objectives.

The thesis has two parts; (i) the scientific assessment of soil trafficability, and; (ii) the development of methods towards the minimization of linear feature disturbance within a geographical information systems framework.

The working hypothesis is focused on providing adequate soil trafficability predictions according to (1) varying soil moisture content (%), soil density (Db), soil texture (sand, silt clay %), coarse fragment fraction, organic matter content, (2) topography, and (3) a vehicle- and load- specific expected tire footprint.

Hypothesis: Soil trafficability can be modeled and mapped based upon the above specifications and the results can be tested through transect studies.

This hypothesis is linked to the following three research objectives:

1. determine ways and means by which soil trafficability under field conditions can be quantified in terms of local soil properties and topography;

2. how the results so generated can be used for the purpose of delineating least cost trail and road routes with cost quantified in terms of potential soil disturbance and compaction risk, and;
3. demonstrate the risk assessment use of this knowledge by way of a least-cost trail and road delineation tool.

Thesis Outline

This thesis has been compiled utilizing Alberta Canada as the location for study. Alberta Sustainable Resource Development as well as Alberta Parks, Recreation and Tourism. Towards the accomplishment of these specific objectives, the thesis is constructed as follows.

Chapter 2 contains a literature review of soil trafficability parameters and GIS techniques towards improved information construction and usage. This chapter is designed to inform about the current state of knowledge regarding the thesis objectives.

Chapter 3 holds a review of the study areas utilized within the thesis to provide an improved understanding of land-use trends within these zones.

Chapter 4 investigates the soil trafficability of the study locations utilizing transect studies which compile a dataset comprising local soil conditions and their relationship to topographically derived variables.

Chapter 5 introduces the TRAIL tool and investigates its utilization upon an industrial forest road application in Northern Alberta.

Chapter 6 contains the concluding remarks summarizing the thesis and outlining how the work addressed the objectives set out in the beginning.

Appendix A provides the TRAIL Tool Manual , including raster processing procedures.

Appendix B provides the data table used within statistical analysis

Appendix C contains the GIS and Field Data CDs, grouped by study area.

Chapter 2 : Review of Fundamentals -Soil Resistance to Penetration and Rutting: Mapping, Least-Cost Path Delineation, and GIS Procedures

2.1 Introduction

Many attempts to model and map soil properties intrinsic for soil trafficability have been proposed. Most notable among these is the WES method of the US Corps of Army Engineers which relates soil trafficability and machine-induced rutting to the local soil resistance to penetration. The latter uses hand-held soil penetrometers to probe the resistance of soils to rutting, and this serves as a guide to ascertain how many vehicles of certain type and load can pass through a particular area on a given day under given weather conditions. In general, soil trafficability and soil disturbance severity including rutting changes across the landscape and in time depending on soil moisture content (MC), soil density (Db), soil texture (sand, silt, clay %), coarse fragments (CF), organic matter content (OM), presence of roots, machine loads, and the number of repeat passes. Rut length, width, and depth are particularly important and easily obtained soil disturbance measures (Duckert *et al.*, 2008), and can be used to determine the extent of soil disturbance on pore space reduction, restrictions of rooting space; interference with water flow, increased surface run-off, and influence of soil erosion and gulley formation (Saarilahti, 1999, Horn *et al.*, 2004, McNabb *et al.*, 1985). Both rutting and soil compaction can lead to direct and indirect soil displacement impacts, and to decreased oxygen diffusion leading to high root mortality and a change in soil moisture regime with additional unintended consequences including de-nitrification, methane gas production, and the methylization of soil mercury (Renault and Stengel, 1994). This

chapter pertains to a review of factors that control soil trafficalibily and to GIS-based matters and methods that can be used to model and map soil trafficability for the purpose of optimizing trail locations across landscapes by way of least-cost analyses. Methods pertaining to the derivation of digital elevation data are reviewed as well (Appendix, this Chapter), because the availability and quality of these data are fundamental for reliable soil trafficability and trail and road layout assessments.

2.2 The Cone Index (DGSI, 2011)

The cone penetrometer is a tool for measuring the resistance of a surface to penetration (Figure 2.1), and is commonly used to test traffic-induced changes in soil compaction (Wronski *et al.*, 1990; Landsberg *et al.*, 2003; Vega *et al.*, 2008; Agodzo, 2003; Saarilahti, 2002; Saarilahti and Antilla, 1999). To generalize, CI readings are often related to specific resistance-inducing soil properties by way of experimentation in laboratories (e.g. Hummel *et al.*, 2004 and others), and in the field (Saarilahti, 2002; Vega et al. 2008). Part of this experimentation deal with changing the shape of the cone. For example, Nowatzki *et al.* (1972) found that CI decreases with increasing cone angle and decreasing surface area. Standardized CI determinations refer to cones with a 60° apex angle and a 1.5 cm^2 cross section (Rooney *et al.* 2000).

Figure 2.1 Standard portable static cone penetrometer.

Balland *et al.* (2008) noted that with increasing organic matter content soil pore space and moisture retention increased leading to decreases in density, hence increasing the penetrability of the soil. Coarse fragment content increases, as noted by Vega *et al* (2008) and others, decreases the penetrability of the soil. Rooney *et al.* (2000) found that with increasing soil depth, penetration resistance increased.

2.2.1 CI affecting soil properties

Soil penetrability is strongly affected by soil texture, coarse fragment content, organic matter content, the presence of soil cementing agents, and the extent of soil freezing (Byrd, 1980; Vepraskas, 1983, Al-Darby, 1988; Shoop 1995, Vega et al. 2008). For example, in coarse textured soils, or "friction" soils, friction forces dominate the resistance, whereas cohesion forces dominate in fine-textured soils, as detailed in Table 2.1. In particular, Nearing (1988) found CI to decrease with increasing sand content (cone slips easily past sand particles), and to increase with increasing clay content (clay particles stick to the cone, especially when wet). Coarse fragment content tends to

increase CI as well, and this is especially so with increasing particle size and increasing soil compaction: the larger the particles and the more surrounded by other fairly immobile particles, the more force is required to force the cone penetrometer through that soil.

Table 2.1. Main trafficability features of friction and cohesion soils.

Friction Soils	Cohesion Soils
Non-sticky, wet or dry; do not shrink; retain high permeability	Very sticky when wet, plastic when moist, hard when dry; subject to shrinking and cracking
Traffic-induced compaction moderate and easily reversible	Traffic-induced compaction severe, esp. when moist, requires high energy inputs to reverse
Trafficability increases under repetitive loading	Trafficability worsens during repetitive loading

In all soils, resistance to penetration increases with increasing bulk density of decreasing porosity of the soil. Generally, soil bulk density (Db; the ratio of the oven dried mass of the soil to its total volume) is a function of texture, CF, and OM as well as the degree of compaction. Changes in Db can affect plant growth if macropore space falls below 10% (DeYoe, 1982). Decreasing in porosities affect the hydraulic conductivity of soils (Jutras and Arp 2011) and, therefore, water infiltration, which, in turn, increases soil erosion, changes on-site drainage and decreases the amount of available water to plants, leading to puddling and altered surface flow patterns (Arnup, 1998). Under natural conditions, soil porosity decreases with increasing soil depth, except for soils in peaty and sandy surface deposits where the resistance to soil porosity and, hence, soil penetrability are not much affected by depth. Adding organic matter increase the state of aggregation of soils, thereby increasing soil friability and pore space at the same time

(Balland *et al.* 2008). In contrast, increasing amounts of $CaCO_3$, and Fe and Al oxides/hydroxides and frozen water within soils lead to increasingly soil cementation with increasing CI values. $CaCO_3$-based cementation is a factor in soils subject arid climates while Fe and Al oxide/hydroxide cementation can be a factor in cool and humid soils. The extent of soil freezing is subject to the combined timing and sub-zero air temperatures and snowpack accumulations on top of the soil, with the earlier and deeper snowpacks able to reduce if not prevent soil freezing under temperate forest soil conditions (Balland *et al.* (2006).

Adding water to soil generally decreases soil penetrability under unfrozen conditions, by increasing the slippage of the soil particles along the penetrating soil surface (Defossez *et al.,* 2002). An exception to this occurs when the soils (sands) are loose and dry. In this case, adding moisture may increase CI at first due to the extra effort required to break the surface tension of the moisture connections. Expressing soil moisture content in terms of percentage of moisture filled pore space (MCps) generally gives the best correlations between soil penetrability and changing soil moisture levels (Vega et al. 2008). Other soil moisture determinations refer to (i) the weight of water per oven-dry soil (gravimetric soil moisture content, or MCg), and (ii) the volume of moisture per volume of soil (volumetric soil moisture content, or MCv). The latter can be obtained through direct in-field measurements using TDR-based soil moisture probes. The relationships between these three soil moisture specifications are as follows:

$$MCg = Db\ MCv \qquad [1]$$

and

$$MCps = (1-Db/Dp)\ MCv, \quad [2]$$

where Dp is the average soil particle density (in g / cm^3), estimated from:

$$1/Dp = OM/1.3 + (1-OM)/2.6, \quad [3]$$

and OM is the soil organic matter fraction within the fine earth fraction of the soil (all coarse fragments > 2mm excluded, through sieving).

Busscher (1997), Agodzo (2003), Saarilahti (2002) and Vega *et al.* (2008) reviewed published CI data and confirmed the general dependencies between CI, soil texture, soil moisture content and Db, or pore space, but there are systematic differences between the field and laboratory derived values. In particular, Vega *et al.* (2008) found that:

$$CI_{Lab} = 1.14 * 10^{(3.99-1.36sand-6.65PS-1.20MC_{PS})} \quad [4]$$

and

$$CI_{field} = 1.08 * 10^{(1.99-0.38sand-2.23PS-0.72MC_{PS})} \quad [5]$$

with PS = 1- Db/Dp as the pore space fraction of the soil.

2.3 Role of CI in soil rut modeling

Determining the depth to which a vehicle will sink based upon loads and soil physical properties has been the focus of many studies. For example, Meek (1996) tested the effects of skidder traffic on a sandy and a clay loam soil. Saarilahti (1999) reported the

ECOWOOD studies in Finland dealing with rutting formation in relation to varying soil conditions. Existing WES-based rut depth models are almost exclusively based upon the wheel numeric NCI which refers to relating CI to tire-exerted foot-print pressures, as formulated by Turnage (1972):

$$\mathrm{NCI} = \left(\frac{1000 * \mathrm{CI} * \mathrm{b} * \mathrm{d}}{\mathrm{W}}\right) * \left(\sqrt{\frac{\partial}{\mathrm{h}}} * \frac{1}{1 + \frac{\mathrm{b}}{2\mathrm{d}}}\right) \quad [6]$$

where W is vehicle load per tire, in kN, b is tire width, d is tire diameter, and h is tire section (height of outer rim of each wheel to end of rubber), all in m, and where (δ = 0.001 (0.365 +170/p) W) is the tire deflection, with p as tire inflation pressure (kPa). Typically, the first wheel or vehicle pass has the most effect upon the soil compaction and rutting (Saarilahti, 2002). Subsequent passes have geometrically diminishing effects so that (Abebe 1989, Meek, 1996, Vega et al. 2008):

$$\mathrm{Z_n} = \left(\frac{1627}{\mathrm{NCI_0}}\right) * \mathrm{n}^{\frac{1}{\mathrm{a}}} * (1 - \mathrm{CF})^2 \quad [7]$$

where Z_n is the rut depth in mm after n wheel passes, CF is the coarse fragment percentage of the soil , a=6 for sand and a=3 for clay, or more generally based on field calibrations (Vega et al. 2008):

$$\mathrm{a} = \mathrm{NCI_0}^{0.6} \quad [8]$$

Once Zn determined, Zn can be used for estimating rut induced reductions in soil pore space and subsequent increases in soil compaction by noting that:

$$PS_n = 1 - Db_0/Dp - {}_{Zn}/h0soil \quad [9]$$

where Db_0 and h0soil refer to the initial soil bulk density and the depth of the originally un-compacted soil. This equation assumes that compaction within the rut-impacted soils is homogeneous. In reality, soil compaction is greatest below the rut surface, and gradually phases into the original soil bulk densities as these would vary naturally vary with increasing soil depth.

2.4 Mapping CI and rut affecting soil properties across the landscape

In order to use Eqs. 5 to 7 for predicting CI, NCI_n and Z_n under general field conditions, it is important to know how texture, soil density (or pore space) and soil moisture content vary

(i) vertically downward across the soil layers

(ii) laterally across the landscape

Balland et al. (2008) developed the following regression formulae to estimate soil bulk density with increasing soil depth:

$$Db = \frac{1.232 + (Dp - 1.23 - 0.75 \cdot SAND)\,(1\text{-}\exp\,(-0.0106 \cdot DEPTH)\,)}{1+6.83 \cdot OM} \quad [10]$$

and soil moisture content at field capacity as fraction of the Db-affected pore space:

$$FC = PS\left(1-\exp\left(\frac{-0.588\cdot(1-SAND)-1.73\cdot OM}{PS}\right)\right) \quad [11]$$

Using lookup values for average sand and OM content for the top 25 cm of soil by soil type, and assuming that each soil is at field capacity regarding soil moisture content allows one to use this formula to predict CI (Eq. 5) across the landscape by soil type, as illustrated in Figure 2.2a. Using the relationship between the cartographically determined depth-to-water DTW and MC_{PS} (Figure 2.3; Murphy et al. 2011), i.e.,

$$\log_{10}(MCPS, \%) = \min(2, 1.71 - 0.094 \log10(DTW, m) + 0.31 (Depth, m) - 0.0028 (Sand, \%) + 0.0045 (Total C, \%) \quad [12]$$

allows one to map the continuous variation of CI from ridge top to depressions for typical summer conditions, as illustrated in Figure 2.2b. To map CI under changing weather conditions Murphy et al. (2009) suggests using:

$$MC_{PS}(DTW) = 1-\{1-MC_{PS}(DTW_{ridge})\}\left[\frac{1-\exp(-k_{DTW}\ DTW)}{1-\exp(-k_{DTW}\ DTW_{ridge})}\right]^2 \quad [13]$$

where $MCPS(DTW_{ridge})$ is daily measured or modeled water-filled pore space % at the ridge top, and k_{DTW} and DTW_{ridge} are soil- and terrain-specific parameters. For example, in undulating and well-drained terrain with DTW_{ridge} = 10 m, k_{DTW} ranges from about 0.2 to 2 from fine to coarse textured soils, respectively, while in rolling to hummock terrain with DTW_{ridge}=100m, k_{DTW} likely decreases to about 0.02 to 0.2 (Figure 2.2c), respectively. This decrease would be due to the slope-length factor and subsoil

permeability: the longer the slope length on impervious bedrock, the more upslope-captured water seeps into the lower-lying subsoils.

In general, many approaches have been suggested for soil moisture mapping across the landscape and by weather, using, e.g., direct field determinations, hydrological models with varying time resolution (monthly, daily, hourly), geospatial model to capture hydraulic flow and water retention patterns, and remote sensing techniques (IR, Radar, MODIS). For example, the Newhall (1996) model uses a network of weather-station data to for mapping soil moisture regimes across the landscape. Gessler (2000), Sorensen *et al*. (2006), Lin *et al.* (2006) and others use the DTM-derived terrain wetness index [TWI = log(flow accumulation / slope)] for a static indexing soil moisture variations across the landscape. Some of the remote sensing techniques specialize in analysing one-time or multi-temporal optical, infrared, hyperspectral and radar images to detect and map changes in vegetation type and soil moisture across the landscape (Grabs 2009). These methods work in principle, but extrapolations beyond the calibration areas tend to be weak (Dubois *et al.* 1995, Creed 2003, Hajnsek 2003) Limiting factors revolve around, e.g., image quality and resolution, light and atmosphere-induced intensity and spectral variations in surface reflectance, surface roughness, and shading.

The above DTW and MCPS mapping suggestions by Murphy *et al.* (2009, 2011) use a cartographic depth-to-water index to map the proximity to the topographically derived water table below the soil surface, and found this index to conform considerably better to field-based determinations for, e.g., texture and water-filled pore space than TWI. The DTW derivation process is outlined in Figure 2.3. To capture soil moisture variations

from dry to wet weather conditions, DTW mapping proceeds by re-setting the DT=0 defining threshold for flow initiation within all DEM-derived flow channels from an upslope flow-contributing area of 4 ha (summer to early fall) to, e.g., 1 ha (to emulate DTW flowing major precipitation events) and 0.25 ha (to emulate DTW during spring melt).

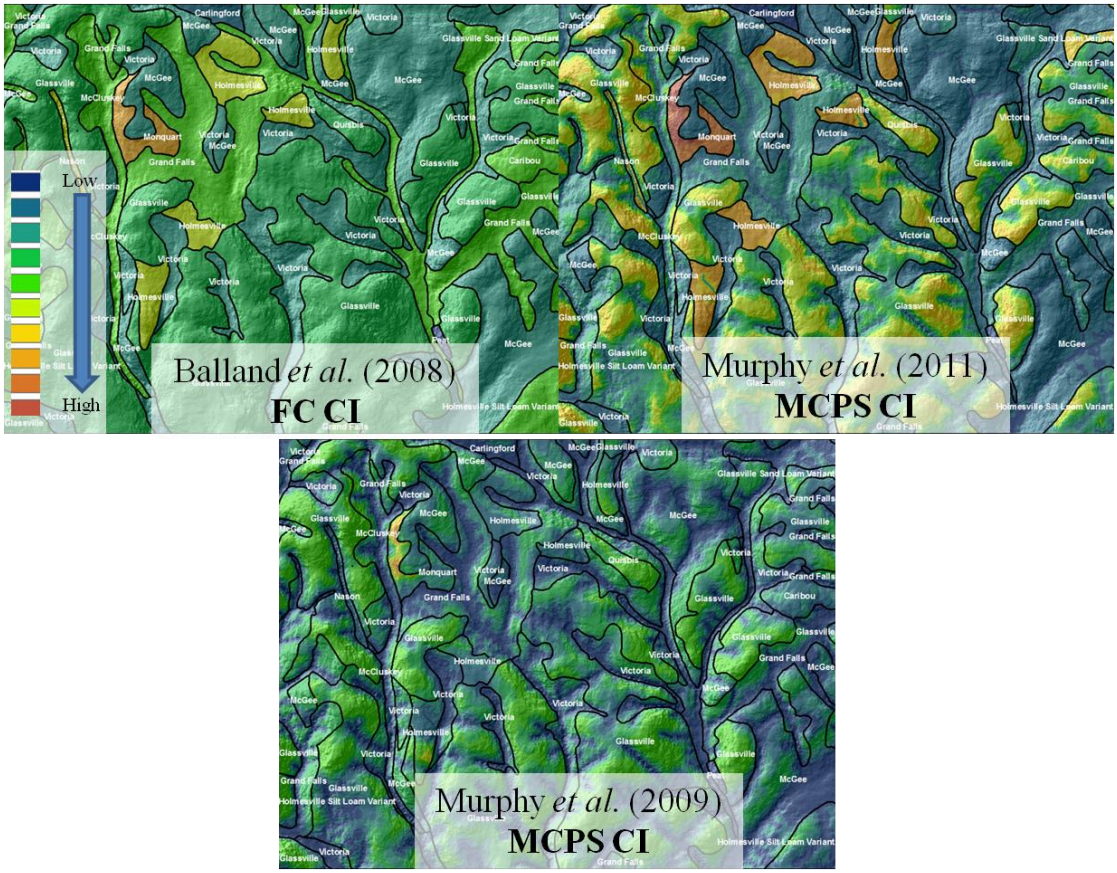

Figure 2.2 A depiction of CI as predicted by (A) field capacity, (B) moisture content of the porespace for Murphy (2011) and Murphy (2009; C) predictions.

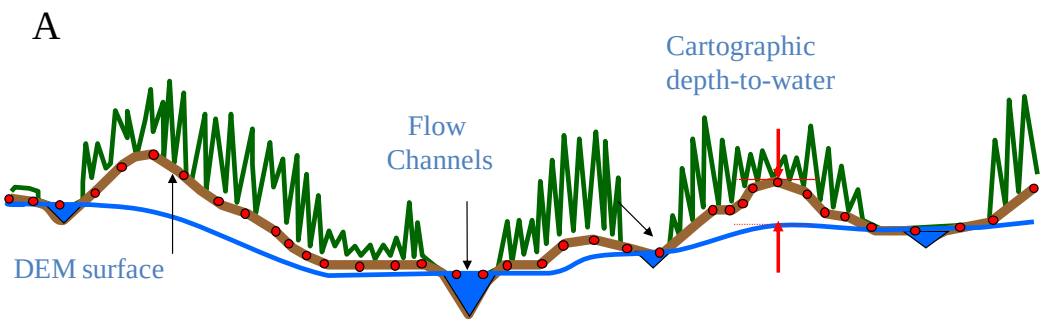

1. Prepare bare-ground DEM surface from LiDAR data (last returns)
2. Predict locations of stream channels
3. Use the wet-areas delineation algorithms to determine the cartographic depth-to-water index (DTW) across the landscape
4. Subtract DTW from DEM to get the cartographically referenced water table elevation
5. Overlay the first LiDAR returns to obtain vegetation height.

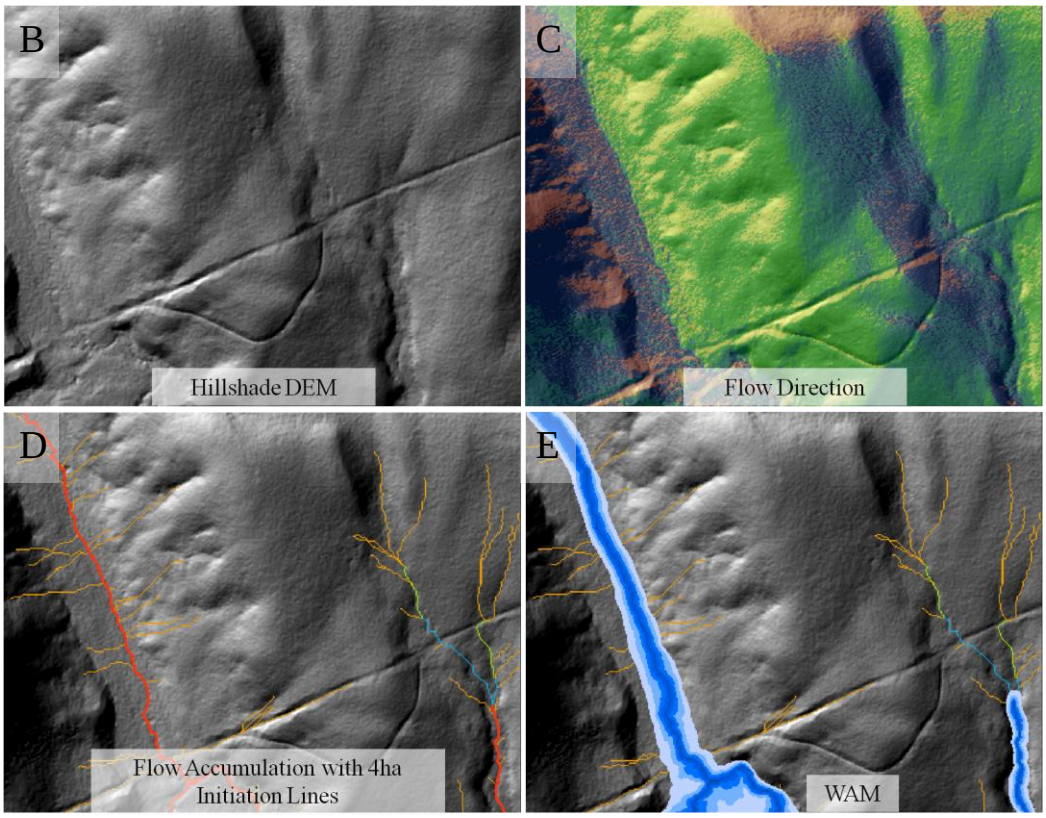

Figure 2.3 (A) LiDAR-based methodology used to derive the cartographically correct depth-to-water index (DTW), needed to model and map soil moisture as well as tree height and density variations across landscapes (LiDAR: light detection and ranging; for details, refer to the Appendix of this Chapter). (B) Hill-shaded DEM. (C). ESRI ARCGIS derived flow direction (D), flow accumulation network classified by the area-based flow-initiation thresholds (E), and the blue-shaded 0 – 1 m cartographic depth to water index (DTW) associated with the flow channels starting with the 4 ha flow initiation threshold.

2.5 **Road and trail delineation**

There are many factors and issues to be considered for least-costing trail and road locations. Some of the factors and issues arising deal with:

1. Access limitations: by ownership, terrain conditions, conservation and limited use rules
2. Intended road and trail functions: recreational, residential, industrial, habitat connectivities
3. Road and trail design: slope challenge, view factor, vehicle type, line-of sight
4. Construction and maintenance costs: cut & fill, road length, hydrological infrastructure requirements (culverts, bridges, wet-area fill-in, frost heaving, road repairs
5. Ecological footprint: soil compaction, invasive species vectorization, water diversion, sediment generation, wildlife interference
6. Placement of new roads and trails within existing road and trail networks and transport facilitating infrastructure
7. Safety regulations and related risk assessments
8. User preferences

2.5.1 GIS methods for route delineation

Least cost paths are a useful application of geographical information systems (GISs, Collischonn *et al.*, 2000; Snyder *et al.*, 2008). The process requires two primary steps;

the creation of an accumulated cost, or friction, surface and the derivation of a least accumulated path between two points. The process is used in assessing habitat connectivity (Adriansen *et al.* 2003), designing habitat corridors (Kautz *et al.*, 2006), and locating hiking trails and optimizing road layout to name a few (Xiang, 1996; Atkinson *et al.*, 2005).

Friction surfaces are composed of the combined considerations in a landscape as represented by values of 'low' friction to 'high' friction. These considerations are typically constant for every user, but the perception as to which considerations are of more importance or pose the most danger or risk, are extremely variable. Each consideration included in an analysis can be weighted and given precedence over others. ESRI ARCGIS has a suite of tools composed to address layer weighting and accumulated cost raster creation. The process is intensive and requires in-depth knowledge of how GISs work.

Friction surface creation involves the contemplation of a number of problems before analysis can proceed. Raster source issues, the number of considerations on the table, and the perceptions of the users have to be recognized in any solution. The more considerations that are to be contemplated in friction surface creation, the more complex the solution becomes (Table 2.2). Combine the fact that not all GIS layers are in the same value ranges (apples to oranges), and that every user has a variable view on what constitutes 'friction', the creation of a usable, accurate friction surface becomes difficult. Other areas for concern include, but are not limited to:

- User perception - usually expressed as qualitative data (nominal) making the incorporation of perception a factor in problem complexity.
- The data - expressed in raster format; often created at different times, at different projections, and at different resolutions. All information is needed to be created equal, in these terms, before processing can truly start.

Table 2.2 Important factors that influence trail and road locations.

Slope	Viewshed Vistas
Stream Crossings	Limited Use Zones (LUZs)
Wet Area Crossings	Restricted Zones
Earth Moving Requirements	Existing Access
Vegetation Removal	Construction Costs
Trail Braiding	Trail Width
Rutting	User Type

2.5.2 Least-cost paths

Least-cost paths (LCP) have been used in GISs to solve networking problems in transportation systems. The most widely accepted form of LCP deduction was created by Dijkstra (1959) and features a moving window kernel utilizing a spreading function which determines the 'cost' of moving between vertices. Dijkstras' algorithm is contained within the ARCGIS tool 'CostDistance', and is accessible with a spatial analyst license.

Many researchers have noted fundamental flaws with this algorithm; in particular, Collischonn *et al.* (1999) noted that a LCP on a flat surface raster should produce a straight line connecting the points; however, this is not the case. Collischonn attributed

this to the small search window of the kernel in the deduction of distance between vertices. Dijkstra utilizes a D8 algorithm search window, and as an improvement, Collischonn offered a D16 algorithm that preformed mildly better then the universal Dijkstra algorithm. The process offered by Collishonn increased computational processing times 2 fold while still only offering mildly improved results. Indeed, as the distance between start and end points increase, the larger the search window needed. Utilizing the methods of Collischonn and Dijkstra, one would need to have a search window with a radius equal to the Euclidean distance between the starting and end point to create a truly straight line.

Further flaws in algorithm processes deal with the methods in which slope is handled. Slope, as viewed from an object capable of movement, is direction dependant. Walking parallel to the grade of a hill results in a perceived slope of 0%, whereas walking perpendicular to the grade, slope can reach un-scalable values. The problem is not necessarily how Dijkstras' algorithm handles slope, but how slope maps are created. ESRI slope procedures create static maps of maximum slope values for each pixel. With a point at the base of a hill and another at the top, Dijkstras' algorithm computes the least accumulated cost path straight up the hill, which in many cases, is not possible. Anderson *et al.* (2004) utilized a node connection method where every node is connected to all of its neighbours and assigned a distance value. The process then utilizes Dijkstras algorithm to connect each node to the network through an iterative loop that steps through the problem node by node. This process is extremely computationally intensive and has yet to be programmed for use in ESRI software.

2.6 Digital elevation data derivation methods

The acquisition of reliable digital terrain models (DTM) for the earth surface involves a variety of air-borne and satellite-based technologies (Welch *et al.,* 1998; Li *et al*, 2005; Farr *et al*., 2007): (i) GPS surveying; (ii) photogrammetry; (iii) radargrammetry; (iv) synthetic aperture radar (SAR) interferometry; (v) airborne laser scanning; (vi) GPS-based surveying. Table 2.3 presents an overview of the resulting DTM products in terms of overall data accuracy, speed of acquisition, costs, and application domain.

Table 2.3 A comparison between DTM data from different sources (Li et al., 2005).

Acquisition Method	Data Accuracy	Speed	Cost	Application Domain
GPS Surveying	High	Slow	High	Small
Photogrammetry	Medium to High	Fast	Low	Medium to large
InSAR	Low	Very Fast	Low	Large
Radargrammetry	Very Low	Very Fast	Low	Large
LiDAR	High	Fast	High	Medium

2.6.1 Geographic positioning systems

The Global Positioning System (GPS) is a satellite-based navigation system made up of a network of 24 satellites originally placed into orbit by the U.S. Department of Defence. GPS satellites emit two radio waves, named L1 and L2. L1 is for civilian use. Position on the ground is determined by measuring the time it takes the radio wave to travel back to the satellite. Measurements are calculated through triangulation among con-currently user-accessed satellites on the ground. While most GPS devices do not offer < 1 m accuracy, some do. Increased GPS precision and accuracy is a function of

device cost (antenna sensitivity), availability of accurately calibrated elevation points (geodesic points) within the neighbourhood, length of time for signal tracing, density of forest canopy, and post-processing differential GPS signals. In practice, on-the-ground XY locations can be GPS-located fairly quickly (1 min or less) within a radius of 5 m using currently available low-end GPS devices. Z accuracies (elevation) are dependent upon multiple factors, with a general range of 1cm to 20m given the quality of GPS receiver in use.

2.6.2 Photogrammetry

In photogrammetry, a photographic sensor captures the visible light and infrared (IR) spectrum and stores them as bands. Images (bands) are then compiled in a mosaic and analyzed as stereo-pairs (Li *et al*, 2005, Figure 2.4). The images are analyzed utilizing mathematical equations to deduce the elevation of any particular point. Relationships between coordinate systems, points on the ground, camera perspectives, image capture height, and angular orientation elements are utilized within the equations. The creation of the DTM can occur through manual transcription of the information or through preferred digital methods which save on time and reduce error.

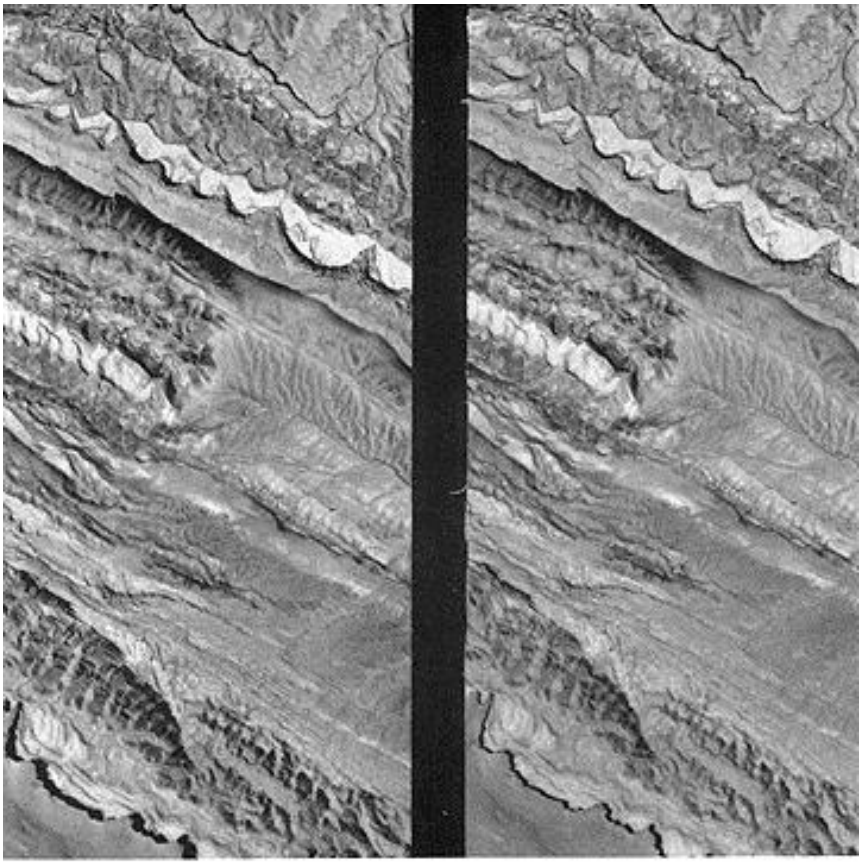

Figure 2.4 An example of stereo images used in photogrammetry. Each image must contain overlap with other images and is taken at a slightly different angle to create a 3-D stereo pair.

There are multiple platforms that capture photogrammetric images, both space based and aircraft based. (Hirano *et* al, 2003) The French satellite SPOT 1 (satellite pour l'observation de la terre) captured 10-20 meter resolution stereo images in 1986, while today SPOT 5 has 2.5-10 meter resolution and a 20km swath for the creation of DTMs. ASTER (advanced space borne thermal emission and reflection radiometer) is another example with 14 spectral bands collected, including visible and IR wavelengths. ASTER has a 15m spatial resolution with a 60km swath (Fujisada *et al*, 2005; Hirano *et al*, 2003; Welch *et al*, 1998).

Walker *et al* (1999) found that rasterizing existing contour maps of a study area in Australia performed better than photogrammetric methods when compared to ground based studies of elevational data. Walker attributed this to the inability of photogrammetric methods to identify actual ground positions versus tree tops or buildings. This problem resonates throughout this method as automatic delineation between natural or manmade objects and the ground is difficult while effects caused by atmospheric process (e.g. clouds) can create further problems (Li *et al*, 2005; Rabus *et al*, 2003). Rabus (2003) noted that photogrammetrically derived optical data are generally inhomogeneous as their quality depends on image feature contrasts.

Franklin (2001) noted that the cost of aerial, or aircraft based, photogrammetry is astronomical when compared to equivalent space based methods of DTM collection. Aircraft imagery is 2 fold more expensive than its space based counterparts; multispectral, hyperspectral and radar deduced DTM are 15 fold more cost effective.

2.6.3 Synthetic Aperture Radar (SAR)

SAR technology is currently the most vastly utilized method of topographic map creation (Li *et al*, 2005). SAR is imaging radar which sends and receives echoes; received echoes come from targets and information from targets is recorded as intensity images (grey scale). Platforms for SAR can be airborne or satellite/space based. There are three basic techniques of SAR collection, two of which are effectively utilized in the creation of DTMs: radargrammetry and interferometry. Radargrammetry utilizes the

measurements of parallax to acquire DTMs, while interferometry determines phase shifts between echoes.

2.6.3.1 Interferometry

Graham (in Li *et al*, 2005) discovered that an over looked component of the typical SAR capture process could be utilized to produce topographic information. He noted that a pair of SAR images taken of the same area at different positions could be used to create an interferogram and the phase differences within could be used to derive DTMs. This process is known as InSAR. InSAR utilizes information captured by the SAR system. Platform heights, the difference in height between image captures, the angle of that difference, and distance from each platform to the target are all variables within the InSAR calculations. The collection of the two images can be created by either single-pass (platform utilizes two antennae) or multi-pass (platform utilizes one antenna; minimum of two passes for same location is required) methods. The advantage lies with the single-pass method due to reductions in mathematical error and source change (i.e. fall and summer tree returns).

The Shuttle Radar Topography Mission (SRTM; Nielsen, 2005) was the first InSAR system to capture a 30m resolution DTM for much of the earth (between latitudes 60ºN and 57ºS; Rabus *et al*., 2003). The platform utilized a one pass approach, capturing data continuously day and night over an 11 day mission (February 2000). Other techniques (photogrammetry in particular) cannot capture information at night due to the lack of source signal or capture data continuously as receiving and sending echoes is not

affected by cloud cover. In addition, the InSAR method does not require homologous point identification or require variable contrast images for DTM derivation. Currently, SRTM-DEM data are available worldwide (90 m resolution for latidudes < ı60° ı; 30 m USA (http://srtm.csi.cgiar.org/).

2.6.3.2 Radargrammetry

Radargrammetry follows the same procedures as photogrammetry only the process utilizes stereo SAR images rather than stereo spectral images. SAR capture by the SRTM or from Canada's RADARSAT constellation program produces multiple bands of information. Different bands are utilized based upon the information that is being researched. Applications range from forestry to glacier changes.

Sanli *et al* (2006) compared radargrammetric DTM creation to interferometric DTM creation and found interferometric DEM results poor when compared to radargrammetric evaluations. They found that radargrammetric methods were more successful in flat and agricultural areas then in variable terrain conditions. Clark *et al.*, (2009) utilized a multi-temporal method of generating predications of hydrologically sensitive zones utilizing archived SAR images for an area within the Boreal plain in Alberta. 54 images captured over a ten year period were selected and classified to reflect hydrological sensitivity yielding a probability map of zones which are wet to dry.

2.6.4 Light Detection and Ranging (LiDAR)

LiDAR sensors offer a significant improvement to alternative methods of high resolution DTM creation. Depending upon the application, data derived from this method has a resolution of 10 – 100cm. The accuracy and resolution seen with LiDAR data in 3-D forest structure and ground features makes this data source highly valuable in the natural resource fields of: ground surface modeling, geology, habitat assessment, timber resource planning, post disturbance assessment, fire and fuels, slope stability, hydrology, fisheries, and costal change, to name a few (Evans *et al.*, 2009).

The LiDAR method creates a high density of points and features multiple echoes per laser pulse, intensity measurements for the returning signal, and centimetre accuracy for horizontal and vertical positioning (Popescu *et al.* 2004). While the cost of acquiring this data source is often a limiting factor, users of this data source attest to its land management application (Evans *et al.*, 2009). There are three types of LiDAR sensors utilized today: profiling, discrete return, and waveform. Profiling sensors capture 1 return at course sampling densities and is not typically used in resource planning.

Discrete pulse LiDAR systems are typically airborne or terrestrial and utilize lasers to capture information on the ground. The physical capture of the data consist of a laser range finder, a computer system for data acquisition, a scanner, a storage medium, and a GPS system for continual position information (Figure 2.5, Li *et al.* 2005). Laser pulses are emitted from a source utilizing scanning frequencies of 50,000 pulses per second (can be 10 times higher), and the returning pulse intensity is registered and stored. The

typical footprint of discrete pulse technologies is 20-80 centimetres. The information is stored as a point cloud and requires algorithms to classify the point cloud information and extract the bare earth topology. Alternatively, algorithms can extract the full feature data providing accurate depictions of trees, buildings and other attributes of the land Figure 2.6.

(Evans *et al.*, 2009) Waveform LiDAR systems are the newest form of laser altimetry. Waveform LiDAR, unlike discrete return LiDAR, emits a constant laser pulse with footprints ranging from 3-8 meters. Waveform LiDAR gives more control to the end user in the interpretation process of the physical environment by providing structural detail of captured images. This method is more accurate in estimating tree heights then the discrete return method, but this system is far less mature for resource planning as it creates an overwhelmingly large dataset that is difficult for analysts to utilize (Bretar *et al.*, 2008).

Mobile LiDAR solutions are being utilized within an urban planning context to fill the demand of highway asset monitoring and other infrastructure (Haala, *et al.,* 2008). This data product is typically mounted to a vehicle which travels upon existing roadways. Accuracies of this method are typically less then 30mm, providing a very detailed 3D surface for planning and maintenance.

White *et al* (2003) amongst others are utilizing the bare earth LiDAR DEMs to study the spatial morphological change in coastlines over time. Popescu *et al* (2004) and others are utilizing LiDAR point cloud information to derive vegetation height and densities

with great success. Soil moisture prediction algorithms (wet areas mapping) are seeing an improvement in accuracy from 0.7 R^2 to 0.9 R^2 (Murphy *et al.* 2009).

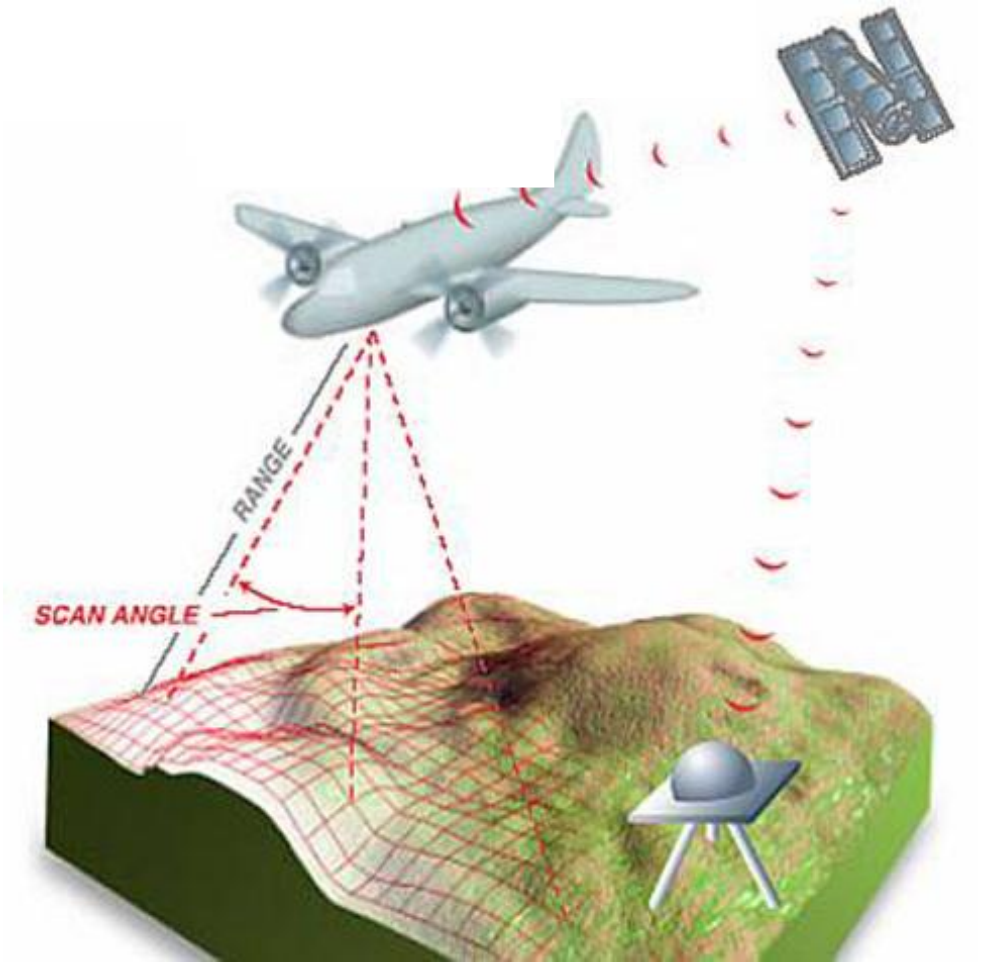

Figure 2.5 The LiDAR collection method. Edited from: http://www.dot.state.oh.us/Divisions/ProdMgt/Aerial/Pages/LiDARBasicS.aspx

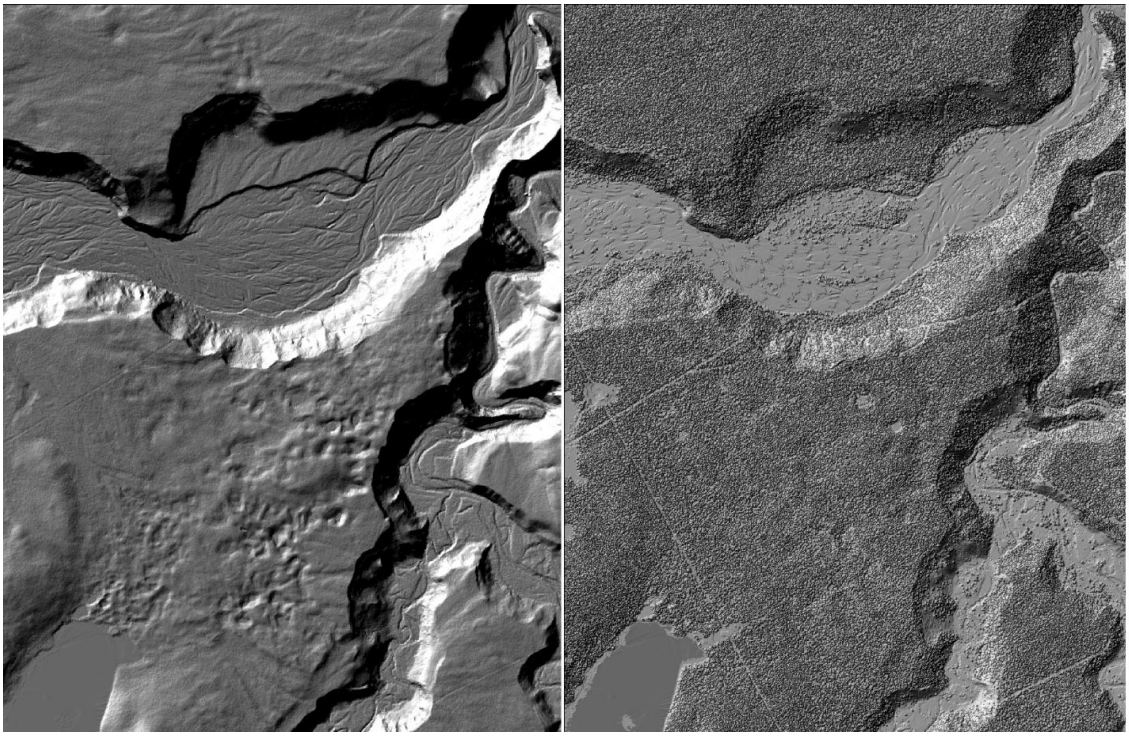

Figure 2.6 Bare earth topography with accompanying full feature LiDAR topography.

2.7 References

Abebe, A., Tanaka, T., Yamazaki, M. 1989. Soil compaction by multiple passes of a rigid wheel relevant for optimization of traffic. J Terramech 26, pp. 139-148.

Agodzo, S., Adama, I. 2003. Bulk density, cone index and Water Content Relations for Some Ghanian Soils. In: Gabriels, D.M. *et al*. (Eds.). ICTP Lecture Notes Series. Volume XVIII.

Al-Darby, A., Baneir, A. 1988. Cone index of loamy sand and loam soils as affected by compaction. J Agric Res 33, pp. 17-30.

Anderson, A., Nelson, J. 2004. Projecting vector-based road networks with a shortest path algorithm. Can J. For Res 34, pp. 1444-1457.

Adruansen, F., Chardon, J., DeBlust, G., Swinnen, E., Villalba, S., Gulinck, G. 2003. The application of 'least-cost' modeling as a functional landscape model. Landscape Urban Plan 54, pp. 233-247.

Arnup, R., 1998. The extent, effects and management of forestry-related soil disturbance, with reference to implications for the clay belt: a literature review. OMNR, Northeast science and technology. TR-037

Atkinson, D., Deadman, P. Dudycha, D., Traynor, S. 2005. Multi-criteria evaluation and least cost path analysis for an arctic all-weather road. Appl Geogr 25, pp. 287-307.

Balland, V., Pollacco, J., Arp, P..2008. Modeling soil hydraulic properties for a wide range of soil conditions. Ecol Model 219, pp. 300-316.

Bretar, F.; Chauve, A.; Mallet, C.; Jutzi, B. Managing full waveform LiDAR data: A Challenging Task for the Forthcoming Years. In Proceeding of XXIst ISPRS Congress, Beijing, China, 3–11 July 2008 37, pp. 415-420.

Byrd, C., Cassel, D. 1980. The effect of sand content upon cone index and selected physical properties. J Soil Sci 129, pp. 197-204.

Busscher, W., Bauer, P., Camp., C., Sojka, R. 1997. Correction of cone index for soil water content differences in a coastal plain soil. Soil Tillage Res 43, pp. 205-217.

Clark, B., Pellikka, P. 2009. Landscape analysis using muti-scale segmentation and object oriented classification. Recent Advances in Remote Sensing and Geo-information Processing for Land Degradation Assessment. Röder & Hill (eds.). Taylor & Francis Group, London. ISBN 978-0415-39769 8, pp. 323 - 341

Collischonn, W., Pilar, J. 2000. A direction dependant least-cost-path algorithm for roads and canals. Int J Geogr Inf Sci 4, pp. 397-406.

Creed, I., Sanford, S., Beall, F., Molot, L., Dillon, P.. 2003. Cryptic wetlands: integrating hidden wetlands in regression models of the export of dissolved organic carbon from forested landscapes. Hydrol Processes 11, pp. 203 – 210.

Defossez, P., Richard, G. 2002. Models of soil compaction due to traffic and their evaluation. Soil Tillage Res 67, pp. 41-64.

Deyoe, D., 1982. Soil compaction and plant physiology. In report on soil compaction course, Oregon State University. B.C. Ministry of Forests. Unpubl rep, pp. 14-47.

DGSI. 2011. Durham geo slope indicator. Instruction manual: portable static cone penetrometer. [ONLINE: Accessed 12/08/2011]. http://web.mst.edu/~rogersda/umrcourses/ge441/Cone%20Penetrometer%20Test.pdf

Dijkstra, E. 1959. A note on two problems in connexion with graphs. Numer Math 1, pp. 269-271.

Dubois, P., van Zyl, T., Engman, T. 1995. Measuring soil moisture with imaging radars. IEEE Trans Geoscience and Remote Sens 33, pp. 915–926.

Duckert, D., Morris, D., Deugo, D., Duckett, S., McPherson, S.. 2008. Developing site disturbance standards in Ontario: Linking science to forest policy within an adaptive management framework. Can J Soil Sci 89, pp. 13-26.

Evans, J., Hudak, A., Russ, F., Smith, A. 2009. Discrete return LiDAR in natural resources: recommendations for project planning, data processing, and deliverables. Remote Sens 1, pp. 776-794.

Farr, T. 2007. The Shuttle Radar Topography Mission, Revi Geophys 45, RG2004, doi:10.1029/2005RG000183.

Franklin, S., 2001. Remote sensing for sustainable forest management. Florida. CRC Press.

Fujisada, h., Bailey, G., Kelly, G., Hara, S., Abrams, M., 2005. ASTER DEM performance. IEEE T Geosci Remote 43, pp. 2700 - 2706.

Gessler, P., Moore, I., McKenzie, N., Ryan, P. 1995. Soil landscape modeling and spatial prediction of soil attributes. Int J Geogr Inf Sci 9, pp. 421-432.

Grabs, T., Seibert, J., Bishop, K. and Laudon, H. 2009. Modeling spatial patterns of saturated areas: A comparison of the topographic wetness index and a dynamic distributed model. J Hydrol 373, pp. 15-23.

Haala, N., Peter, M., Kremer, J., Hunter, G., 2008. Mobil LiDAR Mapping for 3D Point Cloud Collection in Urban Areas - a Performance Test. IAPRS,. 37, 1119f.

Hajnsek, I., Pottier, E. and Cloude, S.R. 2003. Inversion of surface parameters from polarimetric SAR. IEEE T Geosci Remote 41, pp. 727–44.

Hirano, A., Welch, R., Lang, H. 2003. Mapping from ASTER stereo image data: DEM verification and accuracy assessment. ISPRS J Photogramm 57, pp. 356-370.

Horn, 2004. Time dependence of soil mechanical properties and pore functions for arable soils. Soil Sci Soc Am J 68, pp. 1131–1137.

Hummel, J., Ahmad, I., Newman, S., Sudduth, K., Drummond, S. 2004. Simultaneous soil moisture and cone index measurment. Trans ASAE 47, pp. 607-618.

Kautz, R. Kawula, R., Hoctor, T. 2006. How much is enough? Landscape-scale conservation for the Florida Panther. Biol Cons 130, pp. 118-133.

Landsberg, J., Miller, R., Anderson, H., Tepp, J. 2003. Bulk density and sol resistance to penetration as affected by commercial thinning in north eastern Washington. Resource Papers. PNW-RP-551, USDA Forest Service, Pacific Northwest Research Station. pp 35.

Li, Z., Zhu, Q., Gold, C. 2005. Digital terrain modeling: principles and methodology. CRC Press.

Lin, H., Kogelmann, W., Walker, C., Bruns, M. 2006. Soil moisture patterns in a forested catchment: A hydro-pedological perspective. Geoderma 131, pp. 345 – 368.

Meek, P. 1996. Effects of skidder traffic on two types of forest soils. Forest engineering research institute of Canada, Pointe-Claire, QC. Technical report No. TR-117, 12.

McNabb, D., Campbell, R. 1985. Quantifying the impacts of forestry activities n soil productivity. In Foresters' future: leaders or followers? Proceedings 1985 SAF National convention, Fort Collins, Colorado.

Murphy, P., Ogilvie, J., Arp, P. 2009. Topographic modeling of soil moisture conditions: a comparison and verification of two models. Eur J of Soil Sci 60, pp. 94-109.

Nearing, M., West, L. 1988. Soil strength indices as indicators of consolidation. Trans ASAE 31, pp. 471-476.

Newhall, F., Berdanier, C. 1996. Calculation of soil moisture regimes from the climatic record. Soil survey investigations report no. 46. National soil survey centre, Lincoln, Nebraska.

Nielsen, N. 2005. Digital terrain models for use by the centre for Black Sea studies. [ONLINE: Accessed Nov. 2011]. www.pontos.dk/e-resources/terrain-models

Nowatzki, E., Karafiath, L. 1972. Effect of cone angle on penetration resistance. In: Highway Research Record No. 405, Highway Research Board, Washington, D.C.

Popescu, S., Wynne, R. 2004. Seeing the trees in the forest: Using LiDAR and multispectral data fusion with local filtering and variable window size for estimating tree height. Photogramm Eng Rem Sens 70, pp. 589–604.

Rabus, B., Eineder, M., Roth, A., Bamler, R. 2003. The shuttle radar topography mission: a new class of digital elevation models acquired by spaceborne radar. ISPRS J Photogramm 57, pp. 241-262.

Renault and Stengel, 1994. Modeling oxygen diffusion in aggregated soils. I. Anareobiosis inside the aggregates. Soil Sci Soc Am J 58, pp. 1017–1023.

Rooney, D., Lowery, B., 2000. A profile cone penetrometer (PCP) for mapping soil horizons. Soil Sci Soc Am J 64, pp. 2136 - 2139.

Saarilahti, M. 2002. Soil interaction model. In: Haarlaa R, Salo J, editors. ECOWOOD studies made at the University of Helsinki. University of Helsinki, Faculty of Agriculture and Forestry, Department of Forest Resource Management. Publication 31. February 2002.

Saarilahti, M., Anttila, T. 1999. Rut depth model for timber transport on moraine soils. Proceedings of the 9th International Conference of International Society for Terrain-Vehicle Systems, 14 -17. Sept. 1999, Munich, Germeny.

Sanli, F., Abdikan, S. 2006. Comparing a stereoscopic DEM with an interferometric DEM using the same RADARSAT data pair. ISPRS commission VII mid-term symposium “Remote sensing: from pixels to process”, Enschede, The Netherlands, May 8-11.

Shoop, S. 1995. Vehicle bearing capacity of frozen ground over a soft substrate. Geotech J 32, pp. 552-556.

Snyder, S., Whitmore, J., Schneider, I., Becker, D. 2008. Ecological criteria, participant preferences and location models: A GIS approach toward ATV trail planning. Appl Geo 28, pp. 248-258.

Sorensen, R., Zinko, U., Seibert, J.. 2006. On the calculation of the topographic wetness index: evaluation of different methods based on field observations. Hydrol Earth Syst Sci 10, pp. 101 – 112.

Turnage, G. W. 1972. Tire selection and performance prediction for off-road wheeled-vehicle operations. Proceedings of the 4th International ISTVS Conference, Stockholm-Kiruna, Sweden, April 24- 28, 1972. I:62- 82.

Vega-Nieva, D., Murphy, P., Castonguay, M., Ogilvie, J., Arp, P.. 2008. A modular terrain model for daily variations in machine-specific forest soil trafficability. Can J Soil Sci 89, pp. 93 - 109

Vepraskas, M. 1983. Cone Index of Loamy Sands as Influenced by Pore Size Distribution and Effective Stress. Soil Sci Soc Am J 48, pp. 1220-1225.

Walker, J., Willgoose, G. 1999. On the effect of digital elevation model accuracy on hydrology and geomorphology. Water Resour Res 35, pp. 2259-2268.

Welch, R. Jordan, T., Lang, H., Murakami, H. 1998. ASTER as a source for topographic data in the late 1990's. IEEE T Geosci Remote 36, pp. 1282 - 1289.

White, S., Wang, Y. 2003. Utilizing DEMs derived from LIDAR data to analyze morphologic change in the North Carolina coastline. Remote Sens Enviro 85, pp. 39-47.

Wronski, E. B., Stodart, D., Humphreys, N.. 1990. Trafficability assessment as an aid to planning logging operations. Appita J 43, pp. 18-22.

Xiang, W. 1996. A GIS based method for trail alignment planning. Landsc Urban Plan 35, pp. 11-23.

Chapter 3 *:* Study Areas

3.1 Introduction

This section summarizes the study locations used for the collection of soil samples. An area of extremely variable terrain and an area of moderate to minimally variable terrain were chosen to capture as much variability as possible in a single study.

3.2 Ghost River Forest Land Use Zone (GRFLUZ)

This study area is located in the foothills of the Southern Alberta Rockies, Canada (51°19'59"N, 114°57'59"; 113,000 ha, mostly forested, Figure 3.1). The terrain is rolling to hummocky, and includes plateaus, valleys, and steep slopes. Elevation ranges from 1,190m to 2,590 above sea level.

The climate is mostly influenced by western airflow passing over the Rocky Mountains. As such, the area receives 540mm precipitation and maintains a mean annual air temperature of 2°C. January mean temperature does not typically dip below -10°C and July mean temperatures rarely exceed 13°C. The area sees moderate amounts of solar radiation through the year (4400-4800 MJ/m^2).

Bedrock is mostly represented by the Brazeau (non-marine sandstones, conglomerates, shale's and coals), Alberta Group (mudstone interspersed with relatively thin sandstone and conglomerate beds), Coalspur (non-marine sandstones, siltstones, shale's and coals), and Paskapoo (mudstone, siltstone and sandstone, with subordinate limestone and coal) formations (Alberta Geological Survey[1], 2010). Detailed soil surveys have not been

completed for the study area; surficial geology maps for the area are crude but provide valuable information. dominant soil groups for the study area are represented by upland soils (typically Grey Luvisols, interspersed with a small proportion of Brunisols).

The hydrology of the area is characteristic of foothill-mountainous terrain. There are two large rivers in the study area; the Red Deer River in the Northern section, and the Ghost River in the South. The current Provincial hydrology layer (Figure 3.2) has approximately 3400km of linear features (rivers, streams). This layer was likely derived from photo interpretation. Errors associated with this practice are common to such procedures, namely, incomplete networks due in part to image resolution and canopy cover. LiDAR DEMs allow for improved hydrological modeling (Figure 3.3). Wet areas mapping techniques have been created specifically for Alberta LiDAR DEMs (Figure 3.4). Ability to map stream locations within the study area has increased dramatically with this new product (Figure 3.5) versus the largely photo interpreted hydrology layer. The LiDAR derived flow channels find over 7600km of streams, a more than 100% increase in steam identification. Total stream crossings by the Ghost River trail network can now be assessed more completely. Other information derived from high resolution DEMs has seen improvements in accuracy; slope and aspect maps are an example of this.

Access into the area was initially created by the resource extraction industries (mainly oil and gas and coal mining operations) but was expanded to include forestry and recreation (Figure 3.6). The forest within the area contains lodgepole pine (*Pinus contorta*), white spruce (*Picea* glauca) and black spruce (*Picea mariana*) as the

dominant species. The area is actively harvested in the Eastern and Northern sections by Spray Lakes Sawmills, and oil and gas features are prevalent (Figure 3.7).

The GRFLUZ is a heavily utilized recreational area with close proximity to over 2 million people. Government and recreational user groups assist in the creation of the extensive trail system throughout the area (Figure 3.8). Tables 3.1 and 3.2 inform on the current demands within the study area and the related lengths and areas of impact. The Ghost-Waiparous stewardship committee was created with recognition that successful management of public land-use within the GRFLUZ ultimately depends on the support and actions of those who use it. The stewardship council is comprised of, but not limited to groups listed in Table 3.3. These stakeholders collaborate on new trail designation and old trail remediation and closures, mitigate conflicts, and work in partnership with the Alberta government.

Large government interest in the area is large due to the close proximity of the GRFLUZ to Calgary, Cochrane, and the residents of the mountain district of Bighorn. Government bodies involved in the management of values within the GRFLUZ are listed in Table 3.4. The department of sustainable resource development oversees the trail network and is concerned with multiple considerations for the maintenance and construction of access to the area (Table 3.5).

Off highway vehicle (OHV) sales have increased on average 26% per year since 1990 from an original 38,000 registrations to 138,000 in 2009 in Alberta. In 1990, 1.5% of the population owned OHV's while today, in 2010, that number has doubled to 3.6%, an

average 2.2% of the population increase per year (lowest increase of 1.4%). Given Alberta's projected growth rate to 2050 (Figure 3.9, Alberta population projections[1] 2010-2050) with high, moderate and low projections, we can expect to see OHV registration increase (Figure 3.10). Approximately 40% of the Alberta population lives within 300km of the study area, leading to an ever increasing demand for access to the land use zone.

Table 3.1 **Land-use interests and areal footprint of GRFLUZ user groups, including government, industry, clubs and general public.**

Land-use Interests	**Interest**	**Length** km	**Area** ha
Oil & Gas (Shell and Others)	Pipelines	226	113
	Cutlines	1986	993
	Oil & Gas Patches		16
	Access Roads	350	258
	Gas Plants		264
Forest Operations (Spray Lakes Sawmills)	Harvesting		18,352
	Regeneration		-
	Retention		-
	Wildlife Management		-
	Access Roads	150	1,111
Government Departments	Drinking Water Protection		-
	Riparian Protection		-
	Wet Land Protection		-
	Critical Wildlife		12,665
	Prime Protection		10,558
	Facilities		36
	Recreation		-
Public Recreation	Motorized Trails	605	213
	Non-Motorized Trails		-
	Camping		3,652
	Facilities		101
	Area affected	**Total**	**48,332**
		%	**36.8**

Table 3.2 GRFLUZ recreational trail types and their respective lengths.

Trail Class	**Length** km
4 x 4	26
Motorbike Only	16
Quad	217
Quad (Along Pipeline Only)	8
Quad, Closed Dec 1-April 30	142
Quad, Open November Only	45
Un-Mapped Trails	150
Total Trail length	**605**

Table 3.3 Ghost-Waiparous stewardship council members and expert consultants. *Ghost FLUZ Q&A - http://www.srd.alberta.ca/RecreationPublicUse/RecreationOnPublicLand/ForestLandUseZones/GhostFLUZQuestionsAnswers.aspx*

Ghost-Waiparous Stewardship Council Members	
ATV User Group	Industry
Motorbike User Group	Local Governments
4x4 User Group	Ministry of Culture and Community Spirit
Equestrian User Group	Ministry of Infrastructure
Rock Climbing User Group	Ministry of Transportation
Non-motorized Recreation Groups	Disposition Holders
Non-Government Environmental Groups	Federal Department of Fisheries and Oceans

Table 3.4 Governmental ruling bodies within the GRFLUZ.

Governmental Bodies within the GRFLUZ
Sustainable Resource Development
Tourism, Parks and Recreation
Transportaion
Aboriginal Relations
Energy
Environment

Table 3.5 Governmental considerations in access management. *Ghost FLUZ Q&A - http://www.srd.alberta.ca/RecreationPublicUse/RecreationOnPublicLand/ForestLandUseZones/GhostFLUZQuestionsAnswers.aspx*

Governmental Consideration
Watershed Values
Fisheries Values
Wildlife Values
Range/forage Values
Soil and Landform
Historical/Cultural Vlaues
Recreational Values
Public Safety
Minimizing user Conflict
Access Management
Trail Conditons

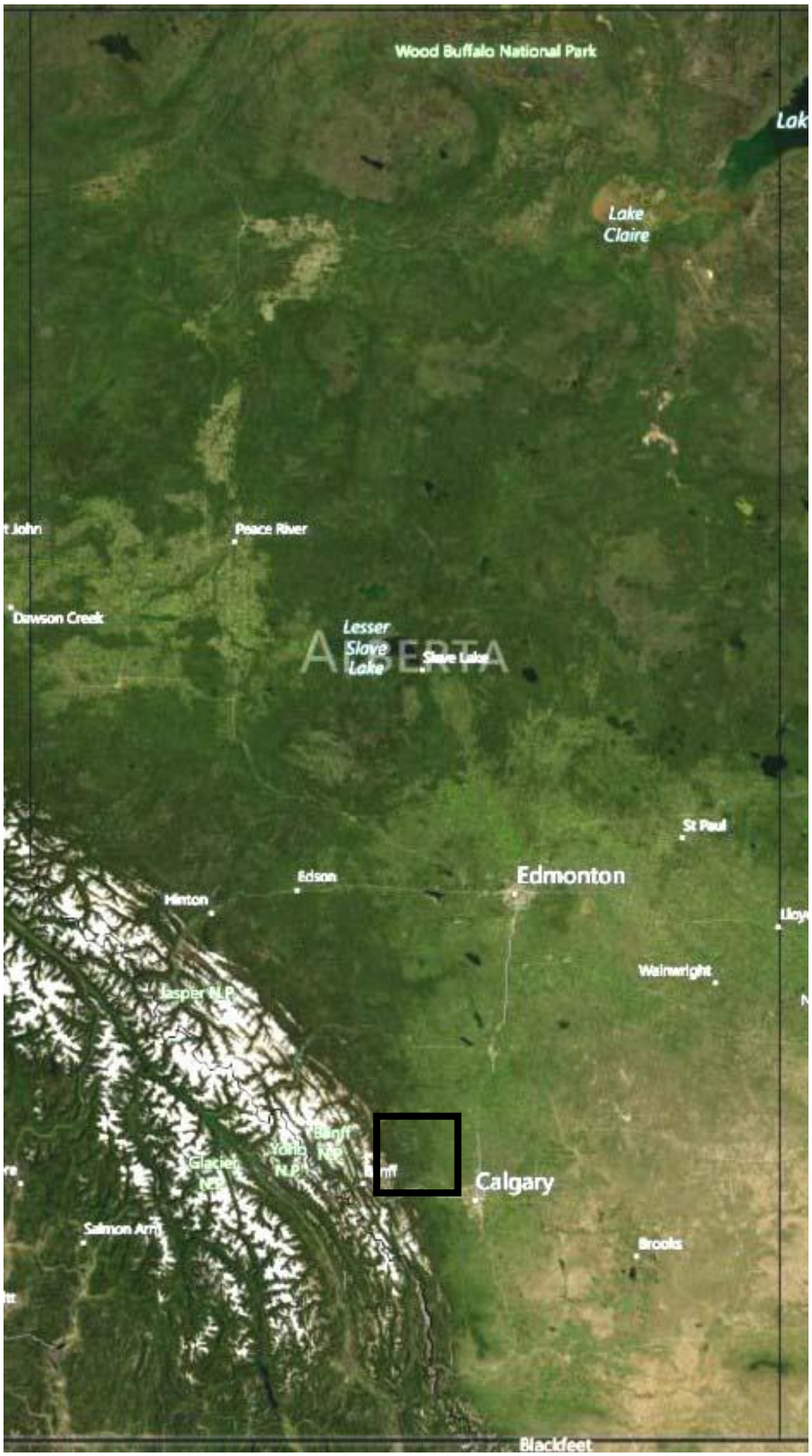

Figure 3.1 Location of the study area in south-western Alberta, Canada.

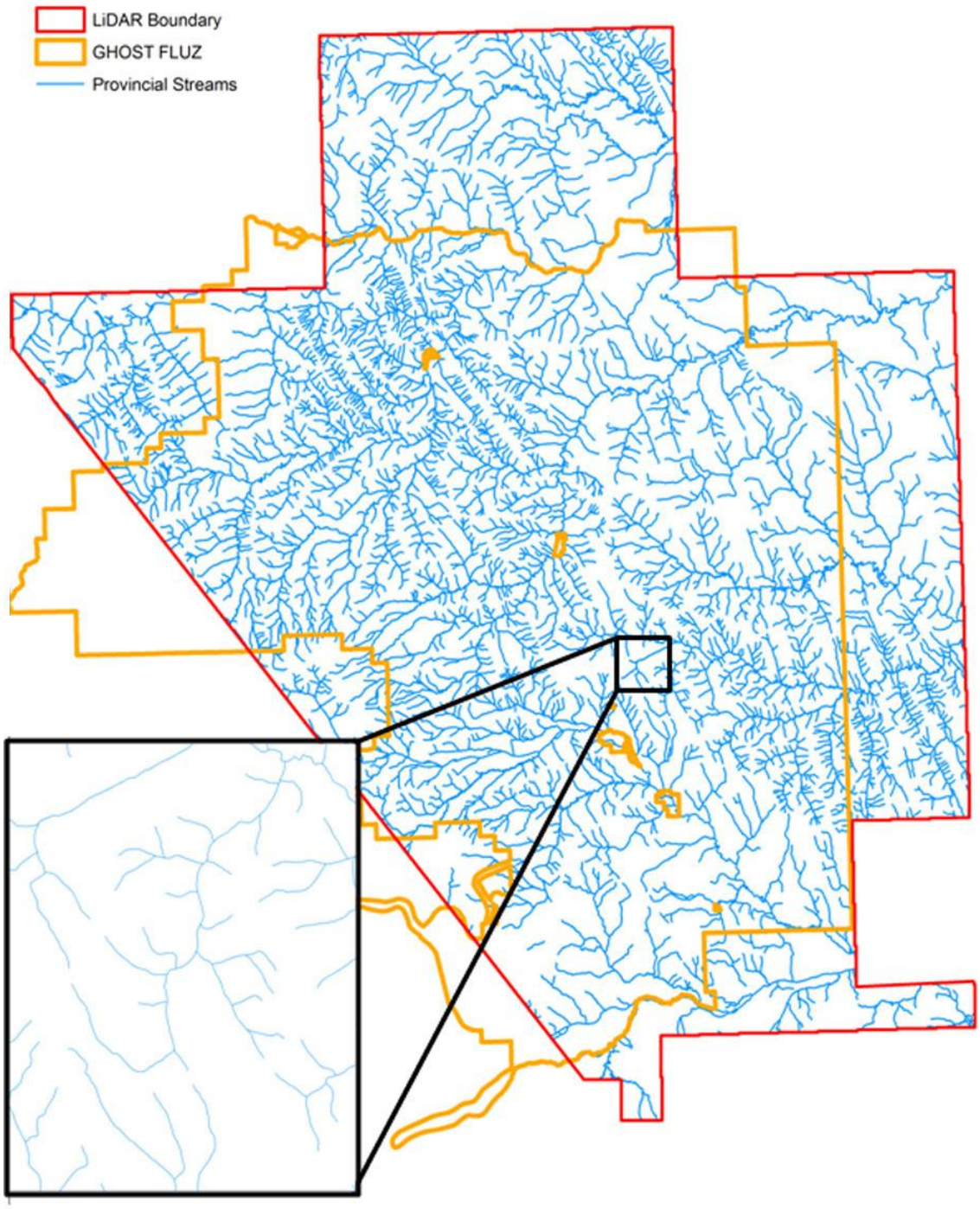

Figure 3.2 Provincial flow channels for the GRFLUZ. *Layers courtesy Alberta government (RIMB).*

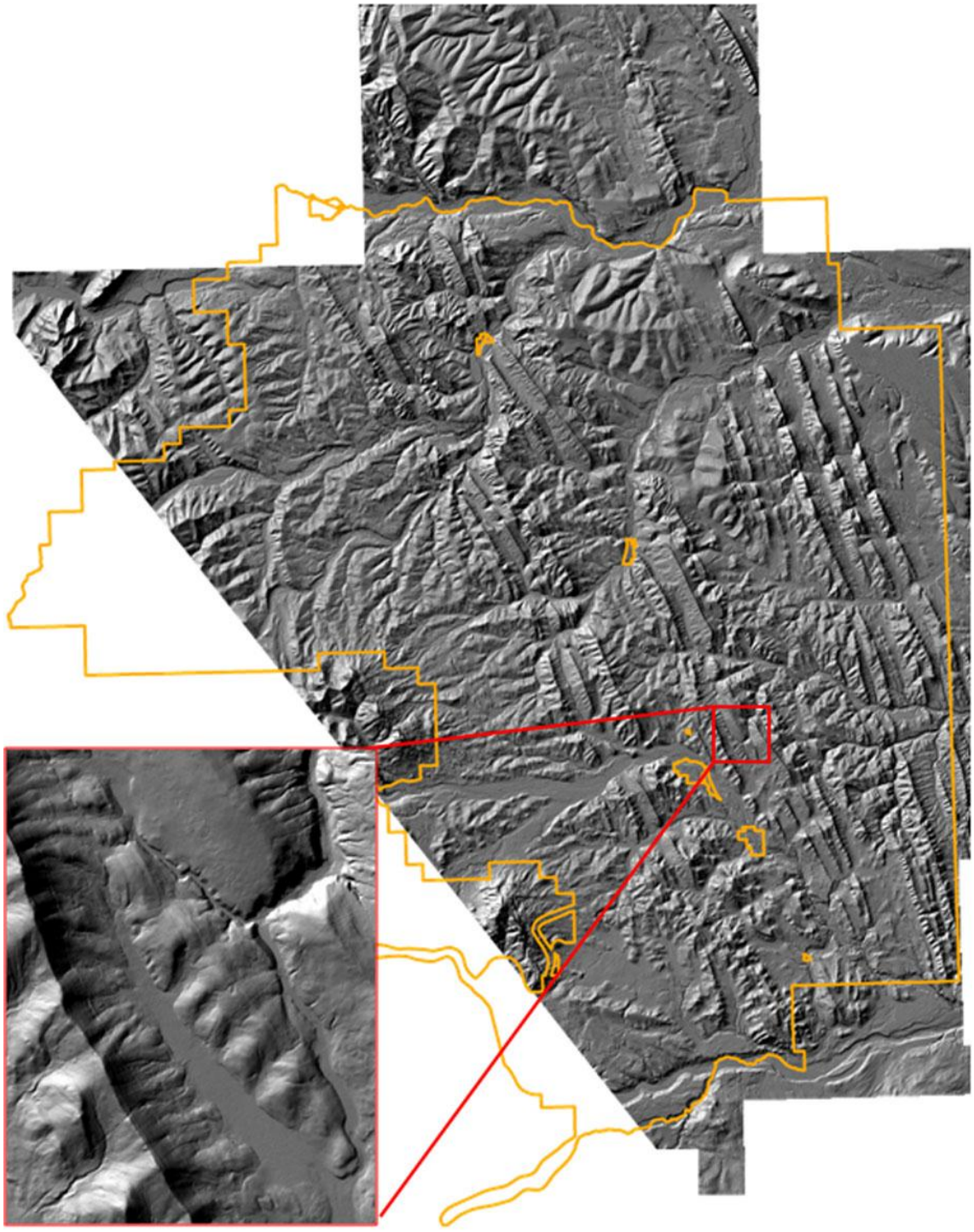

Figure 3.3 Digital elevation map for the study area with close-up insert; 1m resolution. *Layers courtesy Alberta government (RIMB).*

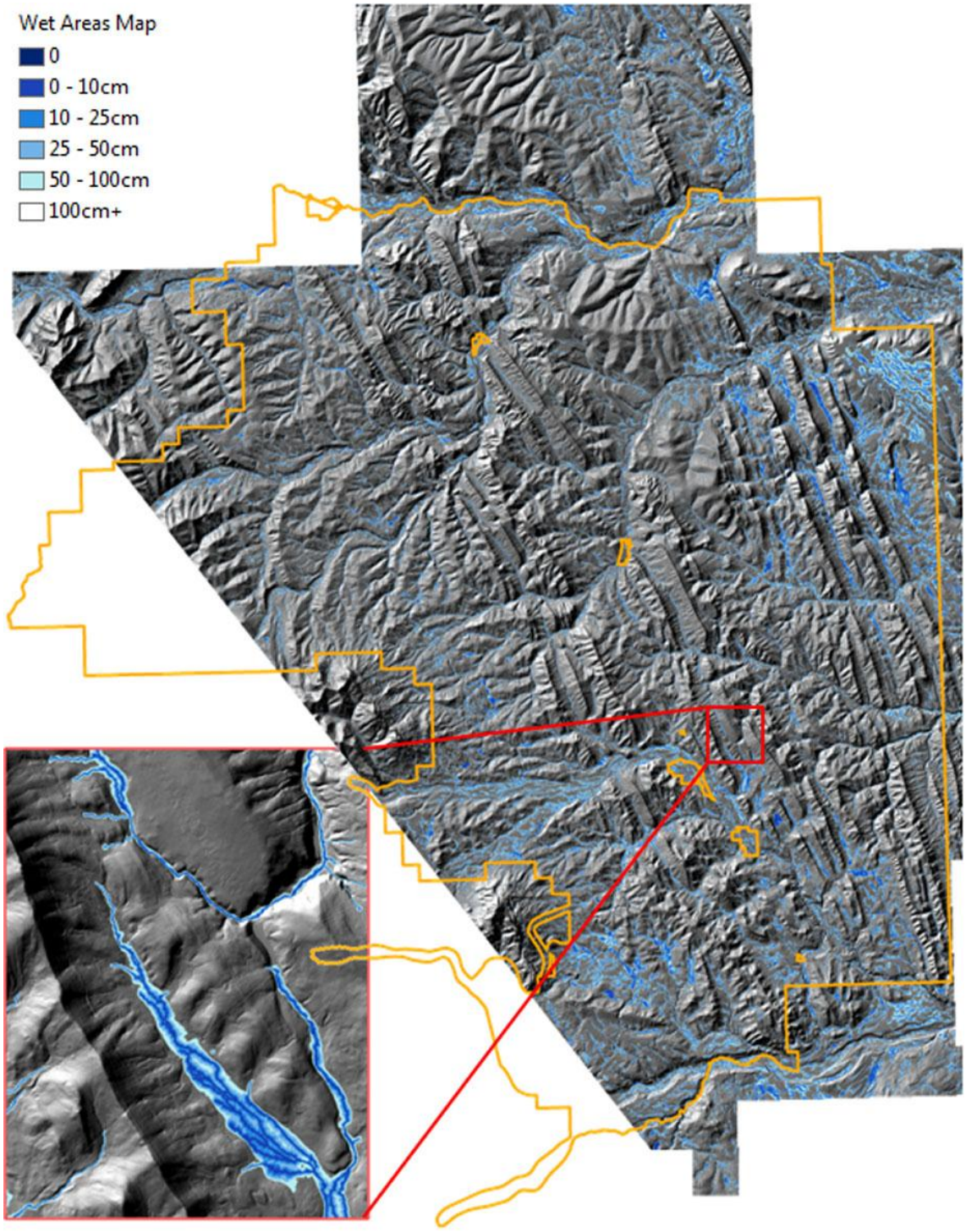

Figure 3.4 Wet areas map for the study area with close-up insert; 1m resolution.

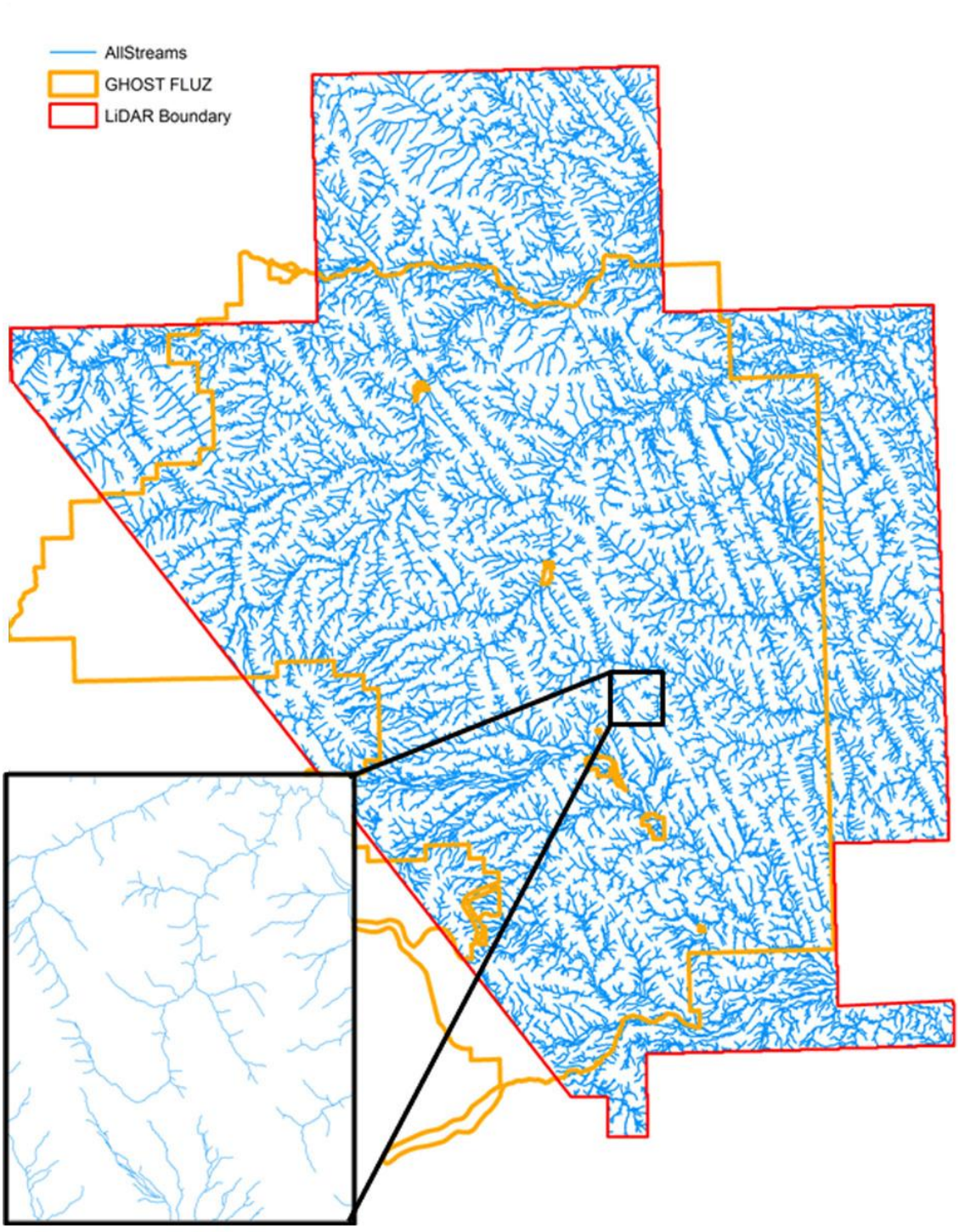

Figure 3.5 LiDAR derived flow channels for the GRFLUZ.

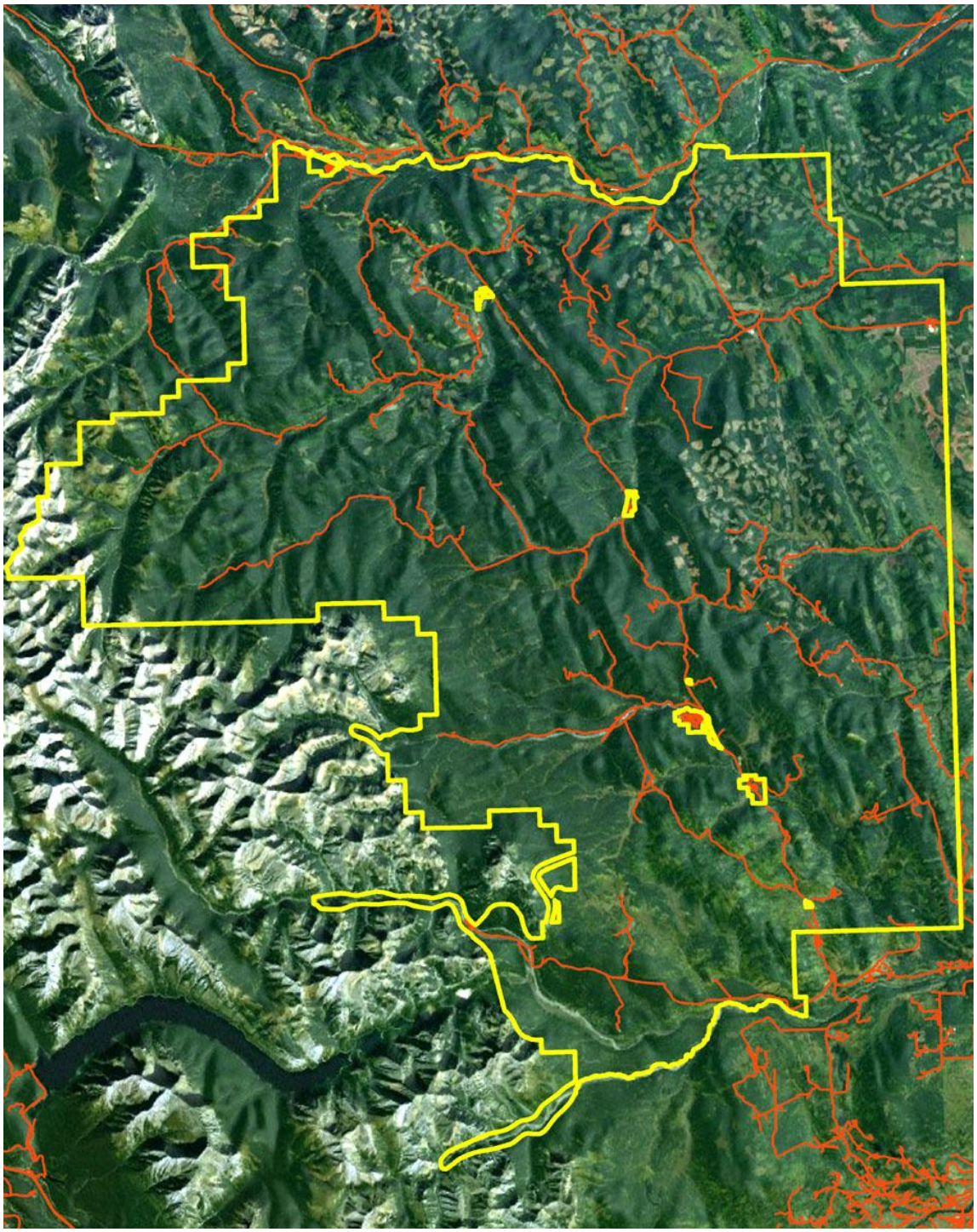

Figure 3.6 Image displaying the extent of road access as created through forest operations, oil and gas requirements, and recreational goals: red lines = roads. *Layers courtesy Alberta government (RIMB).*

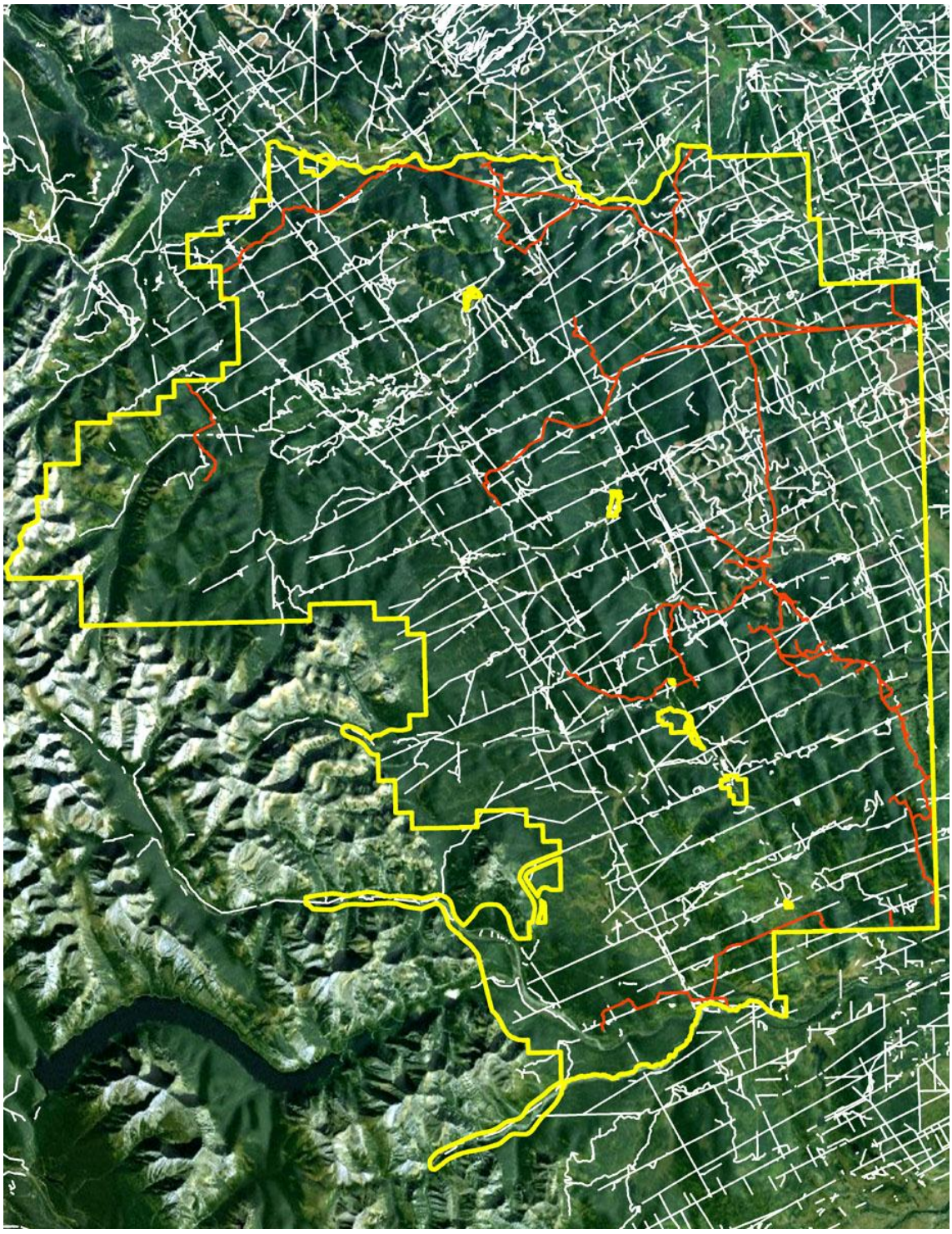

Figure 3.7 A depiction of the Oil and Gas sector throughout the study area: red lines = pipelines, white lines = cutlines. *Layers courtesy Alberta government (RIMB).*

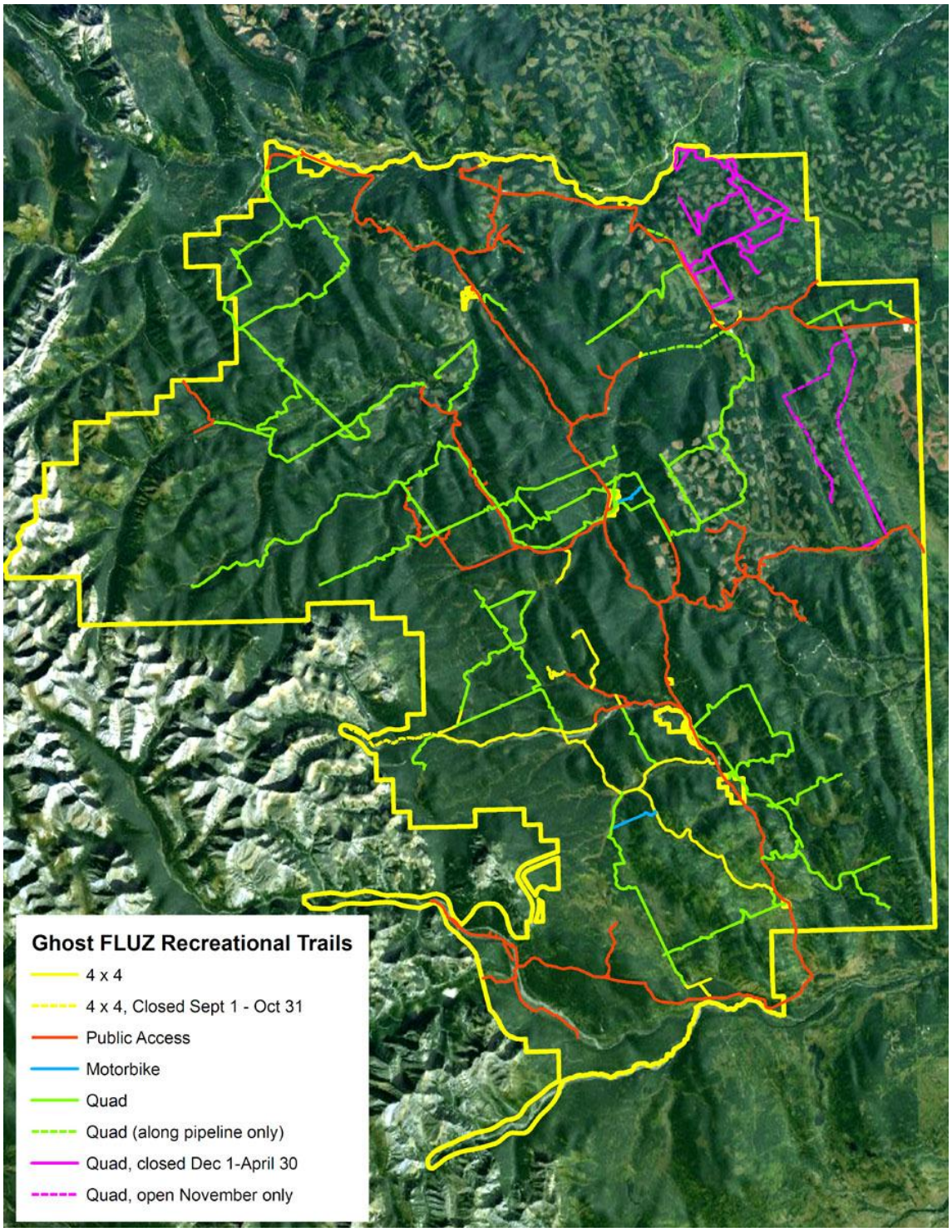

Figure 3.8 The trail system and access map for the recreational users of the area. *Layers courtesy Alberta government (RIMB).*

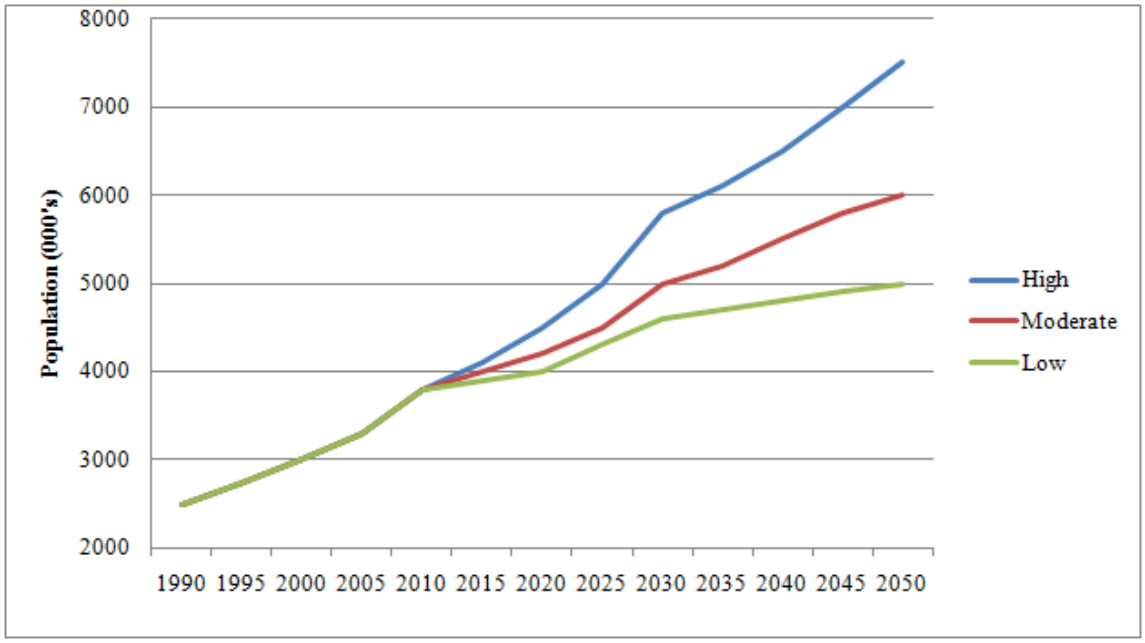

Figure 3.9 Alberta's historical and predicted population growth to the year 2050 with high, moderate and low population growth rate predictions. http://www.finance.alberta.ca/aboutalberta/population_reports/2010-2050-alberta-population-projections.pdf

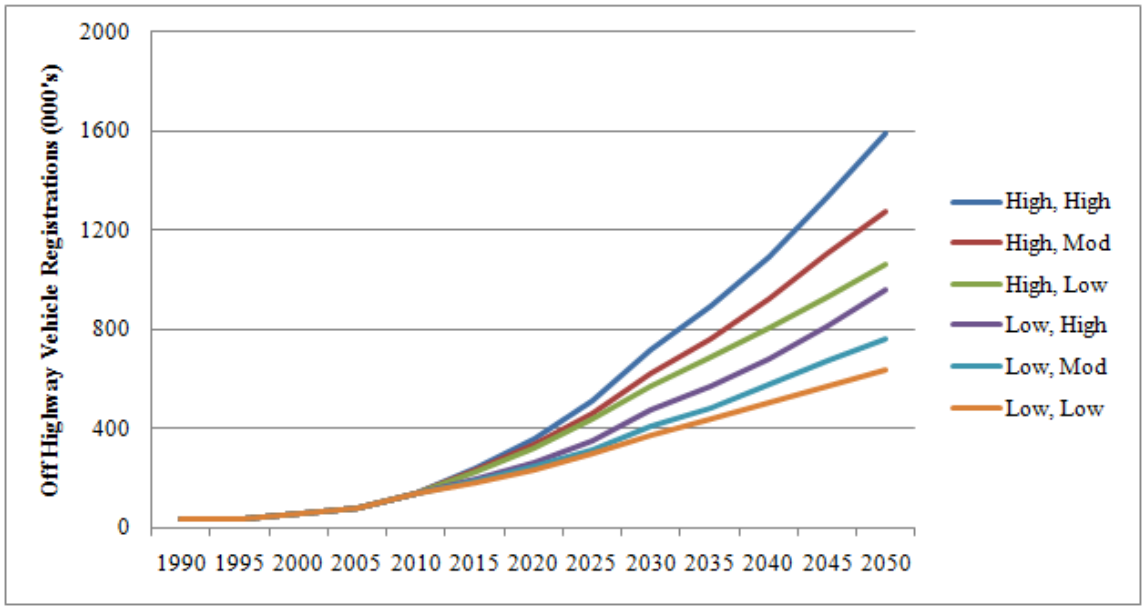

Figure 3.10 Alberta's historical and predicted OHV registration growth as a function of population growth. Predictions utilize average historical registration growth and lowest registration growth in combination with the Alberta growth rate scenarios (OHV registration rate, population growth rate).

3.3 Ecosystem Management Emulating Natural Disturbance Study Area (EMEND)

(Kishuk, 2004) EMEND was established in order to determine management practices that would best emulate natural disturbance. The EMEND research site is located approximately 90km northwest of Peace River, Alberta (Figure 3.11), and approximately 400km Northwest of Edmonton. It is located within the Clear Hills Upland Ecoregion within the Boreal Plains Ecozone. The location is in the proximity of 56° 46' 13" N - 118° 22' 28" W and is approximately 1800 hectares in size. The elevational range of the area is 633-887 meters above sea level and consists of undulating to hummocky terrain in the Southern portion of the research area and typical, low elevational changes in the Northern section consistent to that of Boreal ecoregions.

The climate is that of Boreal with some influence of mountain currents. The mean annual temperature is 1.2ºC with mean January and July temperatures –17.7ºC and 15.9ºC, respectively. Mean annual precipitation is 431 mm. The area sees low amounts of solar radiation through the year (4200-4400 MJ/m^2).

(Kishuk, 2004) Surface material is of a glacier origin; fine-textured glacio-lacustrine, glacial till, and lacustro-till deposits, with localized organic and alluvial materials results. Dominant soil types are of the Gray Luvisol or Brunisol orders with pockets of Luvic Gleysols and Solonetz. The area has been extensively sampled for soil types leading up to a 2004 extensive publication by Kishuk (2004). Vegetation is typically dominated by Trembling Aspen (*Populus tremuloides*), Balsam Fir (*Abies balsamea*), and White Spruce (*Picea glauca*).

The study site drains into the Notikewan and Whitemud rivers which are part of the Peace river drainage. The current hydrology layer has approximately 82km of linear features (streams, Figure 3.12). LiDAR DEMs allow for the improved mapping of hydrological features within the area (Figure 3.13). Through the WAM processing of the area (Figure 3.14), LiDAR predicted stream channels were produced (Figure 3.15). This process has increased the identification of hydrological features by 1180% (968km of features).

Access into EMEND was originally created by resource extraction industries (mainly oil and gas); forestry expanded into the area upon the development of Aspen pulping methods. The area is actively harvest by DMI with supporting structures of the two active industries prevalent (Figure 3.16, Figure 3.17). EMEND is not a heavily used area for recreation or other activities. There are no special zones within the study area depicting protected areas or large scale watershed protection programs.

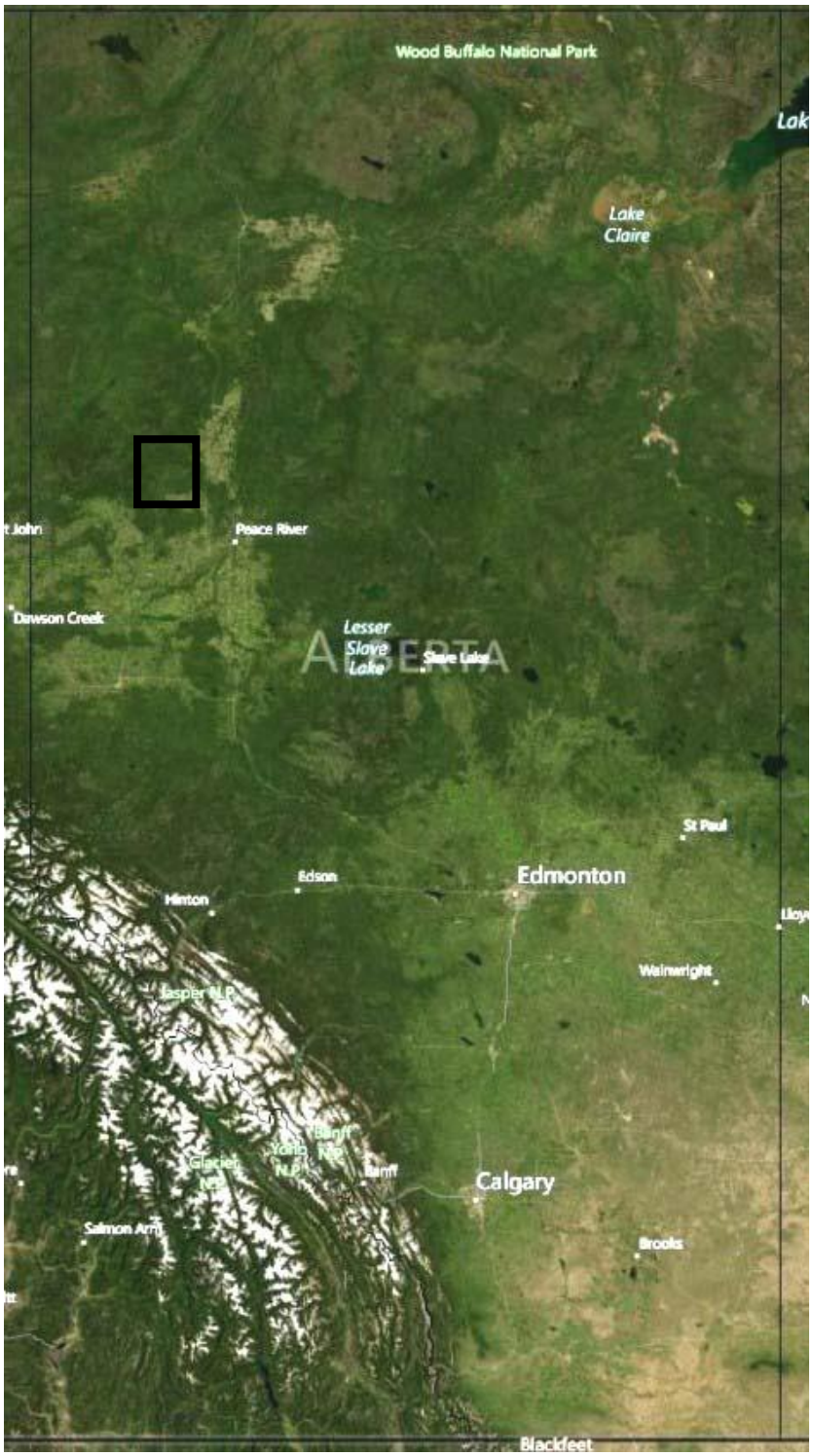

Figure 3.11 Location of the EMEND study area in North-Western Alberta, Canada.

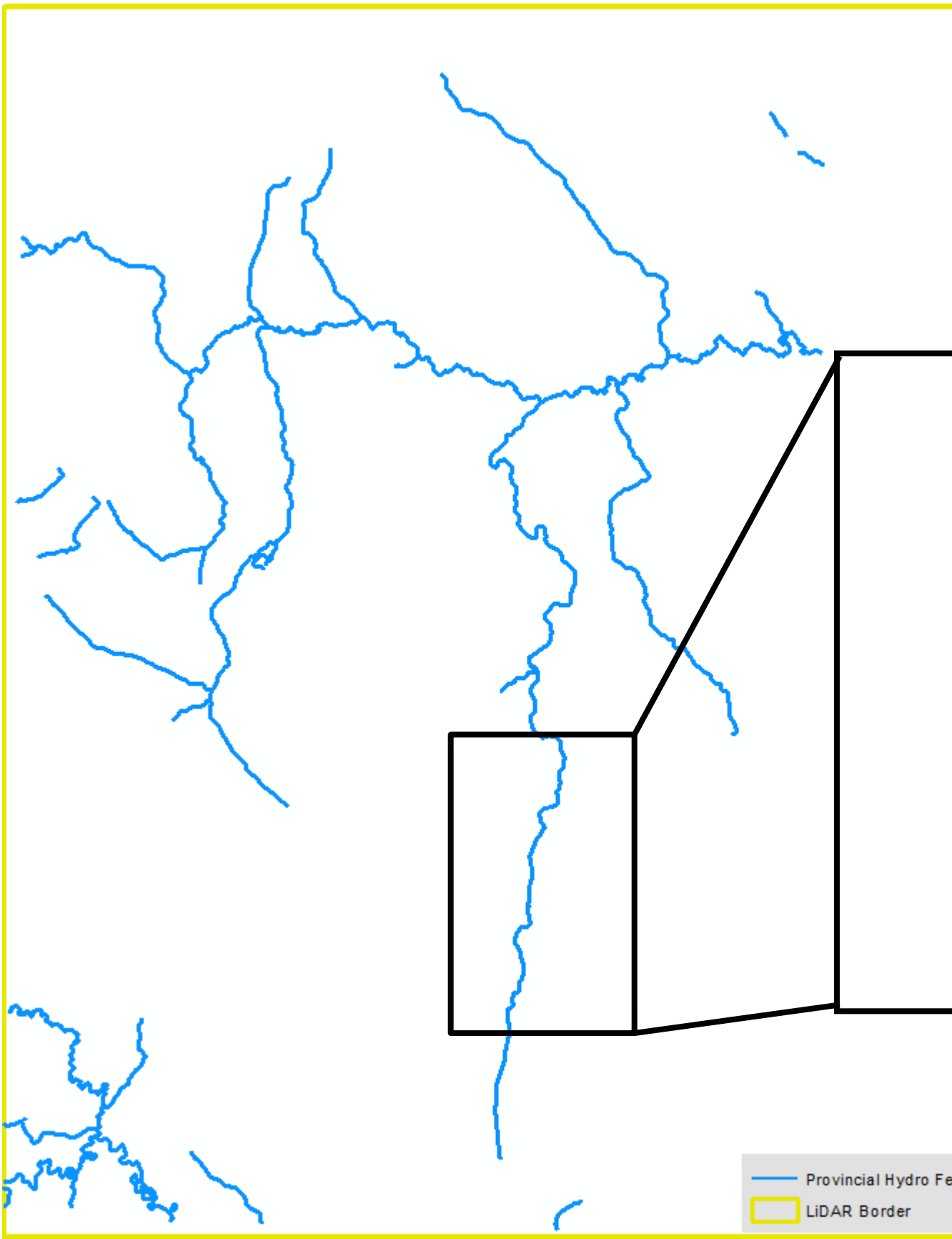
Provincial Hydro Fe
LiDAR Border

Figure 3.12 Provincial flow channels for EMEND. *Layers courtesy Alberta government (RIMB).*

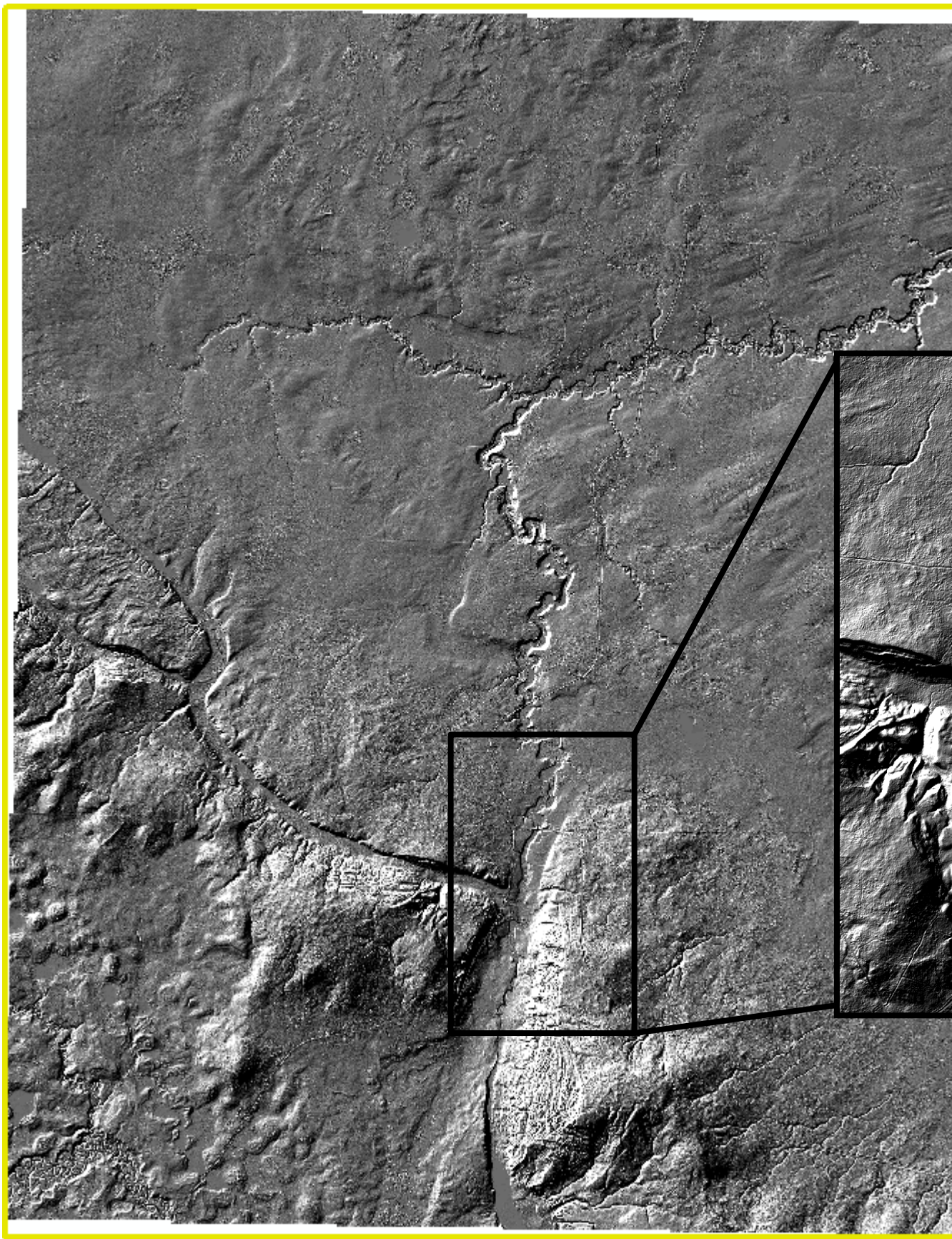

Figure 3.13 Digital elevation map for the EMEND study area with close-up insert; 1m resolution. *Layers courtesy Alberta government (RIMB).*

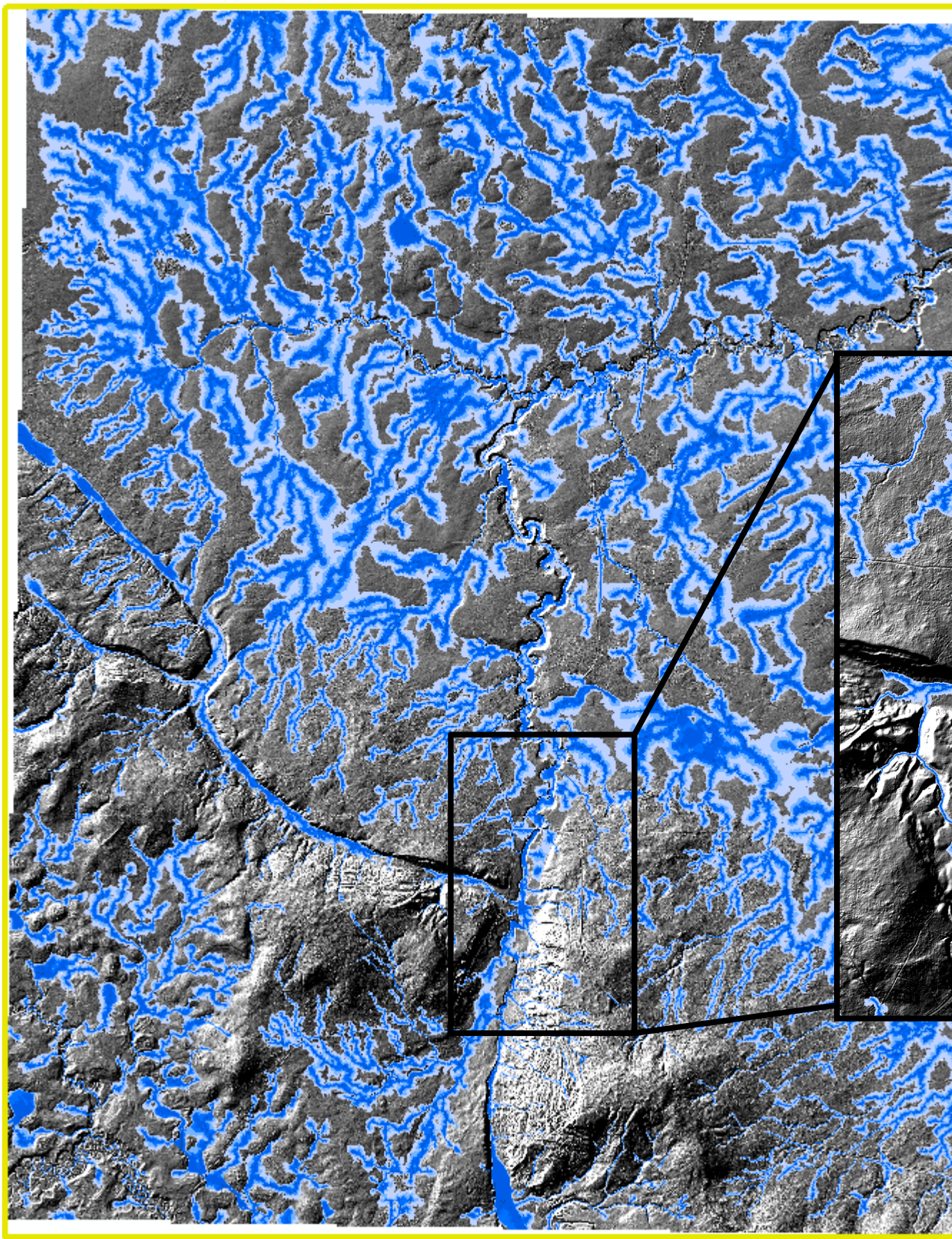

Figure 3.14 Wet areas map for the EMEND study area with close-up insert; 1m resolution.

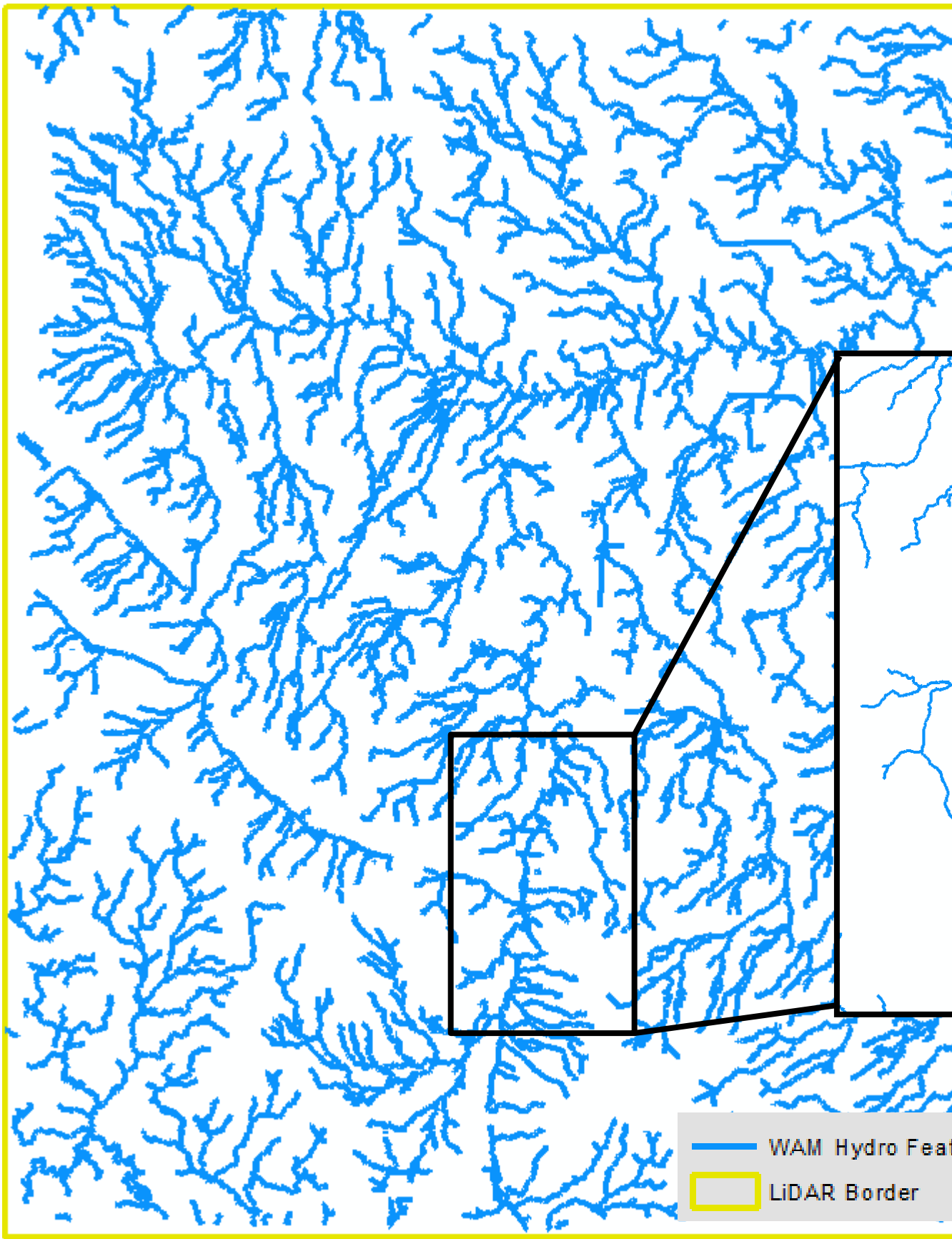
WAM Hydro Feat
LiDAR Border

Figure 3.15 LiDAR derived flow channels for EMEND as part of the WAM process.

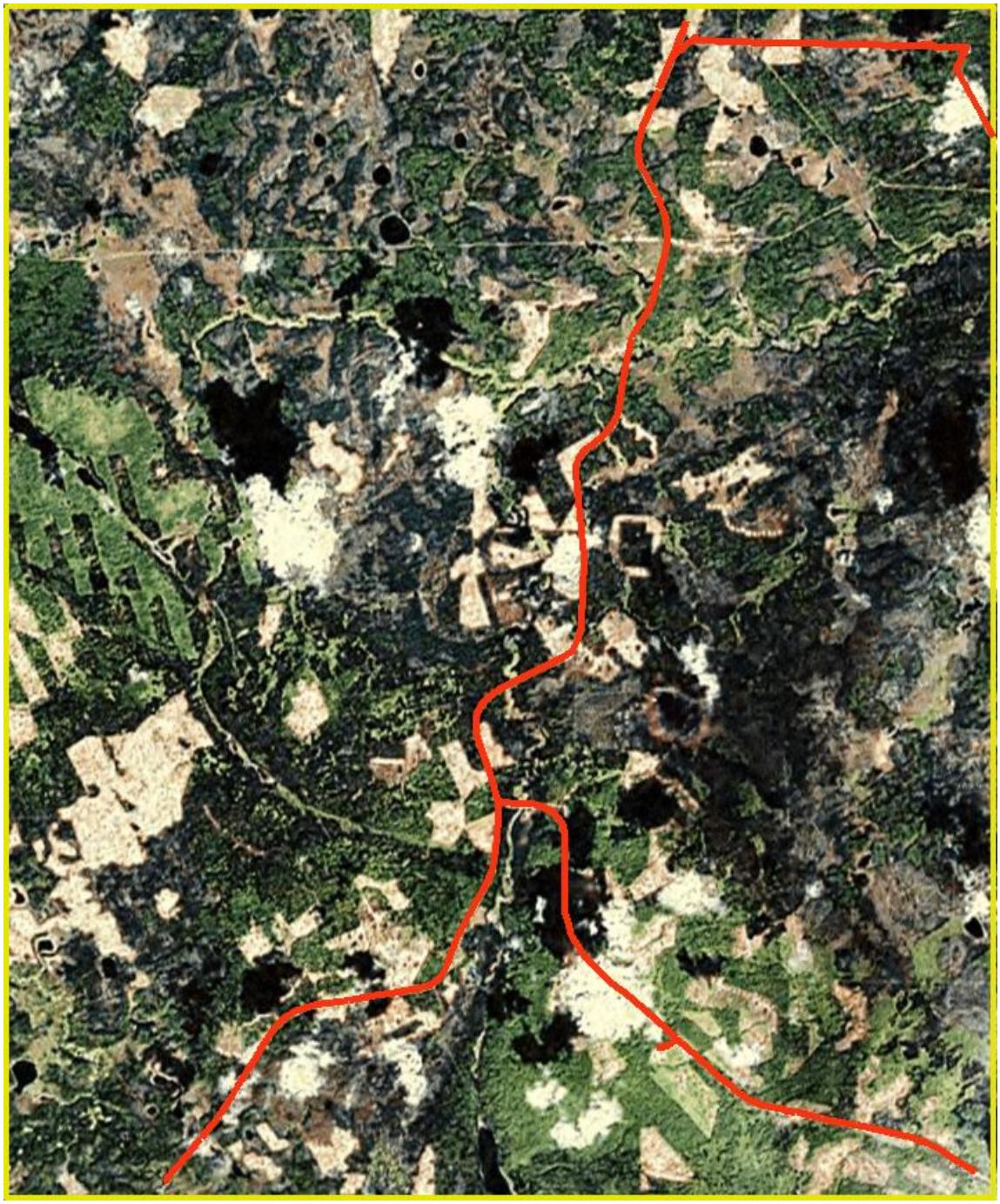

Figure 3.16 Image displaying the extent of road access as created through forest operations and oil and gas requirements: red lines = roads. *Layers courtesy Alberta government (RIMB).*

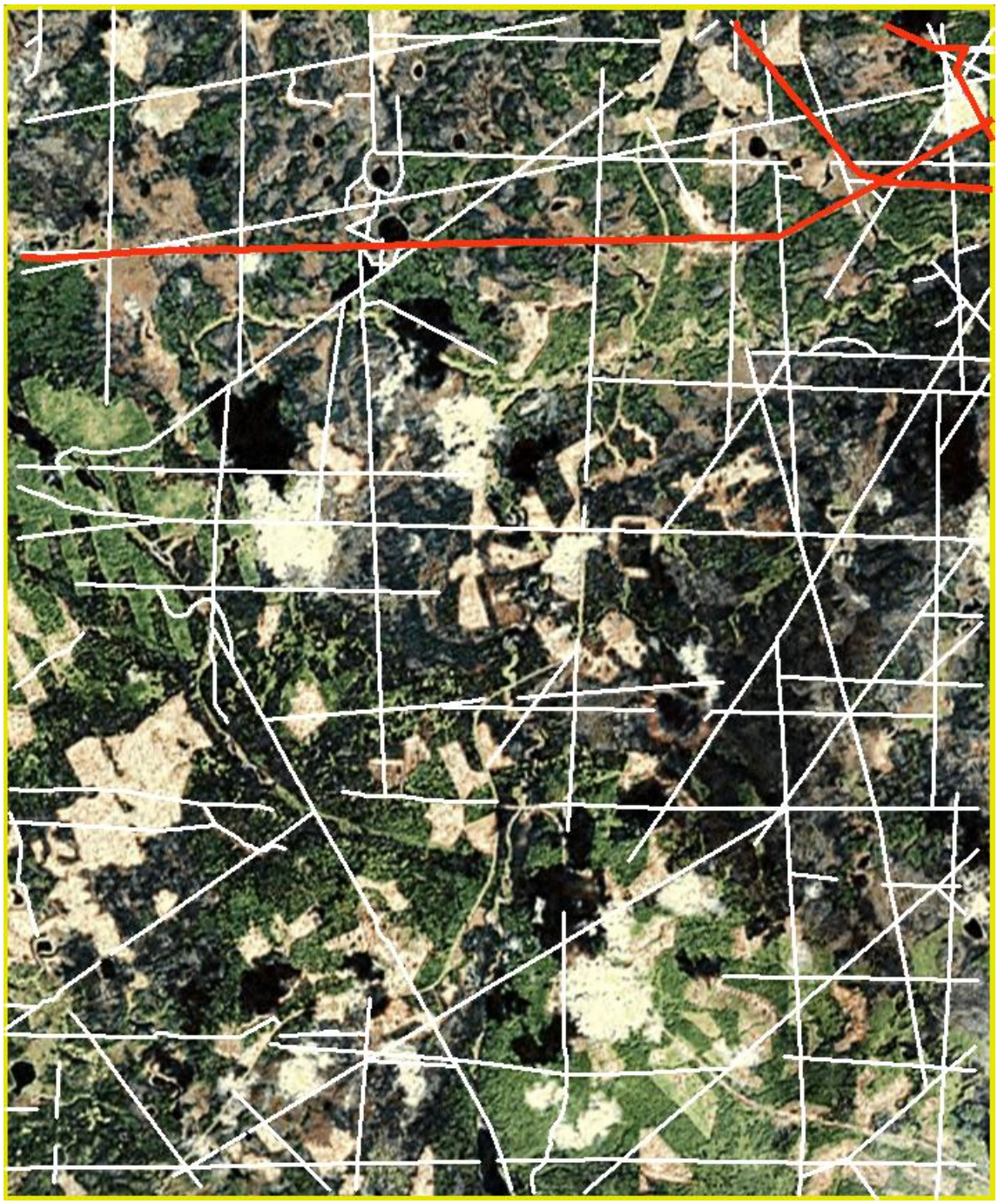

Figure 3.17 A depiction of the Oil and Gas sector throughout the EMEND study area: red lines = pipelines, white lines = cutlines. *Layers courtesy Alberta government (RIMB).*

Chapter 4 : Modeling and Mapping Soil Resistance to Penetration and Rutting Using Digital Elevation Data (LiDAR)

4.1 Abstract

Soil resistances to penetration were probed with a hand-held soil penetrometer across ridge-to-depression transects for two contrasting study areas in Alberta, Canada: one in the foothills west of Calgary, and one in the boreal plain north of Peace River. The results were analyzed in terms of soil moisture, density, texture, organic matter content, soil depth, elevation, slope, slope variability, and the cartographic depth-to-water index (DTW). This index was zero-referenced to all DEM-derived flow channels, each starting with a 4ha flow-accumulation area according to LiDAR-derived bare-ground digital elevation data with at 1m resolution (DEM: digital elevation model; LiDAR: Light Detection and Ranging). The resulting cone index values (CI) conformed to a previous formulation that relates CI to soil texture, density, and water-filled pore-space quite closely. This formulation could be improved for both study areas through direct calibration. In terms of topographic position, CI increased with increasing DTW, in parallel to decreasing soil moisture content and increasing soil density. The resulting regression equation between CI, $\log_{10}$(DTW) and elevation (or study area) was used to map CI and CI-expected rutting depth for all-terrain vehicles (ATVs), and the maps so generated were partially verified with a soil disturbance survey along a 40 km long ATV trail segment within the foothill area.

Key words: soil resistance to penetration, cone index, rut depth, digital elevation model, cartographic depth-to-water index, soil disturbance survey, ATV trails, LiDAR

4.2 Introduction

Forecasting soil trafficability is an important aspect of regulating on- and off-road recreational, agricultural and industrial activities across landscapes as uncontrolled traffic leads to considerable soil degradation in terms of rutting, compaction, and erosion (McNabb *et al.* 1985, Wilson and Seney 1994; Horn *et al.*, 2004, Eliasson 2005, Foltz 2006; Nahdi et al. 2009). Additional side effects refer to inefficiencies in field operations, reductions in future crop production, unnecessary release of sediments and pollutants to surface water, unsightly post-operational aesthetics, unsafe working conditions, and increasingly negative public perceptions (Rab et al. 2005; Raper 2005; Zenner 2007; Stokowski and Lapointe 2000; Marion and Olive 2006; Wilkerson and Whitman 2009). Soil rutting is of particular concern because ruts reduce soil pore space, injure and cut roots, interfere with new root growth, obstruct natural flow paths, produce stagnant water pools, and initiate gulley formation and washouts along slopes (Saarilahti, 2002; Carter et al. 2000, 2007; Blouin 2005; Foltz 2006). Activities intended to curb the negative effects of soil trafficability refer to (i) seasonally imposed rules and regulations, (ii) soil disturbance monitoring (e.g., Duckert *et al.*, 2008; USDA 2009; Miller et al. 2010), and (iii) best-management practices and related guidelines and certification requirements. Impact controlling activities involve, e.g., proactively reducing the severity (length, depth) and frequency of rutting through operations timing, placing gravel, boards, cords or mats including geosynthetics to reduce rut impacts and along trails (Grenier et al. 2008), and prohibiting road and trail use either selectively by segments, or regionally during wet weather conditions.

This article focuses on determining soil resistances to penetration as primary means to model and map soil trafficability in general, and rutting depth specifically, with the primary concepts derived from the WES method of the US Corps of Army Engineers (Carter et al. 2000; Saarilahti, 2002; Priddy and Willoughby 2006). This method uses soil penetrometers (i) to probe the resistance of soils to rutting, (ii) to ascertain how many vehicles of certain type and load can pass through a particular area under given soil and weather conditions, and (iii) to evaluate the effect of rutting on soil compaction or soil strength. In general, soil penetrability generally increases with increasing sand and moisture content, but decreases with increasing clay content (Nearing, 1988). In addition, soil penetrability typically decreases with increasing soil depth due to increasing soil densities (Rooney *et al.* 2008; McNabb *et al.* 1985). Wronski *et al.* (1990), Landsberg *et al. (*2003), Agodzo (2003) and Saarilahti and Antilla (1999) reported similar results. Vega *et al.* (2009) noted that soils are less resistant to penetration under re-constituted laboratory conditions than under field conditions, i.e.:

$$CI_{Lab} = 1.14 * 10^{(3.99-1.36sand-6.65PS-1.20MC_{PS})}; R^2 = 0.77; \quad [1]$$

$$CI_{field} = 1.08 * 10^{(1.99-0.38sand-2.23PS-0.72MC_{PS})}; R^2 = 0.85 \quad [2]$$

where CI is the cone index for soil penetration up to ≈ 7 MPa, PS is the pore space, and MC_{PS} is the water-filled fraction of PS. Hence, Eq. 2 can, at least in principle, be used to estimate CI based on existing soil survey reports that inform about soil texture, density and specific moisture conditions by soil type. CI mapping by soil type, however, is quite coarse by assuming uniform soil conditions within each mapped soil polygon. In reality, soil moisture conditions vary significantly by topographic position, and according to

antecedent to current weather conditions. Similarly, soil depth, texture, organic matter content and densities also tend to vary with topographic position, with soils generally being shallower, coarser, denser, and less enriched with organic matter along slopes and upland positions than in depressions (Murphy et al. 2011). The objectives of this article address these variations:

1. by determining how changes in cone penetrometer readings can be related to (a) changing soil texture, moisture, density, and organic matter content, and (b) changing topographic position;
2. by using the resulting relationships to map soil penetrability and machine-specific soil rutting potentials according to landscape position.

The work regarding Objective 1 involved soil penetration and properties sampling along ridge-to-depression transects. This was done for two contrasting forest areas in Alberta: with within the foothills west of Calgary, and within the boreal plain north of Peace River. The spatial analysis work required for mapping soil CI, rutting potential, soil moisture, texture, organic matter content, soil moisture and density as per Objectives 1 and 2 proceeded by compiling (i) the digital elevation data layer for bare ground (referred to as digital elevation model, or DEM), (ii) DEM-derived attributes pertaining to elevation, slope, surface roughness, flow direction, flow accumulation, flow-channel networks, and flow-channel referenced depth-to-water (DTW; Murphy et al. 2011), and (iii) available soil survey maps and reports. This mapping effort is partially verified by tracking and rating the extent of soil disturbance along 40 km of all-terrain vehicle (ATV) trail segments. Potential rut depths can be inferred from:

$$Z_n = (1656/NCI)\, n^{1/2} \quad [3]$$

where

$$NCI = CI\,(b\,d / W)\,(\partial/h)^{0.5}\,/(1 + b/2d) \quad [4]$$

with b as tire width (m), d as tire diameter (m), h as section height (m), δ as tire deflection (m) = 0.001 (0.365 +170/p), p as tire inflation pressure (kPa), W as vehicle load (kN per number of wheels) and n as number of vehicle passes along the same track.

4.3 Materials and Methods

4.3.1 Study sites

The area west of Calgary (GRFLUZ, 51°19'59"N, 114°57'59"; elevations ranging from 1,190m to 2,590 asl; area = 113,000 ha) represents a mostly forested mountainous terrain. The second site 90km northwest of Peace River (EMEND; 56° 46' 13" N -118° 22' 28" W; elevations ranging from 633m to 887m asl.; area = 1800ha) represents the boreal forest conditions of Northern Alberta (Figure 4.1). Both sites record on average 540mm and 431mm of precipitation with a mean annual air temperature of 2°C and 1.2°C, respectively. Bedrock within the GRFLUZ is mostly represented by the Brazeau, Alberta Group, Coalspur, and Paskapoo formations. Bedrock within EMEND is of a glacier origin; fine-textured glacio-lacustrine, glacial till, and lacustro-till deposits, with localized organic and alluvial materials (Kishuk, 2004, Alberta Geological Survey, 2010). Soil groups for the GRFLUZ are represented by typically upland soils (Grey

Luvisols, interspersed with a small proportion of Brunisols); EMEND is dominated by Gray Luvisol or Brunisol orders with pockets of Luvic Gleysols and Solonetz. Vegetation within the GRFLUZ forest contains lodgepole pine (*Pinus contorta*), white spruce (*Picea glauca*) and black spruce (*Picea nigra*) as the dominant species; EMEND vegetation is typically dominated by Trembling Aspen (*Populus tremuloides*), Balsam Fir (*Abies balsamea*), and White Spruce (*Picea glauca*).

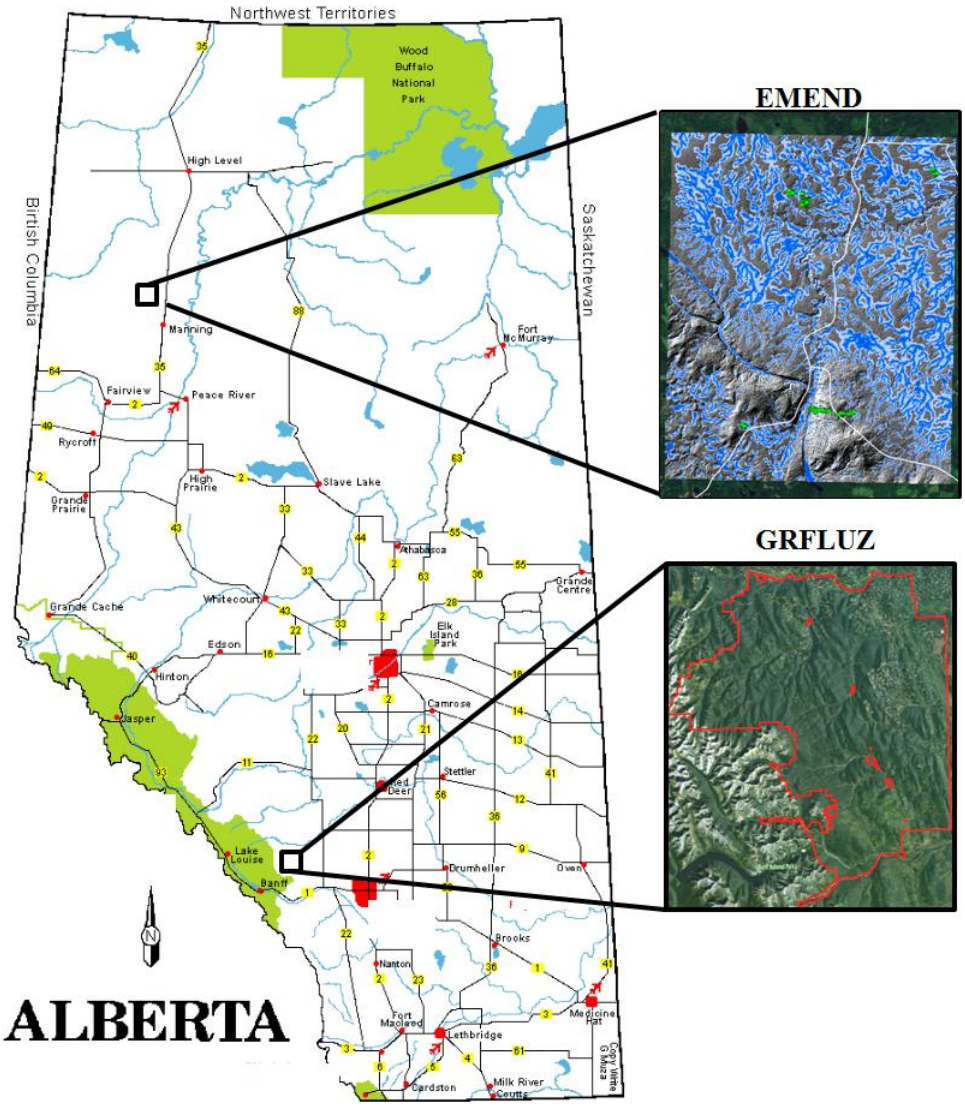

Figure 4.1. Locator map for the two study areas in Alberta, Canada.

4.3.2 Digital elevation data

All spatial data layers were created utilizing ESRI ArcGIS software. Digital elevation rasters for bare ground (DEMs) were obtained from the Research Information Branch of the Alberta Government. DEMs were LiDAR derived, and have a resolution of 1m with vertical accuracies of ±15cm. Wet Area Maps (WAM) were created for the study area from the 1m resolution DEMs. Wet area mapping techniques were applied to the DEMs following Murphy *et al.* (2011) yielding flow accumulation, flow direction, and depth-to-water (DTW) rasters for each study site, with DTW set equal to 0 along the local flow channel network, for which each flow channel was set to have a 4ha area for flow initiation. Slope rasters were created using ESRI's slope functions and ruggedness maps (TRM) were created using the standard deviation of the slope on a 3x3 neighbourhood window.

4.3.3 Transects

Transect sampling was done at both study locations in reference to the DEM-generated DTW map, from low to high, as shown in Figures 4.2-4.4. At EMEND, this was done along 6 transects involving 82 sampling plots (replicated 3 times = 253 samples including streams). At GRFLUZ, this was done along 16 transects and 97 plots (replicated 3 times = 247 samples including streams). Sampling occurred from July to August, 2009 (EMEND) and from mid-July to mid-August, 2010 (GRFLUZ). All plots were geographically registered. Soil cores (5 to 40cm deep; 1.78cm diameter) were collected and aggregated within each 5m plot to yield about 100 g for analysis. Soil core depth and soil layer type were recorded. The depths of organic horizons on top of the

mineral soil layers were also measured. Also determined for each plot was (i) the resistance of the soil to cone penetration, using a hand-held 50-cm long Cone Penetrometer (Humboldt HS-4210; cone angle = 60°; diameter at cone base = 1.53 cm; penetrometer length 50 cm; max. supported load: 7.6 MPa) to determine "Cone Index" or CI, and (ii) soil moisture content by volume ($MCv_{field,}$ top 10 cm of the mineral soil), using a time domain reflectance probe (Theta Moisture Probe). The CI and MCv_{field} measurements were repeated 5 times and averaged for each plot. CI was recorded at 5cm depth increments up to the maximum attainable value (CI_{max}). Typically, soil penetration resistance increased with increasing soil depth. Maximum penetration pressure, however, was limited by (i) the upper body weight of the sampler, and (ii) a general inability to maintain a constant penetration velocity with increasing soil resistance. Typically, the CI_{max} values so generated were more consistent per plot than the CI values at any particular soil depth.

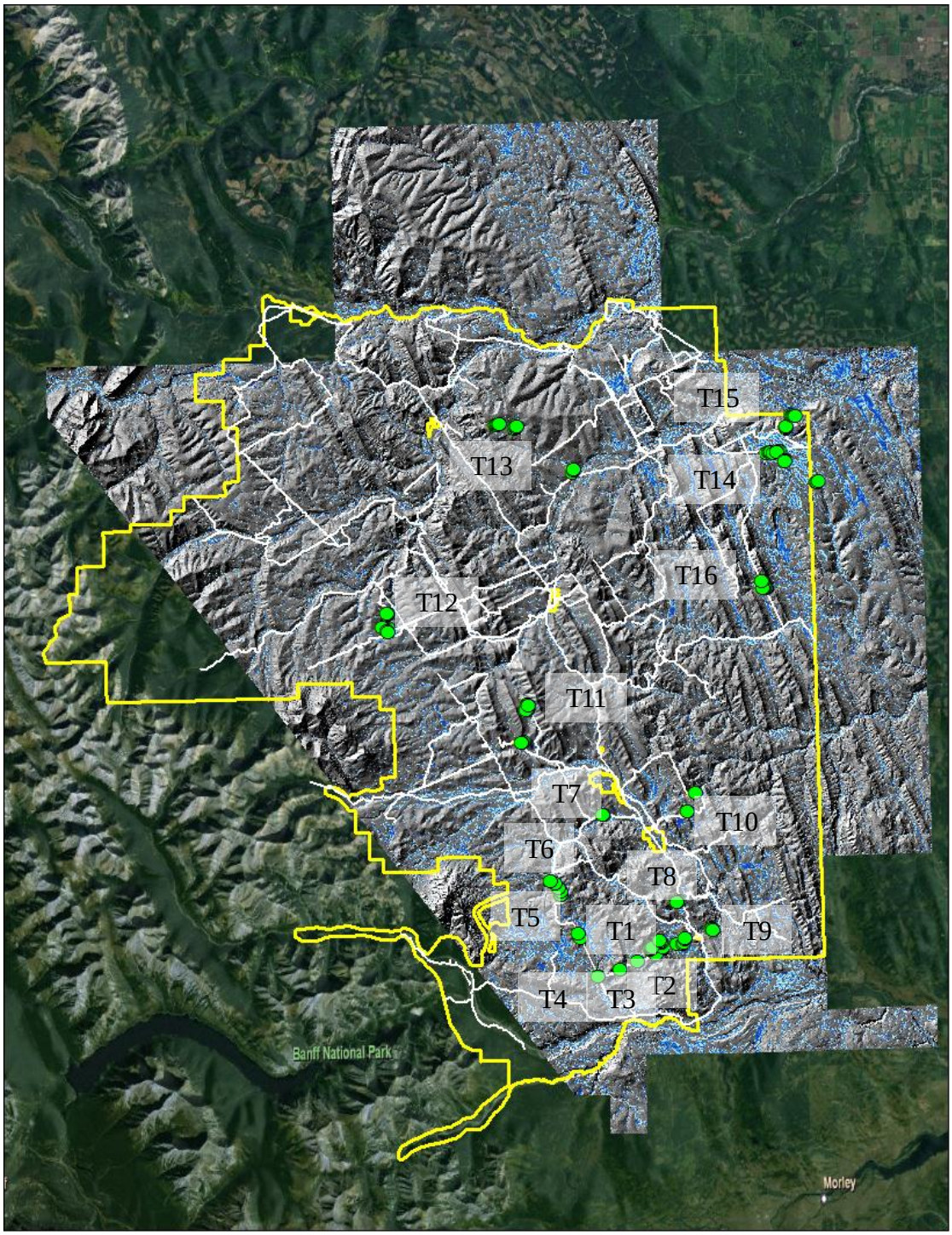

Figure 4.2. Transect locations within the GRFLUZ study area (yellow border) with Lidar-derived DEM (hill-shaded) and existing trails and roads (white), all placed on ESRI .

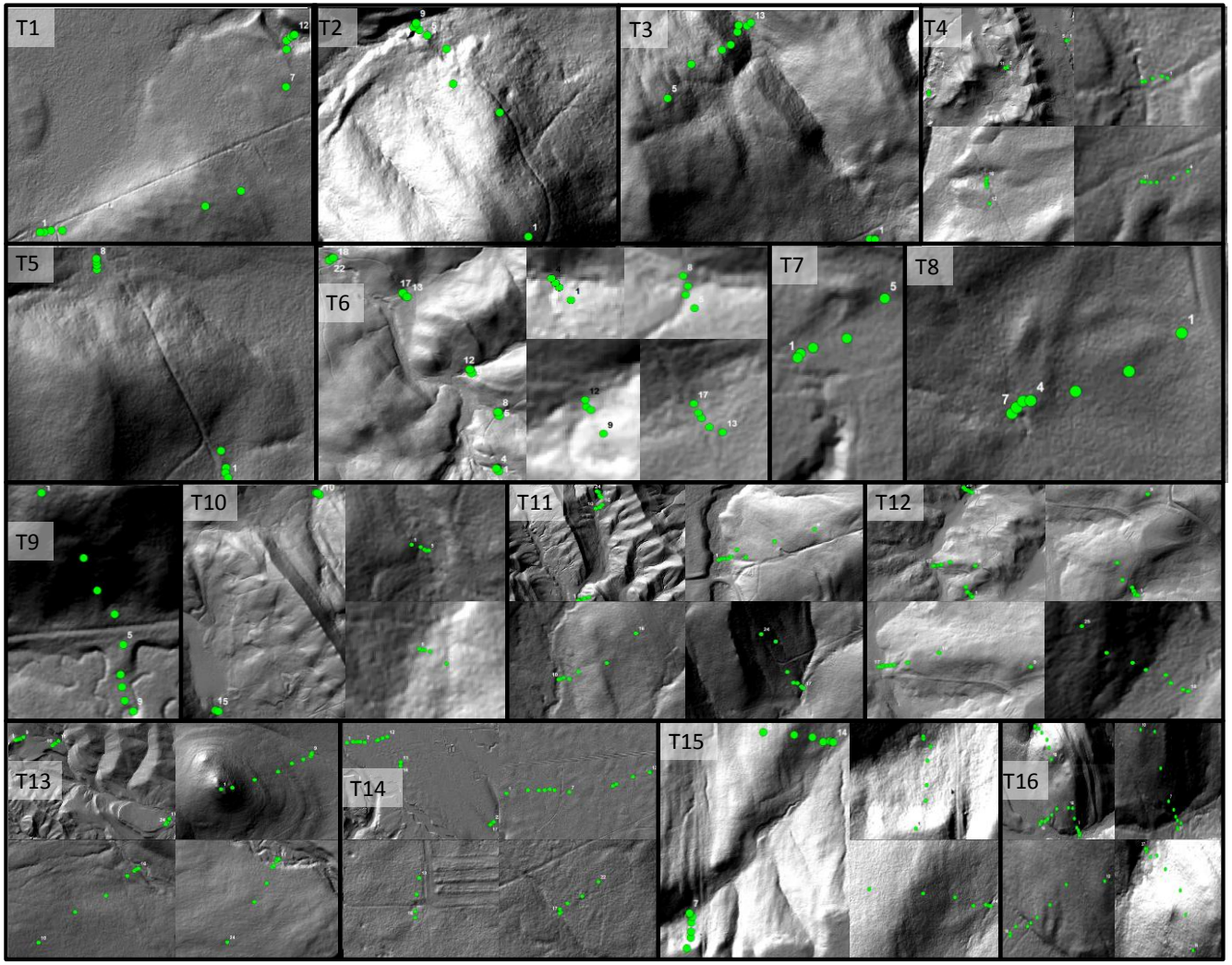

Figure 4.3. Mosaic of the transect locations within the GRFLUZ study area, on hill-shaded DEM.

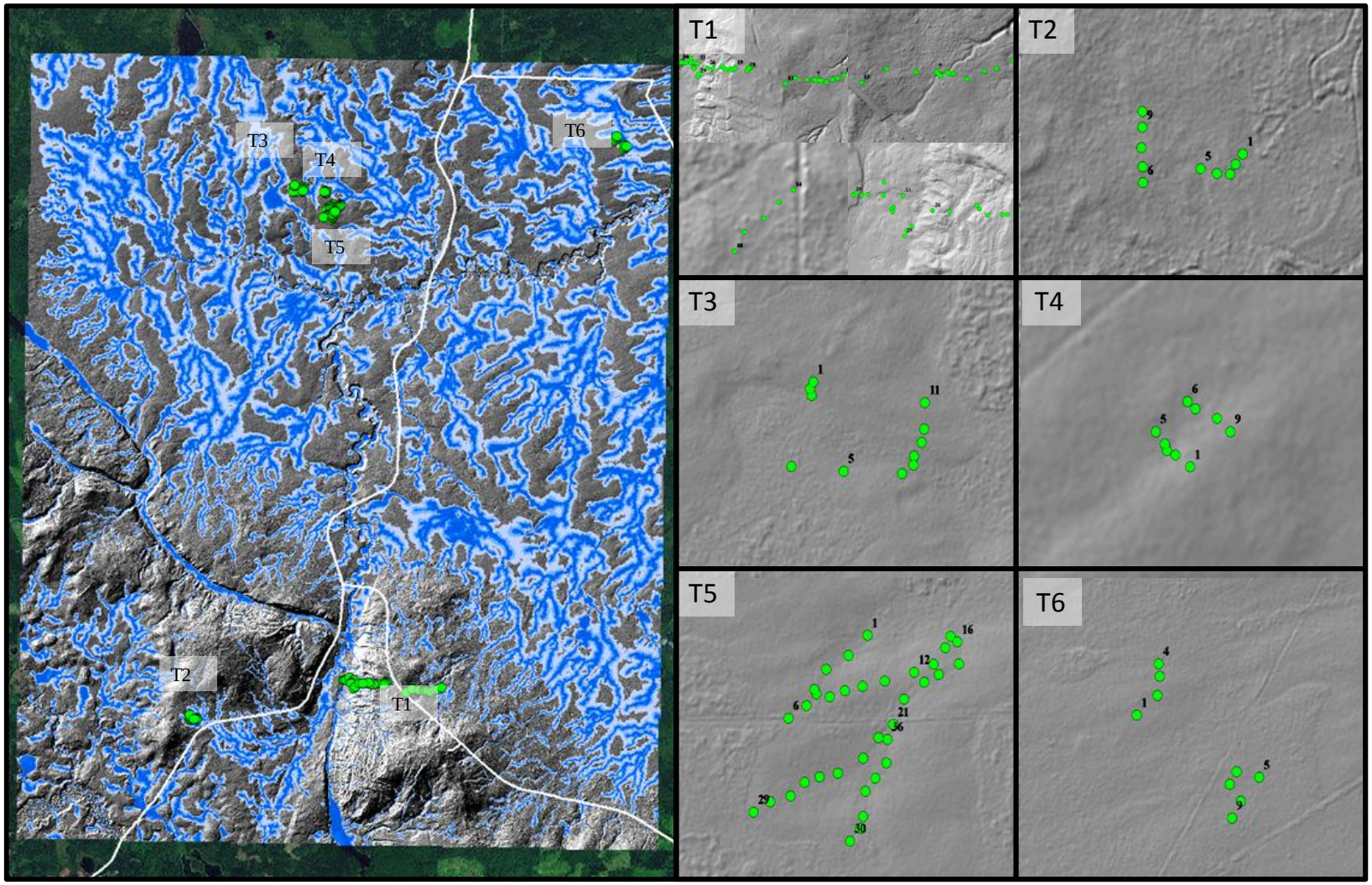

Figure 4.4. study area with the 0-1m depth-to-water index (dark to light blue, resp.) plus transect locations on hill-shaded DEM.

4.3.4 Soil analysis

The aggregated soil core samples were placed into plot-labelled freezer bags, kept cool during transport and dried at 75ºC for 24 hours. Soil aggregates were crushed and the resulting fine-earth fraction was separated from coarse materials through sieving (2 mm). The fractions, so separated, were weighed to estimate the coarse fragment content (CF) within each sample. The sedimentation method was used to determine the sand, silt, and clay proportions within each of the sieved samples (50g). Soil carbon (C) was determined using the LECO CNS-2000, using 500 mg portion of the sieved soil. Soil organic matter (OM) was estimated by setting OM = 1.7 * C. The gravimetric soil moisture (MC_g) was determined as part of the soil drying process. MC_g was then converted into volumetric soil moisture (MC_v) and water-filled pore space (MC_{PS}) based upon soil particle density (Dp), soil bulk density (Db) and pore space (PS) estimates as described in Chapter 2 (Vega, 2009, Balland *et al.*, 2008).

4.3.5 Data processing

The data so generated yield 500 rows of information. Data quality checking was done by examining the general correlation pattern among some of the primary variables referring to sand, silt, clay, OM, LOI, soil depth, CI, MC_g, MCv_{field}, CF. Where feasible, missing or erroneous data were substituted by way of multiple regression analysis. The resulting dataset was processed in several ways:

1. by determining and compiling the average soil properties for sand, silt, clay, OM, Db, Dp, PS, MC_g, MC_v and MC_{PS} for each aggregated soil sample, as specified in Chapter 2;
2. using the sample-generated sand and OM to infer the field values for (Db_{field}), Dp (Dp_{field}) and PS Db such that Balland et al. 2006):

$$Db_{field} = \frac{1.23 + (Dp - 1.23 - 0.75\,SAND)\,(1 - \exp(-0.0106\,DEPTH))}{1 + 6.83\,OM}, \quad [5]$$

$$1/Dp_{field} = OM/D_{om} + (1\text{-}OM)/D_{min}, \quad [6]$$

with D_{OM} = 1.3 g cm^3 and D_{min} = 2.65 g cm^3 are the particle densities of organic matter and mineral soil, respectively;

$$PS_{field} = 1\ Db_{field}/Dp_{field}, \quad [7]$$

and,

$$MCPS_{field} = MCv_{field} / PS_{field;} \quad [8]$$

3. by relating the CI values so obtained to Eq. 2 based on (a) the core-determined values for sand, silt and clay, PS, and MCPS, (b) the field estimated values pertaining to Db_{field}, PS_{field} and $MCPS_{field}$ and (c), soil depth;
4. by prorating CI_{max}, Db_{field}, PS_{field} and $MCPS_{field}$ to 10 cm soil depth and relating the values so generated to elevation, slope, and $\log_{10}$(DTW) for the 1m resolution mapping purpose.

The resulting relationships among CI and the CI-predictor variables were explored through step-wise multiple regression analysis (Statview 5.0, 1998). Potential ATV-specific rut depths (15 passes along the same track) were inferred from Eqs. 3 and 4 by setting W= ATV weight + load = 624 KN; b = 0.254m; d =0.62m; h = 0.33m; p =34.4 kPa. The number of vehicle passes was set at n = 10 as a benchmark.

4.3.6 CI and rut depth mapping and partial verification

CI and rut depth were mapped at 1m resolution for both study areas using the DEM-derived rasters for $\log_{10}$(DTW) and elevation, based on the regression-generated CI versus $\log_{10}$(DTW) and elevation calibration. A soil disturbance survey was done within the GRFLUZ in August, 2010. The 605 kilometers of trails throughout the GRFLUZ were classed into vehicle classes (Figure 4.5). Approximately 320 km of ATV dirt-bike trails and 55km of 4x4 trails were available for sampling. 10% of each trail type was selected and traveled with GPS tracking devices. A total of 40km of trails were sampled for soil disturbance, length of disturbance, and disturbance severity, disturbance severity assigned to 5 classes, using rut depth and extent of root exposure as primary severity indicators.

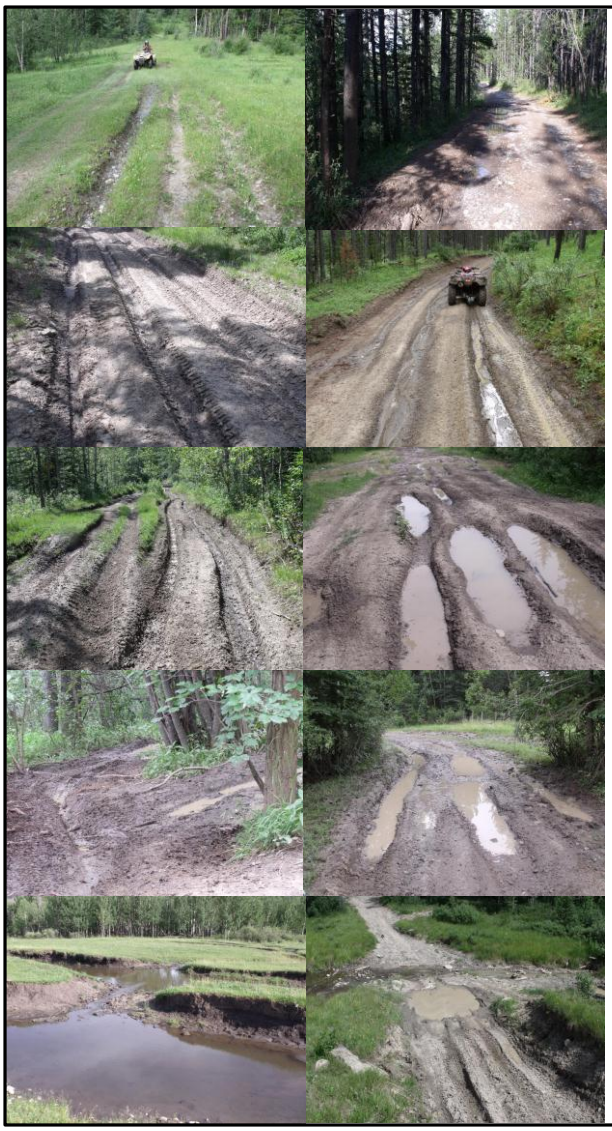

Severity Class	
1	Root Scuffing; small sediment loss; occasional puddling; little potential for further damage.
2	Single to double track rutting and water retention with occasional braiding; potential for further damage.
3	Triple track rutting with substantial water retention and frequent braiding; potential for further damage.
4	Multiple track rutting beyond intended trail corridor with substantial water retention and frequent braiding; sediment loss to nearby waterways substantial; potential for further damage.
5	Multiple track rutting with water course alterations and destabilization of stream banks and shorelines; frequent braiding; potential for further or continual damage substantial

Figure 4.5. Severity classes of trail damage rating, with examples.

4.4 Results and Discussion

Table 4.2 presents average minimum, maximum, and standard deviation values for each of the CI determining variables including CI, by study area (Table 4.1 shows units for all tables). The correlation coefficients among these variables are compiled in Table 4.3. The general relationship between CI and depth of soil penetration is shown in

Figure 4.6 (top), suggesting CI values above about 1.5 MPa approached CI_{max} asymptotically with increasing soil depth such that:

$$CI = C_{max} [1 - \exp (- 0.1 \text{ soil depth, cm})]. \quad [9]$$

In part, this trend could have been caused by sampler-specific physical constraints to penetrate compacted soils at constant velocity above CI ≈ 3 to 4 MPa. Using hydraulically driven penetrometers for these soils would likely generate higher, and perhaps non-asymptotic CI values, perhaps up to ≈ 8 MPa with increasing soil density, as reported by Domsch et al. (2006) using 30° cone tips (100 mm^2 base) for a glacial drift area with sandy deposits overlying boulder clay. Blouin et al. (2011) reported CI values up to 10 MPa using a 30° cone with a 4 mm base for wood landing sites on a sandy-skeletal glaciofluvial substrate, while CImax remained < 4 MPa using a cone penetrometer with 30° and 12.83 mm at base (ASAE standard). A similar asymptotic CI trend with increasing soil depth towards CI ≈ 3 MPa (ASAE) appeared in Sakai et al. (2008) for soils comprised of sandy surface deposits underlain by clay. Carter et al. (2007) reported linear CI increases with increasing soil depth up to CI ≈ 2.5 MPa ASAE on a pine flat with loamy soils with slow to moderate permeability on unconsolidated sand, clays and limestone.

Table 4.1. Overview of soil trafficability determining variables and units.

Variable	Units	Variable	Units
MCg	%	CF	%
MCPS	%	CI_{depth}	cm
Db	$g\ cm^{-3}$	CI_{max}	$kg\ m^{-2}$
Dp	$g\ cm^{-3}$	LFH depth	cm
PS	%	Soil depth	cm
MCv_{field}	%	DTW	m
PS_{field}	%	TWI	m
$MCPS_{field}$	%	Elevation	m
C	%	Slope	degree
Sand	%	RLM	dimensionless
Silt	%	Point X	decimal degree
Clay	%	Point Y	decimal degree

Table 4.2. Descriptive statistics summary for the soil trafficability determining variables within the GRFLUZ and EMEND study areas.

Variable	GRFLUZ						EMEND					
	Mean	Standard Error	Mode	Standard Deviation	Minimum	Maximum	Mean	Standard Error	Mode	Standard Deviation	Minimum	Maximum
MCg	108	11.1	520	175	14.3	522	18	0.5	14.5	8.6	1.4	60.3
MCPS	72	1.1	100	17.6	25.9	100	51.6	1.2	100	19.6	4.8	100
Db	1	0.02	1	0.3	0.16	1.5	1.35	0	1.4	0.2	0.8	1.9
Dp	2	0.03	2.5	0.5	1	2.6	2.47	0	2.5	0.1	1.8	2.6
PS	51	1.2	0	19	0	87.7	45.5	0.4	44.3	6.5	26.5	62.8
MCv_{field}	44	1.7	100	26.7	9.8	100	22.3	0.9	15.4	14.1	3.9	63
PS_{field}	65	1	100	14	50	100	60	0	60	10	50	80
$MCPS_{field}$	63	1.4	100	21.9	18.1	100	36.6	1.4	100	21.8	6.8	100
C	11	1.3	58.1	19.8	0.7	58.1	3.2	0.2	1.8	2.6	0.7	26.9
Sand	37	1.1	0	17.9	0	84.1	28.7	0.5	25.6	7.9	8.1	55
Silt	33	1	0	15.3	0	63.9	33.8	0.4	31	5.9	15.2	51.6
Clay	16	0.6	0	8.8	0	38	37.5	0.5	32.8	7.3	14.6	63.5
CF	10	1	0	12	0	56	40	0	40	20	0	70
CI_{depth}	3	0.8	0	12	0	50	31.5	0.7	25	10.7	15.0	50
CI_{max}	10	0.4	0	6.9	0	31	17.8	0.6	2	9.5	2.0	35
LFH depth	10	1	0	16.3	0	100	12.7	0.6	9	9.6	3.0	81
Soil depth	21	0.9	0	14.1	0	100	17.2	0.3	17.5	4	0	23.8
DTW	7	0.8	0	12.3	0	73.1	1.9	0.2	0.2	2.5	0	16.2
Elevation	1532	6.5	1569	102	1360	1758	747	2.6	713	42	684	822
Slope	9	0.4	3	6.7	0	32.3	3.9	0.3	2.0	4.5	0.1	25.7
RLM	1	0.1	0.9	1.0	0.2	7.4	1.3	0.1	0.8	1	0.3	5

Table 4.3. Descriptive statistics summary for the soil trafficability determining variables within the GRFLUZ and EMEND study areas.

Variable	MCg	Db	MCv_{field}	C	Sand	Clay	CF	CI Max	LFH	$\log_{10}$ DTW	Elevation	Slope	$\log_{10}$ Soil depth	$\log_{10}$ CI Depth	$\log_{10}$ RLM
MCg	1														
Db	-0.86	1													
MCv_{field}	0.83	-0.73	1												
C	0.99	-0.89	0.84	1											
Sand	-0.67	0.48	-0.56	-0.60	1										
Clay	-0.78	0.68	-0.58	-0.79	0.20	1									
CF	-0.52	0.52	-0.40	-0.49	0.39	0.50	1								
CI Max	-0.43	0.48	-0.75	-0.46	0.32	0.18	0.22	1							
LFH depth	0.79	-0.65	0.79	0.78	-0.54	-0.60	-0.43	-0.49	1						
$\log_{10}$ DTW	-0.27	0.25	-0.44	-0.27	0.28	0.14	0.31	0.51	-0.18	1					
Elevation	0.97	-0.84	0.80	0.96	-0.62	-0.73	-0.43	-0.41	0.76	-0.23	1				
Slope	0.04	-0.16	0.00	0.06	0.04	0.08	0.20	-0.08	0.03	0.36	0.10	1			
$\log_{10}$ Soil depth	0.32	-0.21	0.26	0.30	-0.24	-0.26	-0.16	-0.12	0.38	-0.05	0.28	0.06	1		
$\log_{10}$ CI depth	0.41	-0.46	0.71	0.44	-0.30	-0.21	-0.23	-0.87	0.49	-0.52	0.39	0.02	0.10	1	
$\log_{10}$ RLM	0.08	-0.21	0.19	0.12	0.02	0.06	0.18	-0.2	0.14	0.18	0.17	0.62	0.1	0.18	1

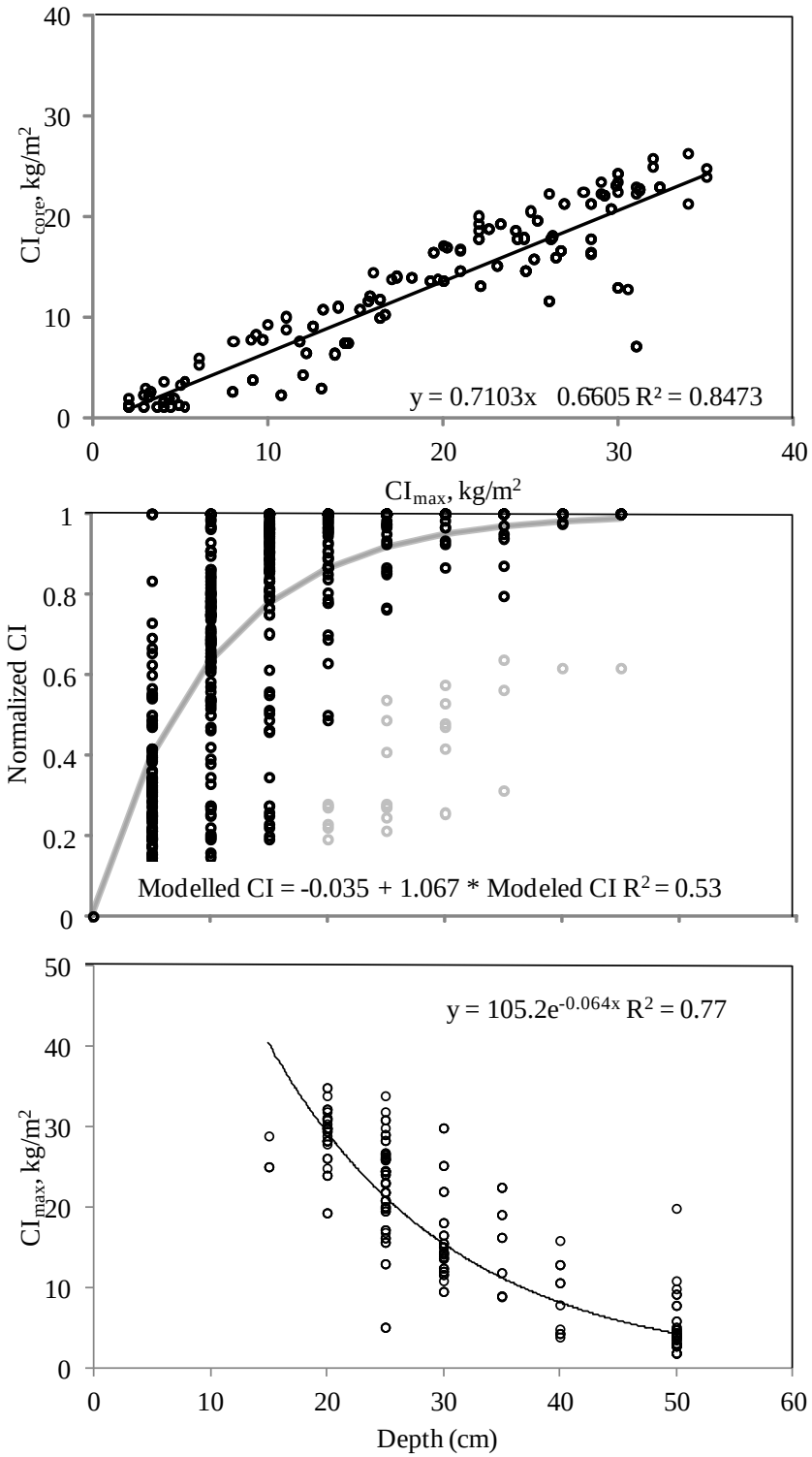

Figure 4.6. Top: Relating the CI of the depth of soil core sample to the CI at maximum penetration depth, with best-fitted model. Middle: Scatter plot and best-fitted model showing CI/CImax against soil depth. Bottom: Scatter plot of CImax versus maximum soil penetration depth, with best-fitted model.

Checking the resulting field-measured CI_{max} against CI(Eq. 2) led to the following result across both study areas:

$$\log_{10}CI_{max} = -0.251(\pm 0.018) + 0.88(\pm 0.04)\ \log_{10}CI \text{ (Eq. 2);}$$
$$R^2 = 0.56;\ RMSE = 0.22;$$
[10]

with the CI predictor variables, namely sand, OM, pore space and MCPS, determined as follows:

1. sand and OM content determined from the soil core samples,
2. Db_{field}, PS_{field} and $MCPS_{field}$ inferred using Eqs 3 to 6, and
3. MCv_{field} as the field-based TDR soil moisture measurements.

The best-fitted scatter plot in Figure 4.7 shows that CI (Eq.2) conforms to the field-determined CI_{max} values quite well, but with a slight bias towards over-prediction. This is likely due to two reasons: (i) the manually produced CI data level off as soil resistance to penetration increases with increasing soil depth (Eq. 9), and (ii) the original, formulation of Eq.2 summarized CI trends across several studies after removing inter-study biases (Vega et al. 2009) presumably due to, e.g., cone angle, size, penetration velocity, extent of soil cementation, etc..

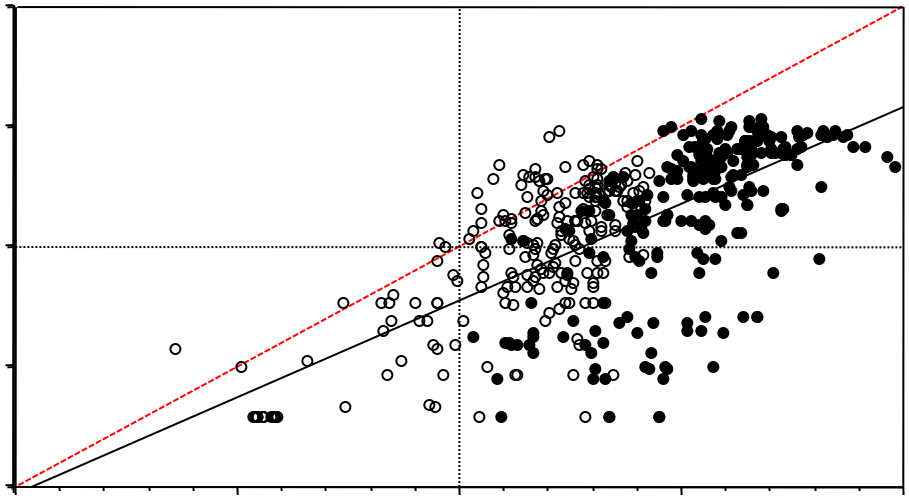

Figure 4.7. Comparing log10CI values predicted from Vega et al. 2009 (Eq. 2) with the field-generated log10 CI data generated for EMEND and the Ghost area.

Checking the Eq. 5 formulation for Db using the core-determined Db values as dependent variables produced the following best-fitted result:

$$Db = 0.25(\pm 0.04) + 1.00(\pm 0.04)\ Db \text{ (Eq. 5)};$$
$$R^2 = 0.62;\ RMSE = 0.18\ g\ cm^{-3}.$$
[11]

In comparison, re-calibrating Db with the core-determined texture, C, and CF values generated:

$$Db = 1.25(\pm 0.02) + 0.003(\pm 0.001)\ Clay - 0.058(\pm 0.003)\ C + 0.36(\pm 0.04)\ CF;$$
$$R^2 = 0.65;\ RMSE = 0.12\ g\ cm^{-3}.$$
[12]

Regressing $MCPS_{field}$ against $\log_{10}(DTW)$ and study area (A) or elevation (B) also produced fairly good regression results, with the soils within the Ghost area generally

being moister than within the EMEND area due to wetter versus drier weather conditions during the Ghost than the EMEND field sampling periods (Figure 4.8 a,b):

$$MCPS_{field} = 62.3(\pm1.1) - 13.7(\pm0.9)\ \log_{10}(DTW) - 28.9(\pm1.5)\ Study\_area;$$
$$R^2 = 0.57;\ RMSE = 16.4\%$$
[13]

$$MCPS_{field} = 7.5(\pm2.3) - 14.0(\pm0.9)\ \log_{10}(DTW) + 0.036(\pm0.002)\ Elev.;$$
$$R^2 = 0.55;\ RMSE = 16.9\%$$
[14]

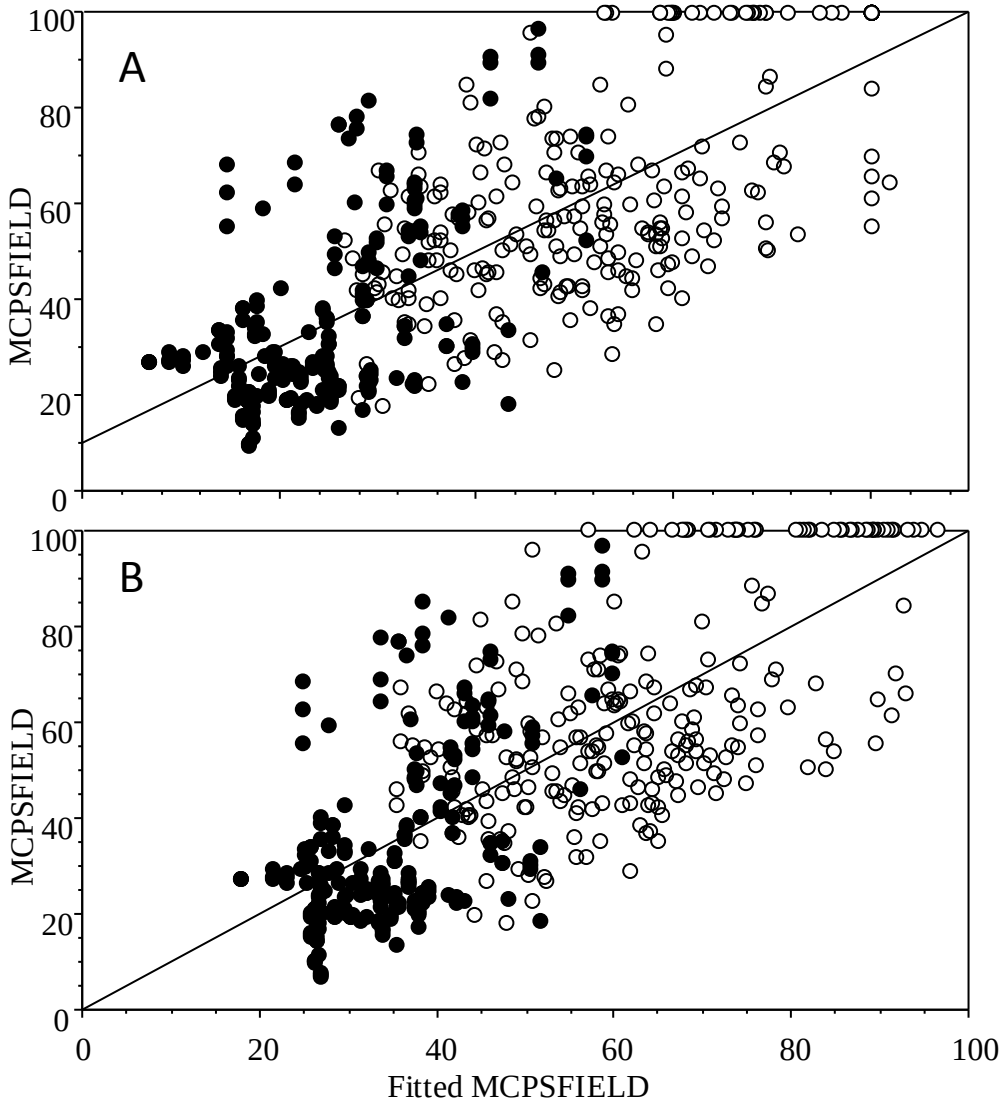

Figure 4.8. Best-fitted scatter plots generated by regressing field-generated MCPSfield values against plot-specific log10DTW and location (A) or elevation (B).

Recalibrating CI(Eq.2) with the field-determined values of the CI predictor variables, namely, Sand, Clay, OM, PS_{field}, and $MCPS_{field}$, improved the best-fitted regression result as follows:

$$\log_{10}CI_{max} = 1.09(\pm0.07) - 1.03(\pm0.11)\ PS - 0.90(\pm0.0003)\ MCPS;$$
$$R^2=0.69;\ RMSE= 19\%.$$
[15]

With this calibration, sand and/or clay and OM (or organic C) content did not enter as additional CI-determining regression variables. However, soil texture and OM do affect CI via Db, Dp, PS and MCPS, according to Eqs. 5 to 8 (Balland et al. 2008). Note that the best-fitted R^2 value for Eq. 15 (R^2 =0.69) is somewhat lower than the corresponding values for Eqs. 1 and 2 (R^2 = 0.77 and 0.85, respectively). This is mainly due to the more limited range of the manually derived CI values, i.e., ≤ 3 (Eq. 9) versus ≤ 7 MPa.

Checking how prorated CI_{max} (CI @ 10cm soil depth) can be mapped according to DEM-derived soil attributes produced fairly good regression results with $\log_{10}$(DTW) and with an additional improvement obtained using elevation or study area (Ghost = 0, EMEND = 1):

$$\log_{10}CI_{10cm\ depth} = 0.27(\pm0.04) + 0.283(\pm0.011)\ \log_{10}DTW - 0.00041(\pm0.00003)\ Elev;$$
$$R^2=0.47;\ RMSE=0.27.$$
[16]

Using the field-determined $MCPS_{field}$ values strongly improved the overall correspondence between the mapped and the plot-specific CI determinations even further (Figure 4.9):

$$\log_{10}CI_{10cm\ depth} = 0.36(\pm0.02) + 0.133(\pm0.012)\ \log_{10}DTW - 1.05(\pm0.004)\ MCPS_{field};$$

$$R^2=0.66;\ RMSE=0.21.$$

[17]

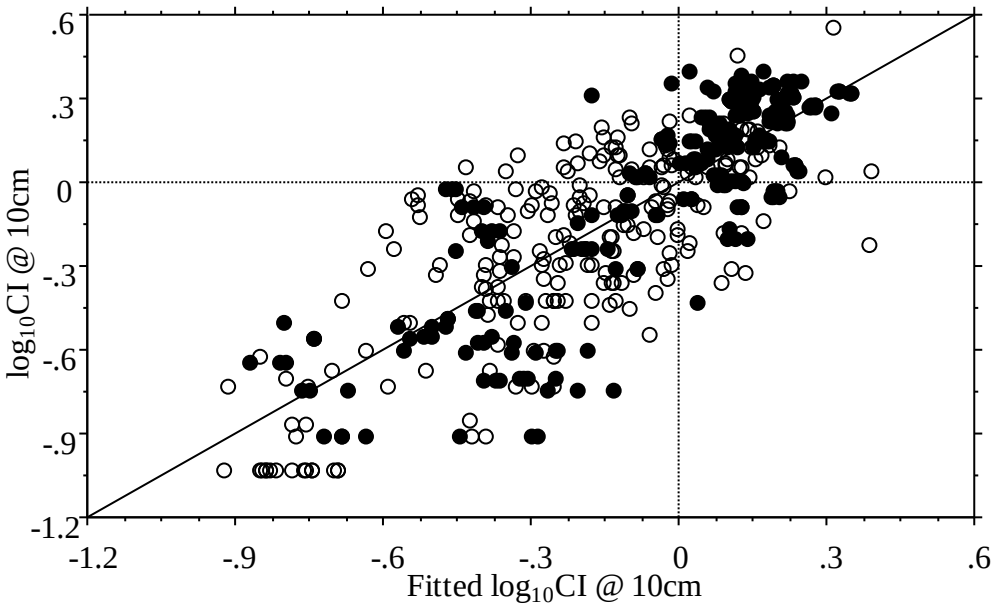

Figure 4.9. Best-fitted scatter plot obtained by regressing CI against field-generated MCPS values and plot-specific log10 DTW values.

Using Eq. 16 produced the GRFLUZ and EMEND CI maps in Figures 4.10 - 4.11, with transect-focused close-ups for a visual comparison between the plot-determined and the map-generated values. While there is general agreement between plot-averaged and mapped values, differences also occur. These differences likely stem from as yet unmapped details regarding local variations pertaining to DTW, soil density, moisture, texture, and organic matter and coarse fragment content. For example, some of the upper

reaches of the flow channels with the 4ha flow initiation areas were found to be dry, thereby suggesting higher DTW values than mapped. These variations occur on account of (i) local variations soil and substrate permeability, and (ii) the weather-dependent extent of water supply from higher elevations. The latter is in part influenced by the extent of vegetation cover, related evapo-transpirational water losses, and upslope soil disturbances including soil compaction leading to faster run-off following precipitation events, and lower soil percolation rates thereafter (Rab et al. 2005; Foltz 2006). Some of these complications can be accommodated to some extent by calibrating Eq. 16 with hydrologically derived soil moisture levels, as outlined by Vega et al. (2009).

Figures 4.10 and 4.11 also show the potential ATV rutting depth based on Eqs. 3 and 4. The survey of the extent of rutting damage along the 40 km trail segments in Figure 4.12 produced a general correspondence between the locations of trail damage by severity class and eq. 16 generated rut-depth projections. Re-mapping the rutting potential with DTW referenced to the local flow channel network with 2 and 0.5 ha flow initiation captured most of the rut locations that were not captured with the 4 ha flow initiation (Figure 4.13). Not surprisingly, the damage was most severe where the soil is soft, mapped CI < 4; mapped rut depth >0.5m; DTW < 2m), less severe on somewhat more elevated ground locations further away from the stream channels (low to intermediate CI and rut depths), and least severe to generally absent on well-drained ground (CI > 20 ; rut depth < 0.2m; DTW > 7m; Figure 4.14).

The $\log_{10}$DTW-based modeling and mapping protocol therefore provides a planning tool for directing or re-locating trails away from areas that would otherwise incur

considerable traffic-induced damage to soils and waterways. Note that rut-induced damage along designated trails would exceed multiple rut-depth predictions due to (i) reduced drainage across tracks, (ii) mud-producing water retention within deepening ruts, (iii) softening of the ground adjacent to tacks, (iv) trail braiding, (v) washouts along trail–crossing seepage flows, (vi) formation of gulleys, and (vii) substantial down-slope sediment transfers and general flow-channel alterations (Bauer 2003; Bruehler and Sondergaard 2004; Marion and Olive 2006; Riedel 2006;).

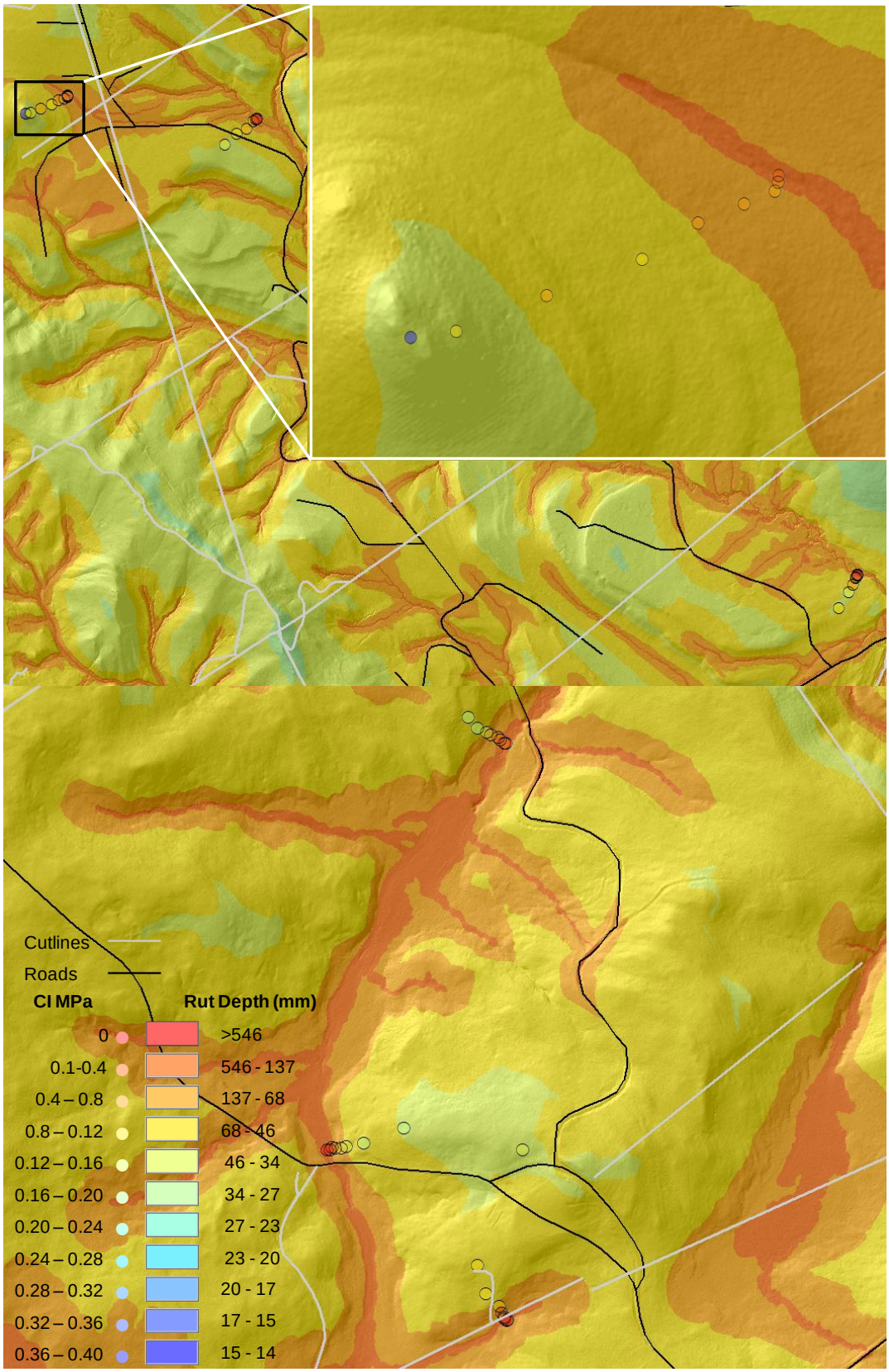

Figure 4.10. Map depicting field-generated and mapped CI at 10 cm depth (Eq. 16), and predicted ATV rut depths (Eq. 3) for two sections of the GRFLUZ study area.

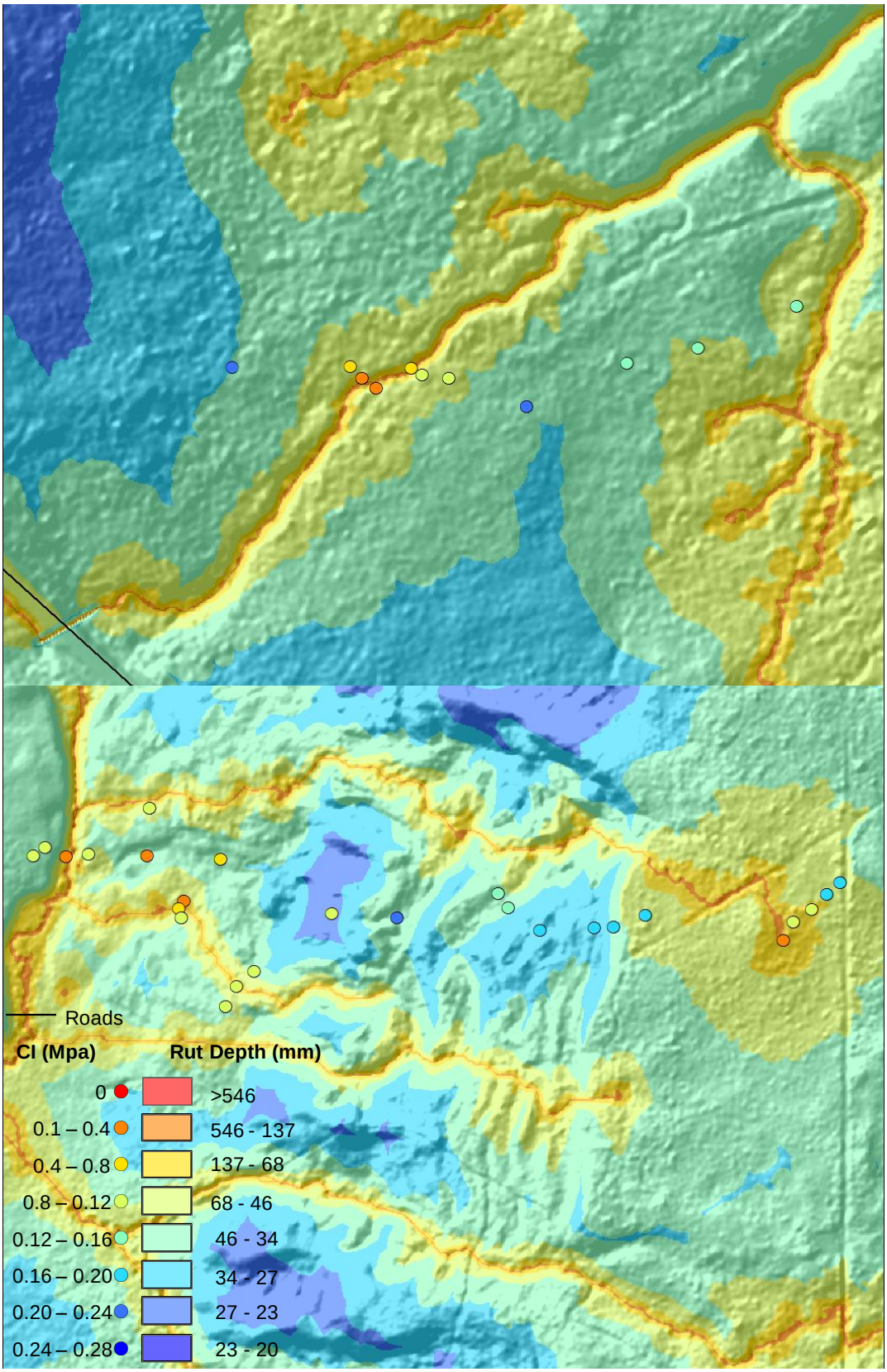

Figure 4.11. Map depicting field-generated and mapped CI at 10 cm depth (Eq. 16), and predicted ATV rut depths (Eq. 3) for two sections of the EMEND study area.

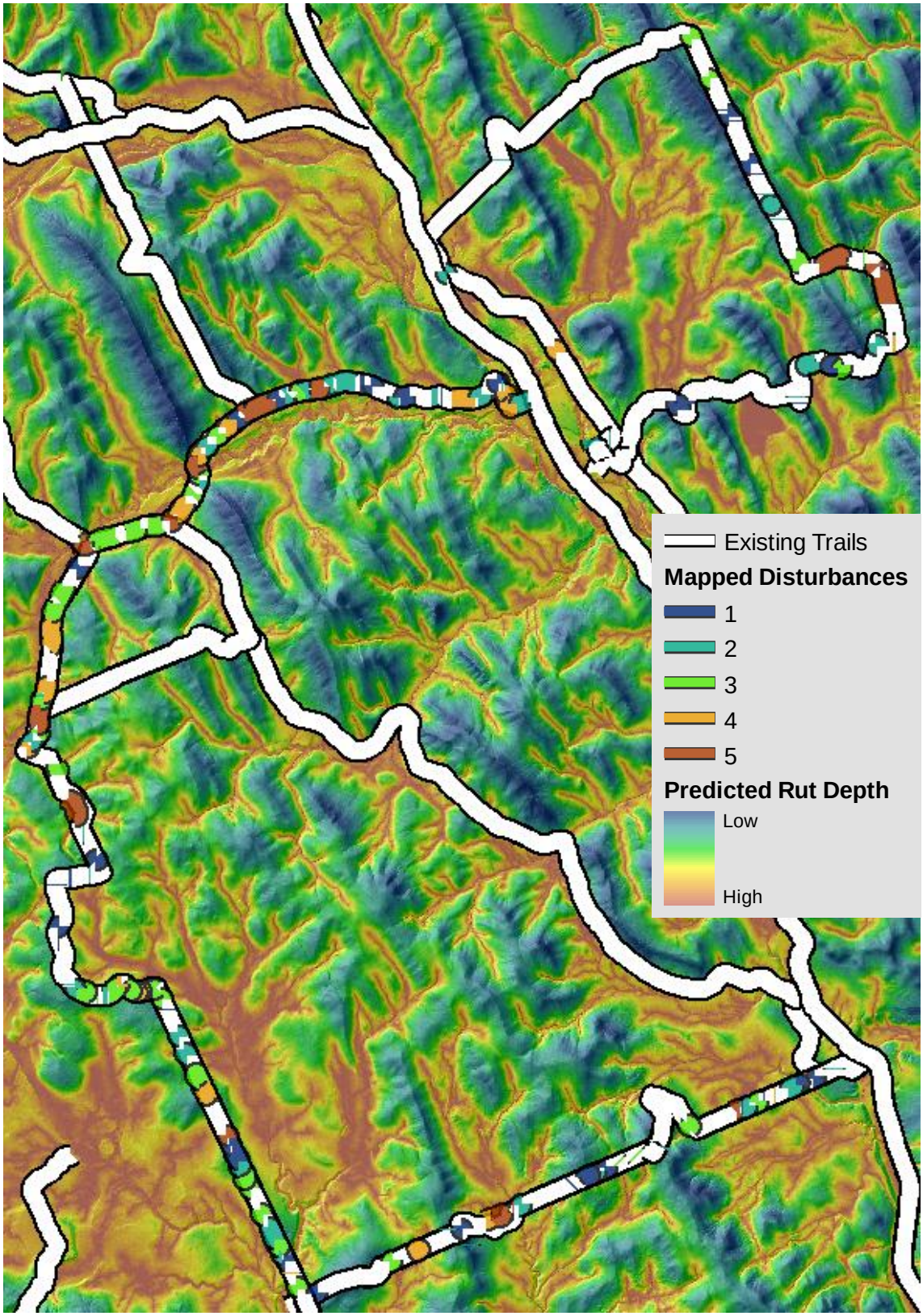

Figure 4.12. Trail damage survey along select trail segments (40 km) within the GRFLUZ study area, overlaid on CI-generated rut-depth map.

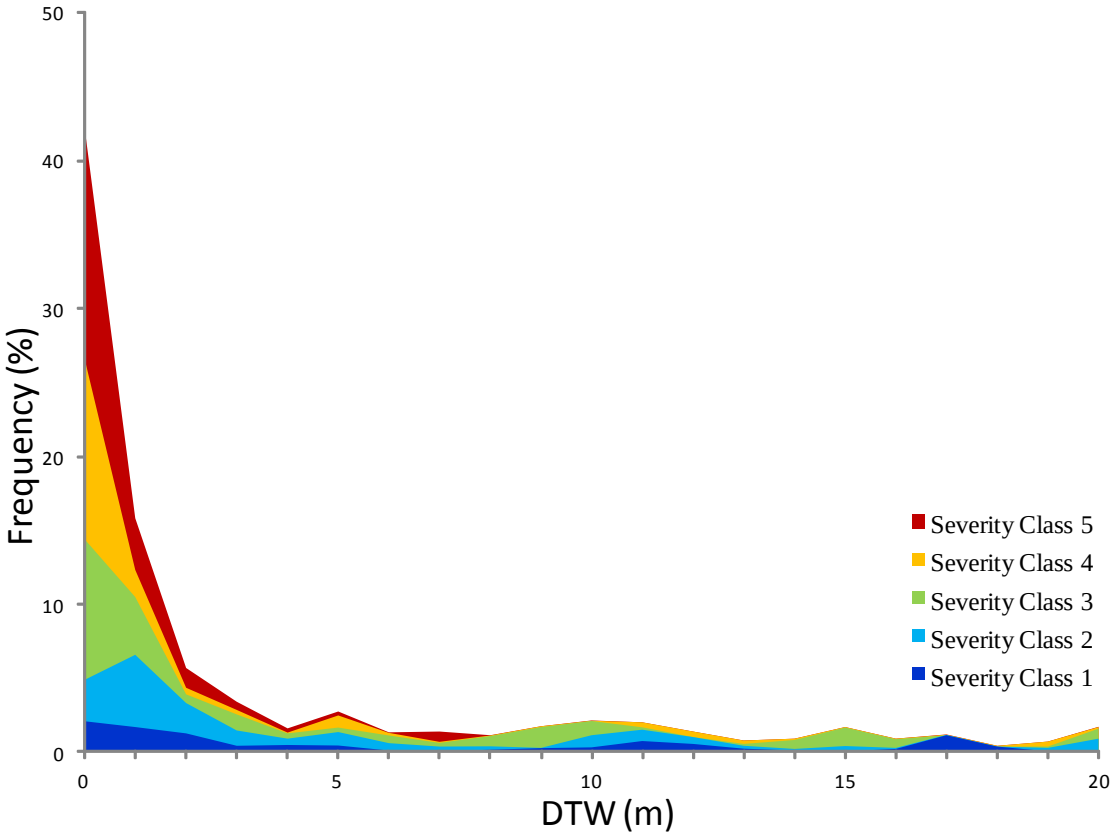

Figure 4.13. Frequency plot of the trail damage severity classes for the trail damage survey versus the cartographic depth-to-water index associated with the DEM-derived flow channel network (4 ha flow initiation threshold).

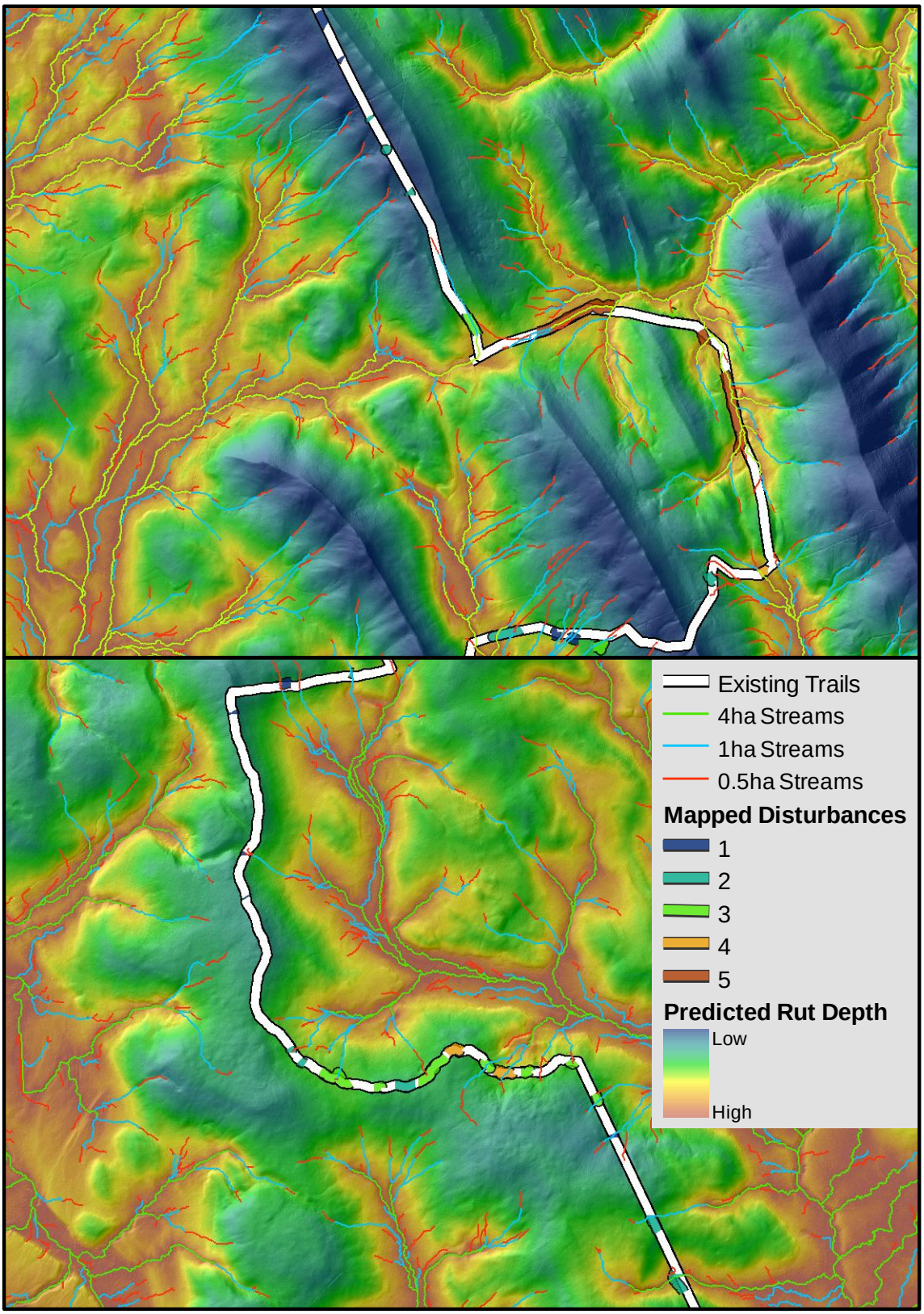

Figure 4.14. Two close-ups of the trail damage survey with the study area, with predicted rut depth and flow channel network using 4, 1 and 0,5 ha for flow initiation, cut offs to 2ha and 0.1ha.

In reference to the WES method and related elaborations (Rab et al 2005; Priddy and Willoughby 2006), the above CI and rut-depth formulation presents a practical, albeit much simplified approach to model and map soil resistance to mechanical disturbances. The role of the DTW index as dominant indicator of soil strength is perhaps not surprising, because DTW itself, i.e., the distance between the soil surface and the surface-influenced level of the water table below the soil surface, not only allows for the direct mapping of soil moisture content, but also for the mapping of soil, vegetation and drainage type as well as other soil properties such as texture, density and organic matter content (Murphy et al. 2009, 2011). For practical consideration, coarse fragments and soil frost effects should also be part of the CI and rut depth calculation. For that purpose, Vega et al. (2009) suggest to use $(1\text{-}CF)^2$ and $1/\max[0, (1- 0.81\ FD^2/W)]$ as CI and rut depth multipliers, respectively. Normally, small CF values representing gravel-like particle embedded in otherwise fine earth do not strongly affect CI as the penetrometer pushes these fragments to the side. With increasing coarse particle size, however, CI readings become erratic and are limited to the distance above the solidly embedded fragments. In total, increasing coarse fragment content and soil frost translate into greater resistance to soil penetration, and - hence – lower rutting depths.

Since considerable attention has been given to the monitoring of extent and recovery of soil from machine-induced disturbances and soil compaction in particular (USDA 2009; Miller et al. 2010), one can convert the CI-based rut-depth projections to estimate the extent of soil compaction and subsequent moisture content within the rut-impacted soil as follows:

$$PS_n = 1 – Db/Dp – Z_n/h_{soil;} \quad [18]$$

$MCPS_n = \min(1, MCPS, PS/PS_n)$; [19]

where Db, PS, MCPS and h_{soil} refer, respectively, to pre-rut soil bulk density, pore space, water-filled portion of the pore space, and depth of compactable soil (mm; Vega et al. 2009). In turn, the estimates for PS_n and $MCPS_n$ can then be used to determine the resulting changes in CI, Db, PS, and MCPS of the soil within the ruts.

4.5 Conclusions

The results of this study suggest that Eq.2 or its re-calibration (Eq. 15) quantify the functional dependency of CI on soil texture, density and moisture content quite well (R^2 about 70%). This particular result should be useful for generating thematically CI and potential rut depth interpretations by soil type, using soil texture, density and moisture content as CI and machine-specific rut-depth predictors for each soil type. Mapping CI and rut depths in topographic detail, however, requires relating the CI predictor variables to topographic position, and this can, in principle, be done by relating the CI determining predictor variables (i.e., soil texture, density and moisture content) to the DEM-derived elevation, slope, and $\log_{10}$DTW variables, as demonstrated. In detail, the results obtained suggest that CI can be mapped across the landscapes of at least two very contrasting areas at 1m resolution with an R^2 level of about 50% based on DEM-generated $\log_{10}$DTW and elevation rasters, and this can be further improved to at least 66% by using locally measured and weather-dependent soil moisture values for soil trafficability mapping during summer conditions. However, further work is required to forecast how soil moisture conditions vary across the landscape with daily weather. Checking the soil disturbance conditions along 40 km ATV trail segments within the Ghost area produced

a general conformance pattern between the field-rated soil disturbance severity classes and the corresponding DEM-derived rut-depth projections.

4.6 Acknowledgements

We are grateful to the Alberta Sustainable Resource Development's Forestry and Land's Divisions for financial and in-kind support. We are also thankful for interest and data support from the Ghost-Waiparous Stewardship Committee and EMEND research partners notably at DMI and the University of Alberta. This soil trafficability research was also supported by an NSERC-supported Industry-University Cooperative Research Partnership (CRD) project.

4.7 References

Agodzo, S., Adama, I. 2003. Bulk density, cone index and water content relations for some Ghanian soils. In: Gabriels, D.M. et al. (Eds.). ICTP Lecture Notes Series. Volume XVIII.

Balland, V., Pollacco, J., Arp, P..2008. Modeling soil hydraulic properties for a wide range of soil conditions. *Ecol Model 219, pp. 300-316.*

Bauer, p. 2003. Rutted and ruined: ATV damage on the Adirondack Forest Preserve. Published by: The Residents' Committee to Protect the Adirondacks, North Creek, New York. http://glorietamesa.org/ATVreport.pdf.

Blouin, V. M., Schmidt, M. G., Bulmer, C. E., Krzic, M. 2005. Mechanical disturbance impacts on soil properties and lodgepole pine growth in British Columbia's central interior. Can. J. Soil Sci. 85, pp. 681–691.

Bruehler, G., Sondergaard, M. 2004. GIS/GPS Trail Condition Inventories: A Virtual Toolbox for Trail Managers. U.S. Department of Interior, Bureau of Land Management Glennallen District, Alaska. Technical Report. UC Proceedings Abstract. http://proceedings.esri.com/library/userconf/proc04/docs/pap1590.pdf.

Carter, E., McDonald, T., Torbert, J. 2000. Assessment of soil strength variability in a harvested loblolly pine plantation in the Piedmont region of Alabama, United States New Zealand J. For. Sci. 30, pp. 237-249.

Carter, E.A., Aust, W.M., Burger, J.A. 2007. Soil strength response of select soil disturbance classes on a wet pine flat in South Carolina. For. Ecol. Managem.247, pp. 131–139.

Domsch, H., Ehlert, A., Giebel, K., Boess, J. 2006. Evaluation of the soil penetration resistance along a transect to determine the loosening depth. Precision Agric. 7, pp 309-326.

Duckert, D., Morris, D., Deugo, D., Duckett, S., McPherson, S.. 2008. Developing site disturbance standards in Ontario: Linking science to forest policy within an adaptive management framework. Can J Soil Sci 89, pp. 13-26.

Foltz, R.B. 2006. Erosion from All Terrain Vehicle (ATV) trails on national forest lands. USDA Forest Service, Rocky Mountain Research Station, Moscow, ID. ASABE Annual International Meeting, Portland, Oregon. http://forest.moscowfsl.wsu.edu/cgi-bin/engr/library/searchpub.pl?pub=2006e.

Grenier, J. 2008. Geosynthetics for trails in wet areas: 2008 Edition. United States Department of Agriculture Forest Service Technology & Development Program. 2300–Recreation 0823–2813–MTDC. http://atfiles.org/files/pdf/ohvbibliogVT00.pdf

Horn, 2004. Time dependence of soil mechanical properties and pore functions for arable soils. Soil Sci Soc Am J 68, pp. 1131–1137.

Landsberg, J., Miller, R., Anderson, H., Tepp, J.. 2003. Bulk density and sol resistance to penetration as affected by commercial thinning in north eastern Washington. Res. Pap. PNW-RP-551, USDA Forest Service, Pacific Northwest Research Station. 35 pp.

Marion, J. L., Olive, N. 2006. Assessing and understanding trail degradation: Results from Big South Fork National River and Recreational Area. United States Department of the Interior. U.S. Geological Survey. Patuxent Wildlife Research Center. Virginia Tech Field Unit. National Park Service. Final Research Report. 80 pp. http://www.imba.org.uk/uploads/papers/marion_nps_report.pdf.

McNabb, D., Campbell, R. 1985. Quantifying the impacts of forestry activities on soil productivity. In Foresters' future: leaders or followers? Proceeding, 1985 SAF National convention, Fort Collins, Colorado.

Miller, R.E., McIver, J. D. Howes, S.W., Gaeuman, W.B. 2010. Assessment of soil disturbance in forests of the Interior Columbia River Basin: a Critique. United States Department of Agriculture Forest Service. Pacific Northwest Research Station. General Technical Report PNW-GTR-811.
http://www.fs.fed.us/pnw/pubs/pnw_gtr811.pdf

Murphy, P., Ogilvie, J., Arp, P. 2009.. Topographic modeling of soil moisture conditions: a comparison and verification of two models. *European Journal of Soil Science. 60, 94-109.*

Murphy, P., Ogilvie, J., Meng, F., White, B., Bhatti, J., Arp, P.. 2011. Modeling and mapping topographic variations in forest soils at high resolution: A case study. Ecol. Model 222, pp 2314-2332.

Naghdi, R., I. Bagheri, I., Lotfalian, M., Setodeh, B. 2009. Rutting and soil displacement caused by 450C Timber Jack wheeled skidder (Asalem forest northern Iran). J. Forest Sci. 55, pp. 177–183.

Nearing, M., West, L. 1988. Soil strength indices as indicators of consolidation. Trans ASAE 31, pp. 471-476.

Priddy, J.D., Willoughby, W.E. 2006. Clarification of vehicle cone index with reference to mean maximum pressure. J. Terramechanics 43, pp. 85–96

Rab, M.A, Bradshaw, F.J., Campbell, R.G., and Murphy, S. (2005). Review of factors affecting disturbance, compaction and trafficability of soils with particular reference to timber harvesting in the forests of south-west Western Australia, Consultants Report to Department of Conservation and Land Management, Western Australia, Sustainable Forest Management Series, SFM Technical Report No. 2, 146 pp. http://books.google.ca/books/about/Review_of_factors_affecting_disturbance.html?id=XJAwNAAACAAJ&redir_esc=y

Raper, R.L. 2005. Agricultural traffic impacts on soil. J. Terramechanics 42, pp. 259–280.

Riedel, M.S. 2006. Quantifying trail erosion and stream sedimentation with sediment tracers. In Fowler, D.L. (ed.), Second interagency conference on research in the wetlands. USDA Forest Service, Southern Research Station, Coweeta Hydrologic Laboratory, Otto, NC. pp. 133-142.

http://www.srs.fs.usda.gov/pubs/ja/ja_riedel001.pdf

Rooney, T.. 2008. Distribution of ecologically invasive plants along off road vehicle trails in the Chequeamegon national forest, Wisconsin. The Michigan Botanist. 44, pp. 178.

Saarilahti, M.. 2002. Ecomodel. In: Haarlaa R, Salo J, editors. ECOWOOD studies made at the University of Helsinki. University of Helsinki, Faculty of Agriculture and Forestry, Department of Forest Resource Management. Publication 31, February 2003; 2002. Available from: http://ethesis.helsinki.fi/julkaisut/maa/mvaro/publications/31/programs/ecomodel.exe

Saarilahti, M., Anttila, T.. 1999. Rut depth model for timber transport on moraine soils. Proceedings of the 9th International Conference of International Society for Terrain-Vehicle Systems, 14 -17. Sept. 1999, Munich, Germany.

Stokowski, P.A., LaPointe, B. 2000. Environmental and social effects of ATVs and ORVs: An annotated bibliography and research assessment. School of Natural Resources, University of Vermont, Burlington. http://www.forestwatch.org/content.php?id=125.

Vega-Nieva, D.J., Murphy, P.N.,C., Castonguay, M., Ogilvie, J., Arp, P.A. 2009. A modular terrain model for daily variations in machine-specific forest soil trafficability. Can. J. Soil Sci. 89, pp. 93-109.

Wilson, J.P., Seney, J.P. 1994. Erosional impact of hikers, horses, motorcycles, and off-road bicycles on mountain trails in Montana. International Mountain Society. Mountain Research and Development 14, 77-88. URL: http://www.jstor.org/stable/3673739. Accessed: 05/11/2009 16:42

Wronski, E. B., Stodart, D., Humphreys, N.. 1990. Trafficability assessment as an aid to planning logging operations. Appita J. 43, pp. 18-22.

Zenner, E.K. Fauskee, J.T., Berger, A.L., Puettmann K.J. 2007. Impacts of Skidding Traffic Intensity on Soil Disturbance, Soil Recovery, and Aspen Regeneration in North Central Minnesota. North. J. Appl. For. 24.

Chapter 5 : Trail Routing, Analysis, Investigation, and Layout (Trail)

5.1 Abstract

This article informs about an integrative GIS-based process to delineate and evaluate trail and road routing through already accessed or non-accessed terrain, with the purpose of avoiding hydrological trouble spots, minimizing trail construction costs and reducing ecological damage due to recreational and industrial use. This process enables Trail Routing, Analysis, and Investigative Layout (TRAIL) on the ESRI ArcMap platform. The process requires:

- uploading the data layers needed for the route-layout and evaluation purpose, e.g., local digital elevation model (DEM), DEM-derived slope and wet-areas map (WAM) with its cartographic depth-to-water layer (DTW), areas available and not available for trail routing;
- setting of risk tolerances pertaining to, and among others, crossing stream channels, wet areas, rugged terrain, steep slopes;
- selecting the beginning and end locations for the proposed route(s), and;
- analyzing alternative route options as proposed or derived through least-cost path analyses (LCP).

TRAIL, primarily intended to address trail proliferation due to off-highway vehicles (OHVs), provides a platform for delineating and evaluating hydrologically and ecologically sensitive yet cost-effective routes for recreational as well as industrial use. This is demonstrated for two case studies in Alberta: one area east of Calgary (recreation) and one area north of Peace River (forest access).

5.2 Introduction

Off-highway vehicles (OHV; Jeeps, Land Rovers, 4x4's, all-terrain vehicles (ATV's) etc.) sales have increased on average 26% per year since 1990, from an original 38,000 registrations to 138,000 in 2009 in Alberta. In 1990, 1.5% of the population owned OHVs. In 2010, that number increased to 3.6%. Assuming that this increase is correlated with Alberta's population growth (an average increase of 2.2% per year since 1990; lowest increase =1.4%), new OHV registrations would then increase to 0.5-1.6 million over the next 40 years. While this prospect is attractive in terms of stimulating local economies, there is concern that this increased traffic will further increase OHV-caused damage on forested and non-forested lands (Wilshire *et al.* 1978; Rooney 2008; Buckley 2004; Eckert *et al.* 1979; Slaughter *et al.* 1990; Weaver *et al.* 1978; Forman *et al.* 1998; Webb *et al.* 1983). OHV-caused damage refers to: un-controlled trail proliferation; forest fire initiation; water and air pollution; all-season disturbances of noise-sensitive birds and animals; alteration and destruction of streams, surface waters and wet/sensitive habitats; vegetation loss; the spreading of invasive species; soil scuffing, rutting and compaction; water- and wind-induced soil erosion and slope destabilization. All of these disturbances are affected by: vegetation cover (forests, grasslands, transitional, bare); topography (slope, slope length, aspect, ridge, valley); soil type (loose to compact, fine to coarse; covered to bare, shallow to deep) and drainage (dry to wet) .

Currently, OHV route planning is facilitated by the availability of existing maps showing the locations of linear features (roads, trails, seismic lines, etc.), lakes, streams, wetlands, ownership, land-use and recreational opportunities, and topography (elevation

contours, digital elevation models or DEMs). Integrating and weighing this information towards least-cost route locations while minimizing traffic-induced damage to soils and habitats, however, is difficult. In general, trail and road planning and building involves least-costing based on a variety of user preferences such as: (i) extending the "time-in-the-saddle", (ii) enhancing the connectivity between points of interest, (iii) ensuring trail stability and ecological viability to prevent trail washouts, rutting, and braiding, (iv) varying recreational trail-challenge from low to high, and (v) adding trail supporting infrastructure such as camps and resting places.

This article introduces the TRAIL platform, designed to facilitate:

1. the compilation of the data layers deemed essential for specific trail developments; these layers inform about the local distribution of flow channels, wet areas, slope and terrain conditions, forest cover, points of interest, sensitive habitats, land management objectives, and land dispositions;
2. the specification of the control points along the desired trail locations, i.e., the beginning, end and desired stops along the trails;
3. the delineation of alternative trail routes, with each route generated through least-cost path analyses (LCP) according to user sensitivities and related risk perceptions;
4. the evaluation of alternative routes among a series of proposed and LCP constrained trail paths.

5.3 Least-Cost Path Analysis

Least-cost path (LCP) methods and analyses (Dijkstra, 1959) are used to optimize network use, transportation costs, and trail and road delineations (Xiang, 1996; Collischonn *et al.* 1999; Adruansen *et al.* 2003; Atkinson *et al.,* 2005; Kautz *et al.*, 2006; Snyder *et al.* 2008). Within ESRI ArcGIS, LCP is featured in several spatial analysis platforms, which use a window kernel to determine the 'cost' of moving between vertices. At least two primary data layers are required to do this: a rasterized friction surface that represents the cost (or penalty, or risk) of moving from point to point, and a layer of nodes that need to be connected. The process of creating a cost surface is part of conducting a suitability analysis (Nonis *et al.*, 2007). In detail, this involves identifying and combining all data layers that are needed for making decisions according to specific land-use requirements, constraints, and management preferences (Malczewski, 2004; Lambert *et al.* 2007). In doing so, all cost (or penalty- or risk-) identifying data layers need to be standardized to a common scale to allow for multi-layer risk-weighing according to user-specified cost and risk perceptions (Miller et al., 1998; Lambert et al. 2007).

In this regard, Lambert *et al.* (2007) suggests that every risk-quantifying data layer should be brought into a standardized and unitless scale x that varies from 0 to 100, to identify no to extreme risks, respectively. According to Cromley *et al.* (1999) and Bodstad (2002), risk perceptions along this scale may not always increase linearly. With TRAIL, non-linear risk scaling for each risk variable is done with the x^c power function, with x = 0 denoting no risk, 1 denoting risk indifference, and 2 denoting high risk. Risk

weighing across the standardized $0 \leq x \leq 2$ range from one variable to the next is done by changing c for each variable from 0 (denoting indifferent risk sensitivity or user preference) to 10 (denoting increasing risk when $x > 1$ or increasing preference when $x < 1$).

For the purpose of road and trail planning, a variety of trail and road delineation platforms are already available (Table 5.1). Each of these platforms have their own specifications and specializations: some platforms deal with optimizing network connectivity's to reduce overall transport costs between single or multiple source and sink nodes (e.g. NETWORK; Chung, 2000); others focus on optimizing engineering layout and minimizing construction cost (e.g. FORPLAN; Johnson, 1986). Some provide simple LCP teaching examples (e.g. MapCalc; Berry, 2001), while others utilize linear and mixed integer goal programming techniques (e.g. PLANEX; Epstein, 2001). The TRAIL platform specializes on optimizing node to node linkages, one link at a time, while using an integrative GIS approach to least-cost trail and road locations according to user-set preference and risk specifications.

5.4 Data Layers

The data layers to be accessed or created for the risk assessment process are listed in Table 5.2, each with a brief description of functionality. The risk types that are to be part of the sensitivity analysis are listed in Table 5.3. These layers (i) may be freely available as part of the public domain, (ii) can be obtained through data-sharing agreements, (iii) need to be purchased, or (iv) need to be created using geospatial analysis procedures.

Table 5.1 Optimizing road design and assessment platforms: overview.

Software Package	Reference	Intended use and objectives	Algorithm	Programming Platform	Inputs	Outputs	Management Level
FORPLAN	Johnson 1986; Weintraub et al. 1994	Forest management planning: harvest-block & access scheduling	Mixed-integer goal programming techniques	FORTRAN 77	Forest inventory polygons: stands, habitats; road network	Forest management & access: cost minimization	Strategic
PLANEX	Epstein 2001; Sessions 2006	"	Linear programming with heuristic decision making	"	As above, coarse-gridded DEM for optimizing road locations	"	Tactical
SNAP	Sessions 2006	Forest management planning; reducing operational costs and env. impacts	Heuristic randomized harvest block adjacency condition, LCP for road building	C, C++	Forest polygons, harvest roads, costs	"	Tactical
UWTHPS	Schiess 1995	Timber harvest planning at a tactical level using a systems approch	"	C, C++, ARC INFO	Management goals, DTM square gridded	Forest operations planning	Tactical
NETWORK	Chung 2000, 2001; Sessions 2006	"	Mixed-integer matematical and heuristic	VC++, AutoCAD	Harvest plan map; haul & road costs; road length, DEM	Network optimization: road attributes & costs	Tactical
ROUTES	Reutebuch 1988; Tucek et al. 1999	Minimizing logging transport costs	Contour-based road-slope design	HP 9000	Air photos, 15 m DEM	Wood forwarding optimization: skidding trails, etc.	Strategic
Pegger	Rogers 2005	Optimized road selection based on road specification	"	Avenue; ARCView GIS	1- 10 m DTM	Road slope and length optimization	Tactical
ROADPAC	Keays 2007	Road design	"	AutoCAD	DTM square grid	Road design optimization	Operational
RoadEng	Heralt 2002	"	"	VC++	DEMs and GPS data	"	Operational
Novapoint	Vianova 2006	Model based road, highway and street design	"	AutoCAD	1- 10 m DTM ; AutoCAD drawings	"	Operational
MapCalc	Berry 2001	Exploring spatial data relationships	LCP based on stream delineation	MAP CALC	Friction surface	Route optimization	Strategic
PATHMATRIX	Ray 2005	Matrix representation of effective geographic distances among populations	LCP	Avenue; ARCView GIS	Zones; Friction surface	Connectivity optimization	Strategic
Linkage Mapper	Vaught 2008	Regional wildlife habitat connectivity	LCP	Python; ArcGIS	Core habitat area; Friction surfaces	"	Strategic
Circuitscape	Shah et al. 2008	Gene-flow pathways	Electronic circuit theory	Python	Friction surface	Integrated circuit optimization	Strategic
TRAIL	This paper	Footprint minimization	LCP	VBA; ArcGIS	Integrated friction surfaces	Alternative route geneartion and evaluation	Tactical

Table 5.2 TRAIL input: data-layer acquisition and processing.

Data layer	Load	Create	Description
Bare-earth digital elevation model (DEM)	×		A digital representation of the elevation at the earth's surface.
Cartographic Depth-to-Water (DTW)	×		DEM derived projection of depth to water below soil surface, derived cartographically according to the elevational rise away from all local open-water features such as flow channels and shorelines.
Flow Channels (streams/rivers)	×		DEM-derived flow channel layer, using flow direction and flow accumulation algorithms (e.g., D8, D-infinity).
Transportation features	×		Maps of linear features dealing with traffic and transportation; include, but are not limited to: paved and unpaved roadways, seismic lines, etc..
LiDAR generated full- feature DEM	×		Needed to determine tree height, stem density, etc..
Non-trafficable areas	×		Areas not to be entered (off-limit).
Limited use zones	×		Areas that are not off-limit for specific purposes, but carry a penalty (cost) to minimize traffic through these areas.
Areas of interest	×		Area that is of special interest for traffic focusing.
Start and end locations	×		Beginning and end of each trail / road segment.
Flow accumulation	×	×	Number of cells that contribute flow into downhill cells (e.g., D8 algorithm to determine flow direction and accumulation, ESRI).
Culvert sizing		×	Data layer indicating culvert size along streams based on Manning's equation (Manning,).
Rutting zones		×	Machine-specific data layer delineating depth of rut ting according to specific weather conditions, e.g., end of summer (Vega *et al.*, 2008).
Slope		×	Data-layer required to steer traffic (i) away from steep slopes, (ii) from areas with strong slope variations, (iii) avoiding continuous slope change along roads (ESRI).
Terrain ruggedness		×	Defined by the standard deviation of the slope; estimated using focal statistics.
Maximum vegetation height		×	Estimated by applying focal statistics to the hull-feature DEM – Bare-earth DEM difference raster.
Openings		×	Open areas within the landscape that are larger than a user defined size.
Cut and Fill		×	Amount of earthwork required for a given road width.

Table 5.3 The risk types that users may change to reflect tolerance to risk acceptance. Each is comprised of a slide bar to which users may test the effects of changing tolerance.

Perceived risk/preference factor
Stream Crossing
Wet area crossing (<0.5m)
Wet area avoidance (minimum distance from)
Slope
Cut & fill
Trail blazing
Rutting
Open areas (proximity and size)
Ruggedness level preference (type of moguls likley to encounter)
Ruggedness level (level of enforcement to ruggedness level preference)
LUZs
Route length

Among the various means to acquire digital elevation data, LiDAR-derived DEMs and associated point cloud data (Figure 5.1 a, b) are thus far the most reliable for delineate roads and trails through vegetated and non-vegetated terrain while minimizing traffic across and along flow channels, wet areas and steep slopes. For wet-to-dry delineation, the DEM derived flow-channel and wet-areas mapping protocol (WAM) by Murphy *et al.* (2009) provides a method to map all hydrologically sensitive zones next to already mapped flow channels and shorelines in a comprehensive fashion (Figure 5.1 c). This is done by determining the cartographic depth-to-water (DTW) below the soil surface through least-costing the elevational rise away from the flow channels and shore lines, where DTW = 0. Once established, DTW can be used to map the drainage conditions across the area as these may vary from very poor (DTW < 0.1), poor (0.1 < DTW < 0.25m), imperfect (0.25 < DTW < 0.5m), moderately well (0.5 < DTW < 1m), well (1 < DTW < 25m), and excessively well (DTW > 25m). Wet areas and wetland borders

generally coincide well with DTW<0.5m (Murphy *et al.* (2009, 2011). The resulting DTW map can also be used to determine the extent of soil rutting as affected by (i) weather and (ii), vehicle type with vehicle load and contemplated number of passes as additional specifications (Vega *et al.* 2008; Figure 1d).

Part of the wet-areas mapping protocol requires the mapping of flow direction and flow accumulation. The flow accumulation layer, automatically derived from the bare-ground DEM using the e.g., D8 algorithm, determines the water-contributing area above each potential route-stream crossing. This area is essential for determining the minimally required culverts diameters, and this can be done by using formulation suggested by, e.g., Rothwell (1978):

$$D = 30.48\left(\frac{n\ C\ I\ A * 2.1 * 10^{-5}}{S^{0.5}}\right)^{0.375}$$

(eq. 1)

where:

D = culvert diameter, cm

S = recommended slope of culvert = .017

n = roughness coefficient for culvert, = 0.015 for the FOZ area, = 0.03 for the RZ area

C = runoff coefficient (depends upon soils, slope and land use; = 0.3 for the FOZ area, = 0.5for the RZ area

I = extreme weather event, assumed to be 40mm/hr for both areas

A = flow contributing area above culvert (ha)

Cut & fill requirements for establishing flat road and trail surfaces can be obtained through using ESRI's focal statistics for local DEM smoothing. Users can set the length and width along which the trail or road beds need to be smoothed. The resulting differences between the smoothed and un-smoothed surfaces can then be used to determine the cut & fill volumes associated with each least-cost path (Figure 5.1e).

Finally, using the LiDAR-generated first-return point-cloud data provides a comprehensive means to map vegetation density and height above bare ground (Figure 5.1 b). Heights are created subtracting the first-return LiDAR point-cloud information from the last-return point-cloud data (bare earth DEM). Vegetation height is classed out according to size (Table 5.4). Vegetation density is classified by the sum of pixels with less than or larger than 0.5m vegetation within a 3x3 pixel block. These vegetation parameters so mapped can then be classified into vegetation-based trafficability classes (VTC) pertaining to vehicular movement restrictions, as shown in Table 5.4 and in Figure 5.1f, where the more open areas are shown in blue, and the more vegetated areas show finely textured variations in accessibility.

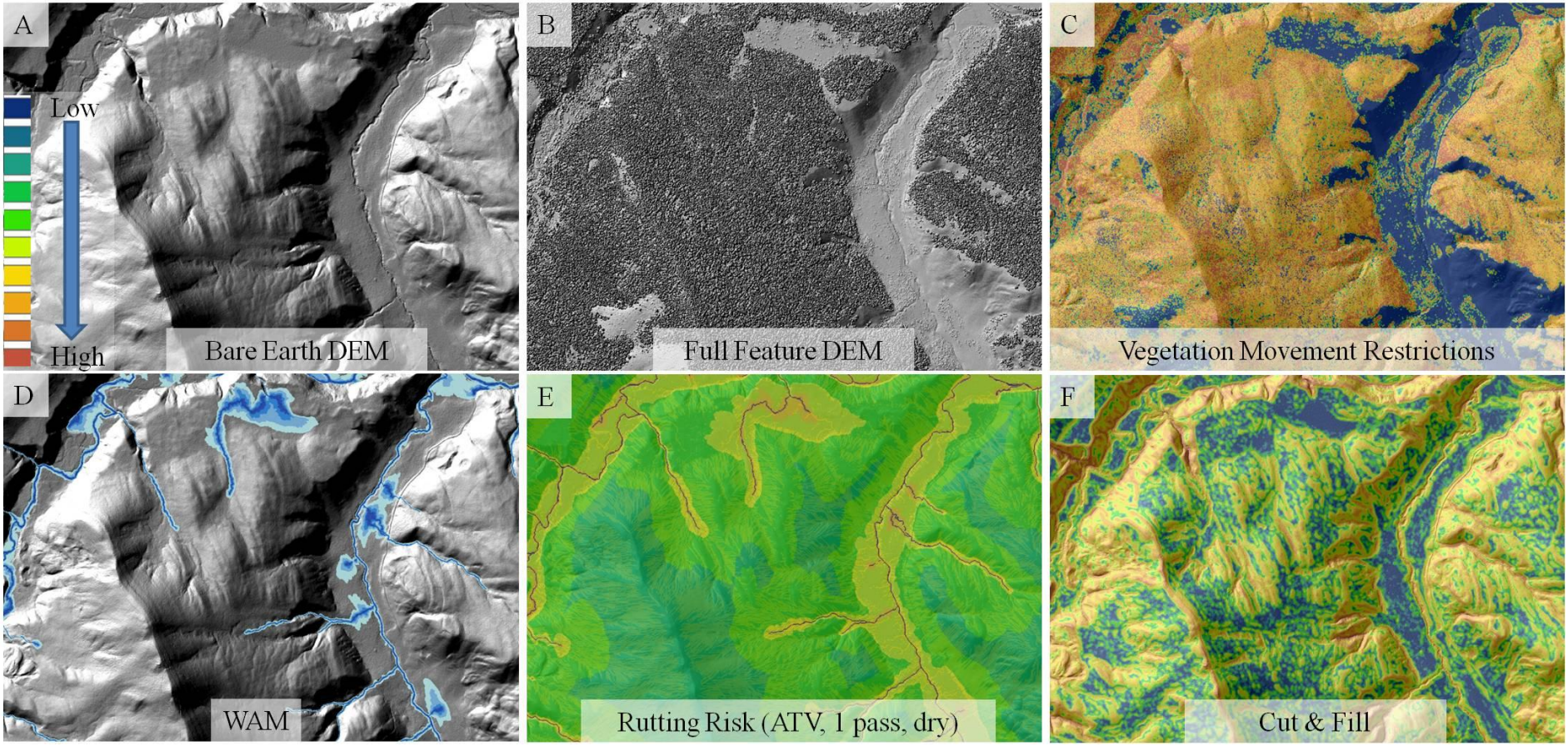

Figure 5.1 Example of data layers used with TRAIL: (A) digital images; (B) LiDAR derived tree heights; (C) depth-to-water (DTW) and flow channels delineation (4 ha flow initiation) on top of the LiDAR derived full-feature DEM; (D) LiDAR derived bare-earth hill-shaded DEM; (E) DEM-derived slope; (F) LiDAR derived terrain ruggedness (= standard deviation of slope; flat - 0 to 1; intermediate - 1 to 2; moderate - 2 to 4; heavy - 4 - 14; extreme >14).

Table 5.4 The method of combining vegetation cover densities and height estimates into a single movement penalty for vegetation.

Vegetaion Cover (%; 3x3m pixel block)	Height Class°				
	0 - 0.5m	0.5 - 4m	4 - 10m	10 - 20m	20m+
0-10	1	1	1	1	1
10-20	1.25	1.25	1.25	1.25	1
20-30	1.5	1.5	1.5	1.5	1
30-40	1.5	1.5	1.5	1.5	1
40-50	1.75	1.75	1.75	1.75	1
50-60	1.75	1.75	1.75	1.75	1
60-70	2	2	2	1.75	1
70-80	2	2	2	1.75	1
80-90	2	2	2	1.75	1
90-100	2	2	2	1.75	1
° Does not consider sub-canopy vegetation					

The bare-ground-DEM can also be used to obtain a measure of machine-impacting mogul-type terrain ruggedness. This can be done by determining the standard deviation (STD) of the DEM-derived gradient for, e.g., each 3x3 m cell neighborhood. Classifying these STD values into, e.g., 5 ruggedness classes from flat (0-5 STD) to extremely perilous (> 50 STD) generated the terrain ruggedness map (TRM) in Fig 2d. The resulting TRM is significantly different from the widely used terrain ruggedness index (TRI; Riley *et al.* 1999; Moreno *et al.* 2003, Crawford 2008) given by:

$$\begin{aligned}\mathrm{TRI} = {} & ((\mathrm{DEM}(0,0) - \mathrm{DEM}(-1,-1))^{2} + (\mathrm{DEM}(0,0) - \mathrm{DEM}(0,-1))^{2} \\ & + (\mathrm{DEM}(0,0) - \mathrm{elev}(1,-1))^{2} + (\mathrm{DEM}(0,0) - \mathrm{DEM}(1,0))^{2} \\ & + (\mathrm{DEM}(0,0) - \mathrm{elev}(1,1))^{2} + (\mathrm{DEM}(0,0) - \mathrm{DEM}(0,1))^{2} \\ & + (\mathrm{DEM}(0,0) - \mathrm{elev}(-1,1))^{2} + (\mathrm{DEM}(0,0) - \mathrm{DEM}(-1,0))^{2})^{0.5}\end{aligned}$$

(eq.2)

where DEM (n, n) is the cell location relative to any center cell at DEM(0,0). This particular formulation indexes terrain ruggedness by slope rather than moguls (compare Figure 2b with Figure 2c). In detail,

$$\text{TRI} \approx 0.348 + 0.096 * \text{Slope} - 0.004 * \text{Slope}^2 + 1.095 * 10^{-4} * \text{Slope}^3 - 1.679 * 10\text{E}^{-6} * \text{Slope}^4 + 1.022 * 10^{-8} * \text{Slope}^5$$

(eq. 3)

such a that TRI(eq. 3) = TRI (eq. 2), with $R^2 = 0.99$. Alternatively, regressing TRI versus TRM yields:

$$TRI = 0.854 + 0.184RLM, with\ \text{R2} = 0.13$$

(eq. 4)

i.e., TRI and TRM represent fairly un-correlated topographic variation components, i.e., large-scale flat to steep variations for the former and versus small-scale flat to mogul variations for the latter.

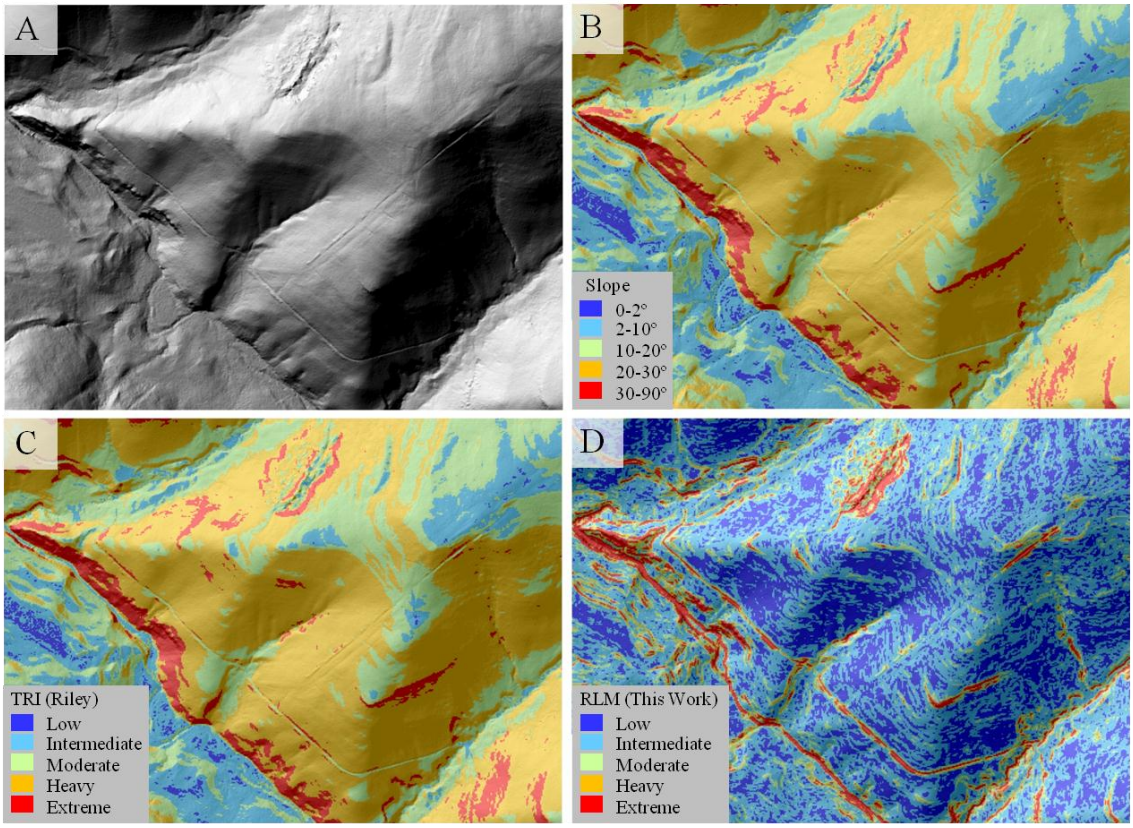

Figure 5.2 A comparison of the TRI map (C) to (A) the hillshaded DEM, (B) the classified ESRI created slope degree map, and (D) the TRM revealing the ambiguity of the TRI. A neighborhood window of 3x3 was used in creating both (C) and (D).

5.5 The TRAIL Platform

Illustrated in Figure 5.3 is the information flow within the TRAIL platform. This platform is controlled through a graphical user interface (GUI) which is used to enable various VBA and ESRI spatial analyst scripts (ArcMap 9.3), raster creation and least-cost analyses. This interface has six tabs (Figs. 5.4 and 5.5).

The '**Load Data**' tab (Figure 4b) prompts the user to:

1. select an analysis window and raster cell size
2. define output feature location
3. define input feature locations

4. execute feature creation routines, by creating
    a) the slope raster
    b) the terrain ruggedness raster
    c) the cut & fill raster
    d) the culvert sizing raster
    e) the vegetation raster
    f) the flow accumulation raster
5. specify the vehicle length

The minimum user operations for this tab deal with:

1. selecting the analysis window and raster cell size
2. defining the output feature location
3. loading the default raster
4. loading the DEM
5. loading the stream layer
6. loading the WAM

The '**Linear Features**' tab (Figure 4c) allows the user to select or avoid potential trail locations from existing linear features (roads, trails, power corridors, seismic lines).

The '**Potential Rutting**' tab (Figure 4d) is used to estimate vehicular impacts upon soils, based on vehicle specifications dealing with vehicle load, number of tires, tire radius, inflation pressure.

The '**Risk Aversion**' tab (Figure 5a) allows the user to analyze and assess risk sensitivities along the routes, as this ranges from aversion to avoidance pertaining to:

1. slopes
2. stream channels
3. wet area
4. limited use zones (LUZs)
5. earth moving (cut & fill).

The '**Constraints**' tab (Figure 5b) allows the user to address trail-building constraints, by:

1. accounting for 'cost' of trail blazing
2. decrease trail braiding by avoiding open, unconstrained areas
3. set trail challenge goals from easy to difficult across rugged terrain
4. shorten length of route according to user preferences
5. minimize hydrological risks through locating optimal flow-channel and wet-area crossings

The '**LCP execution**' tab (Figure 5c) is used: to produce the **risk sensitivity map** from the individual risk-defining data layers, to create several route alternatives, and to generate the route profile tables. There are four buttons:

1. to load or build the desired **risk sensitivity map** according to all of the above considerations and specifications;
2. to execute the LCP analysis by setting the start and end points of the desired route (Figure5d);
3. to generate the LCP route profile regarding elevation, slope, DTW, stream crossings, culvert sized, cut & fill, etc. (Figure5d);
4. to exit (settings stored).

Once the data layers are loaded and created, and users have utilized the slide bars to represent their interpretation of risk, the users select start and end points for the contemplated route and begin with the analysis. Once completed, the platform produces an attribute table that displays the accumulated trail (or road) profile values for each risk type (elevation, DTW, stream crossing flag, cut & fill, etc.). The users may alter the slidebar settings any number of times to create multiple trail or road locations and attribute tables to perform a comprehensive tradeoff analysis among the various LCP selected routes. The additional option allows the user to generate and re-profile smoothed versions of the most desired routes utilizing ESRI smoothing methods. The trade-off analysis is facilitated by displaying:

1. route-specific bar graphs dealing with cumulative costs along the route, e.g., route length, number of stream crossings, length of wet areas and steep slopes to be crossed, total cut & fill requirements; and,
2. route attribute profiles as these change each meter along the least-cost routes, before and after smoothing roadbeds and routes.

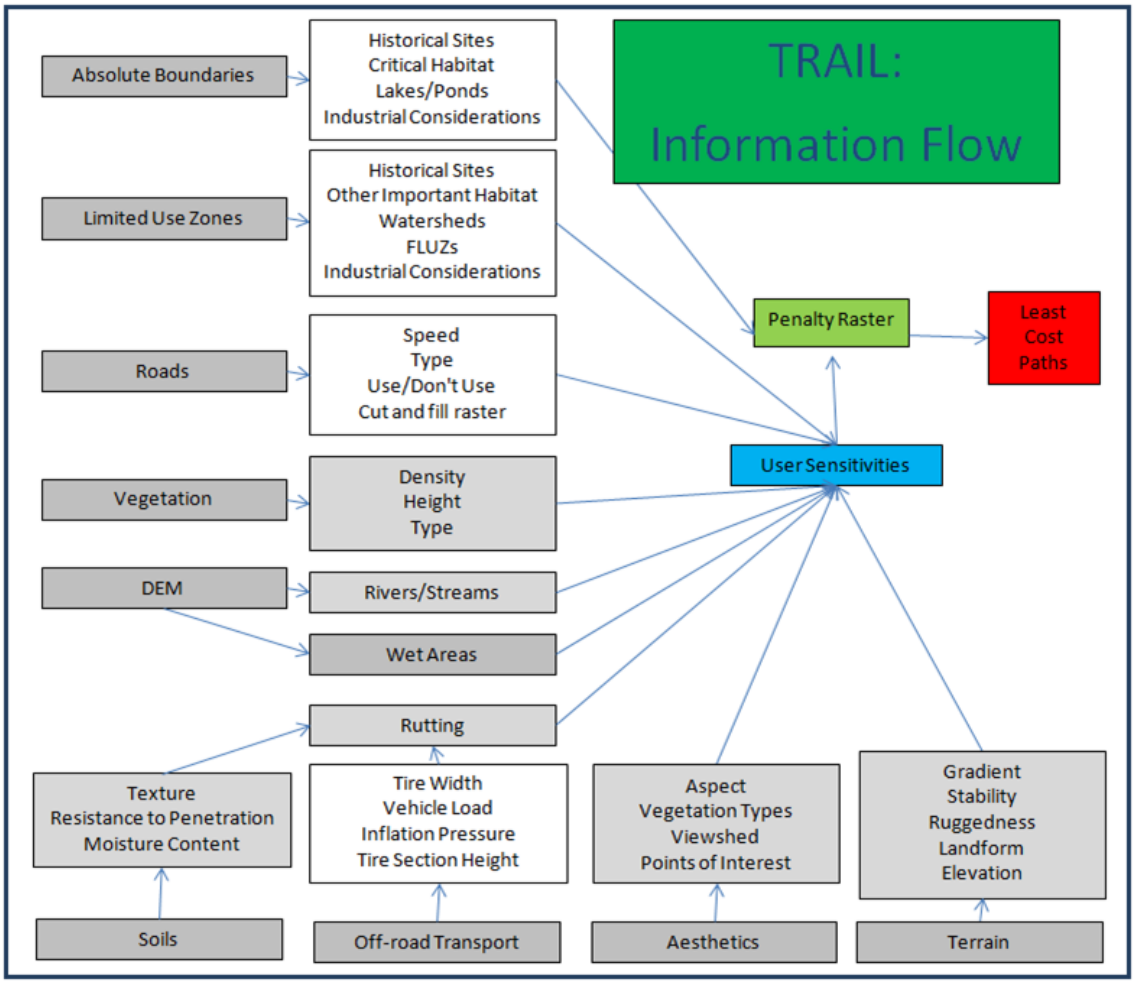

Figure 5.3 The TRAIL platform: information flow. The platform combines multiple data sources at varying scales, resolutions and spatial projection systems, assigns a user defined risk factor, and creates a least cost path between nodes.

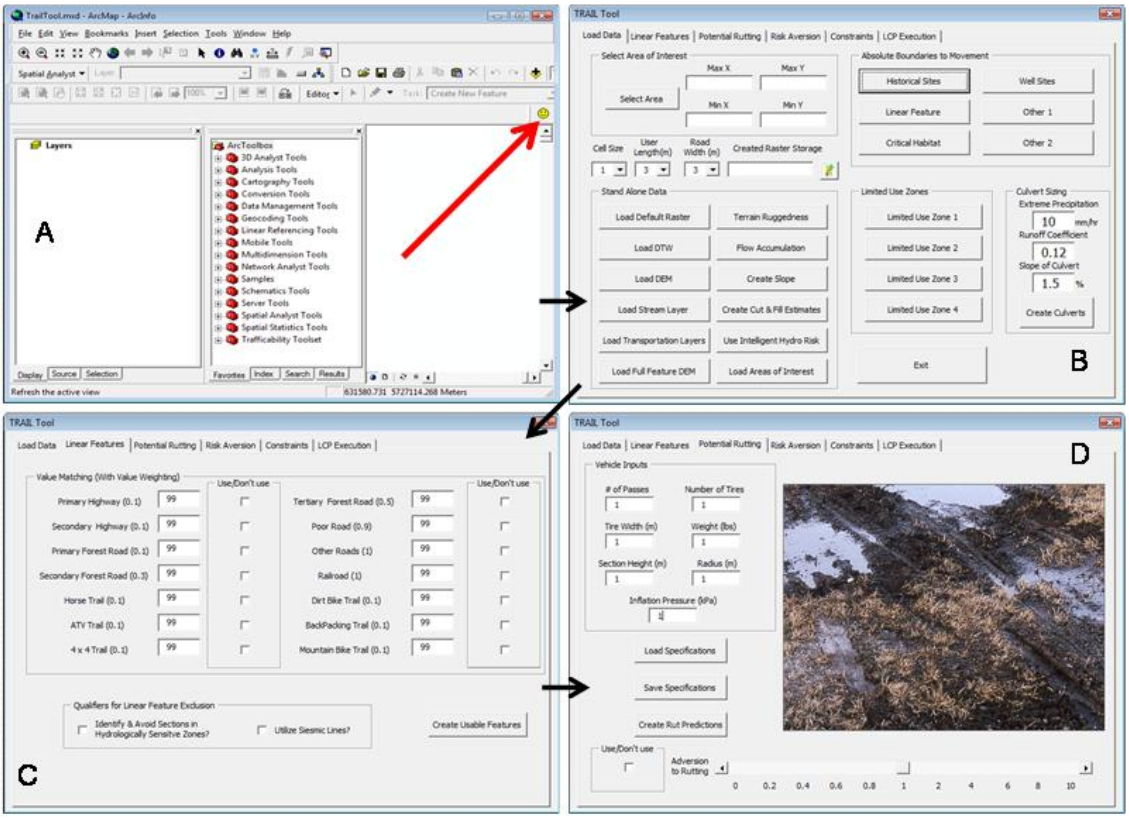

Figure 5.4 TRAIL GUI, Tabs 1 to 3.

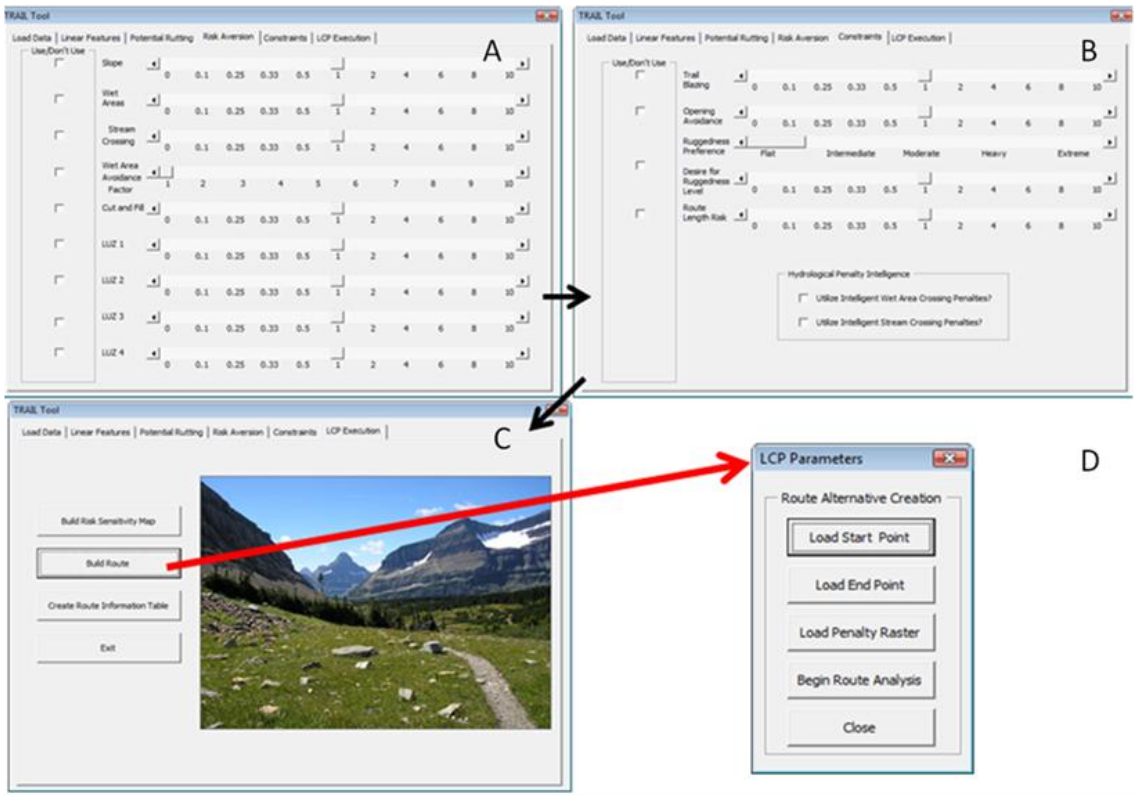

Figure 5.5 TRAIL GUI, Tabs 4 to 6.

5.6 Case Studies

Two contrasting TRAIL-based case studies were performed, dealing with examining alternative routes for (i) two proposed recreational ATV trails within the forested foothills of the Southern Alberta Rockies (termed “recreation zone” or RZ), and (ii) for three proposed forest access road segments within the boreal plain north of Peace River, Alberta (termed “forest operations zone, or FOZ) (Figure 6). These studies were done by:

1. compiling all the required data layers including the data layer for the proposed road locations (see below);setting the beginning and end locations of each trail and road segments along the proposed routes;
2. setting alternative levels of perceived risks and preferences along each segment pertaining to stream and wet area crossings, slope and ruggedness level (RL), cut & fill requirements, and road length; these settings vary from "not applicable" (na) and "does not matter" (0.1) to risky (10);
3. using TRAIL to generate the least-cost paths associated with each preference designed to minimize the crossing to streams, wet areas and steep slopes while still minimizing road or trail length;
4. using ESRI smooth line function to smooth these paths;
5. summarizing the results so generated, by
    a. plotting elevation, slope, stream channel and wet-area locations along the length of each trail and road segment, and
    b. by listing the number of stream crossing, lengths of wet areas and steep slopes to be crossed, total length, and extent of cut & fill requirements of each trail and road segment.

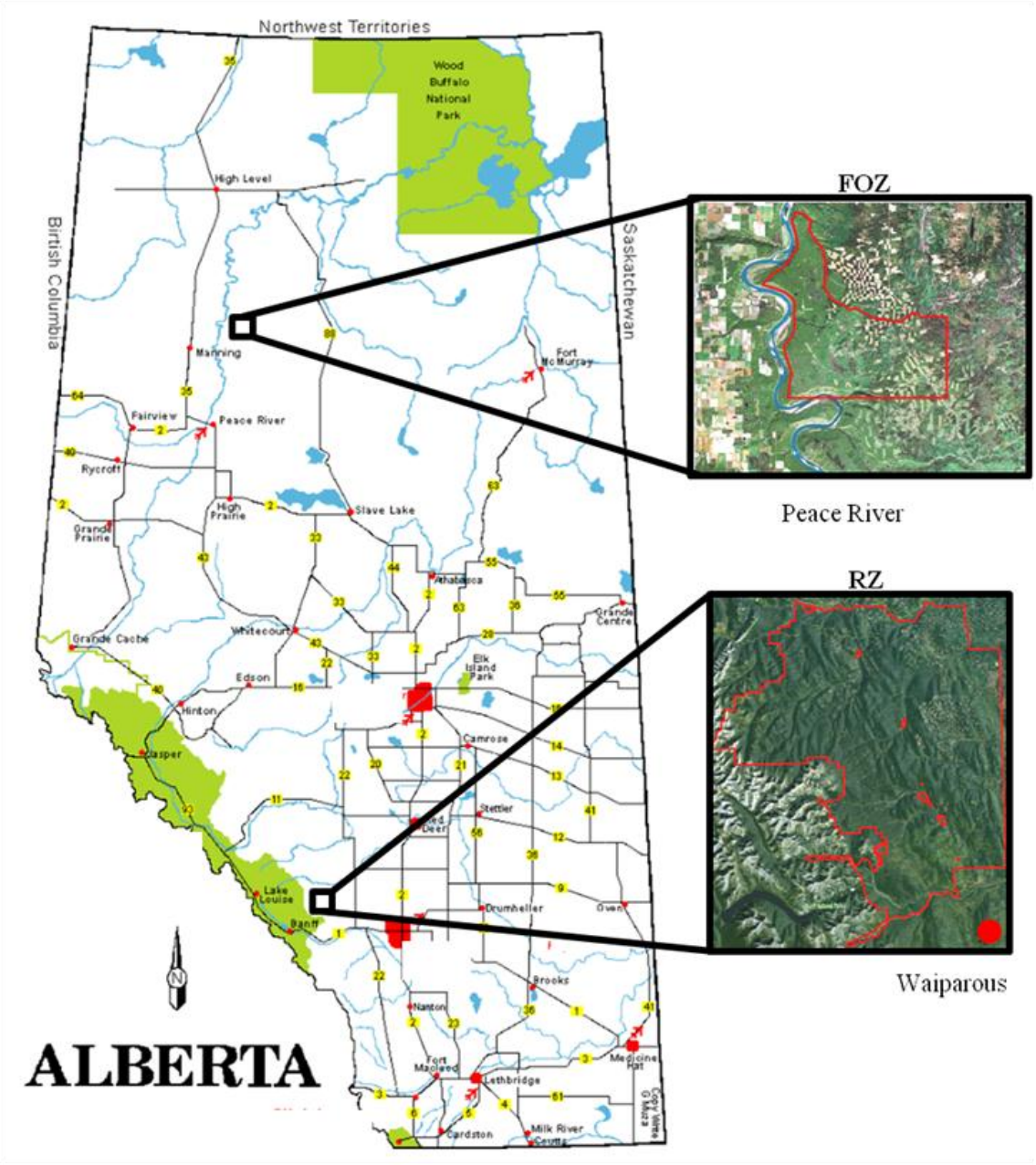

Figure 5.6 Location of the two study locations within Alberta, Canada (map from Watertonpark.com, 2011).

5.6.1 Study Areas

The RZ is located within the forested foothills of the Southern Alberta Rockies 100 km west of Calgary with center at 51°19'59"N - 114°57'59"W: elevation 1,190 to

2,590m a.s.l; mean annual precipitation 540 mm; mean annual temperature 2°C. According to Alberta Geological Survey (2010), bedrock within RZ is represented by the Brazeau, Alberta Group, Coalspur, and Paskapoo formations. Upland soils are mostly bedrock-derived Grey Luvisols interspersed by Brunisols, with Lodgepole pine (*Pinus contorta*), white spruce (*Picea glauca*) and black spruce (*Picea nigra*) as dominant trees. FOZ is located within a boreal plain 90 km north of Peace River, Alberta, with center at 56° 46' 13"N - 118° 22' 28"W: elevation 630m to 890m a.s.l.; mean annual precipitation 431 mm; mean annual temperature 1.2°C. Bedrock within FOZ is represented by Shaftesbury and Loon River shales. Soils have developed on fine-textured lacustrine to coarse-textured till deposits, interspersed by organic and alluvial materials, with soil orders varying from Gray Luvisol and Brunisol orders on the uplands, and Luvic Gleysols and Solonetzs in the lowlands. Vegetation is dominated by Trembling Aspen (*Populus tremuloides*), Balsam Fir (*Abies balsamea*), and White Spruce (*Picea glauca*).

5.6.2 Data Layers and Sources

All data layers were provided in the NAD_1983_UTM_Zone_11N D_North_America_1983 datum. The Research Information Branch (RIMB) of the Alberta Government provided the following data layers for both study areas:

1. LiDAR DEM (minimum 1 bare earth return per meter², ±15cm vertical accuracy)
2. linear feature layers
    a. roads

b. trails

c. seismic lines, pipelines, transmission lines

3. exclusion zones

a. historical zones

b. protection zones

c. habitat

d. industrial use areas

4. aerial photography

5.6.3 Data Processing

The LiDAR-generated point cloud data for RZ and FOZ were rasterized into a 1x1 m format to generate the full-feature (all returns) and bare-earth (last returns) DEMs. The bare-earth DEMs were, in turn, used to derive the data layers for flow direction, flow accumulation using the D8 algorithm, and the cartographic depth-to-water index (DTW) in reference to all DEM-derived flow channels stating with the 4 ha threshold for flow initiation (for details, see Murphy *et al.* 2009, 2011). The TRAIL platform was then used:

1. to access the DEM and DTW layers;
2. to automatically create the slope (ESRI, 2011) and ruggedness layers within a 3x3m for the RZ and a 15x15m for the FOZ;
3. to generate the ruggedness (TRM) and vegetation-based trafficability classes (VTC) as described above;

4. to compile all the other data layers, including the layer for existing and/or proposed trail routes;
5. to re-format all layers towards the same spatial arrangement (cell size, spatial reference, extent).

Once all the needed data layers were compiled, various risk and preference options were selected for each of the proposed RZ and FOZ trail or road segments at a time, as specified in Table 5. The resulting LCP results were then compared with each of the proposed trail and road segments by (i) plotting elevation, DTW, and culvert locations along each segment, and by (ii) tabulating estimates of the number of channels to be crossed, the length of wet areas and steep slopes to be crossed, the cut & fill effort, and flow accumulation areas and minimum predicted culvert diameters for each culvert location along each segment. Sensitivity analyses dealing with the LCP route delineations as affected by route smoothing (smoothing length: 0, 10, 100, 1,000 m; using PAEK and ESRI methods) and raster resolution (1, 3, 9, and 15 m) were also performed.

5.7 Results and Discussion

The TRAIL outcomes for each of the trail and road segments are listed in Table 6 for each of the risk settings in Table 5.5. These outcomes are quite variable, but generally conform to expectations. For example, not avoiding streams and wet areas as part of the TRAIL process leads to increasing the number of streams and wet areas to be crossed. Similarly, not avoiding steep slopes leads to increased lengths of steep slopes along the

TRAIL-generated road and trail locations. However, adding stream, wet-area and slope restrictions to the TRAIL process decreases the initial capital required to construct these features, as detailed in Table 5.7. For example, only an estimated 1 of the originally proposed 12 culverts would have to be installed along Road segment 1; the corresponding length of wet areas to be crossed would decrease from 1806 m along the originally proposed route to 28m along the TRAIL-selected road. Some of these gains are somewhat offset by slightly increased trail and road length requirements. The best TRAIL-generated routes are presented in Figure 5.7. Also shown in Figure 5.7 are the originally proposed and the smoothed LCP route locations (smoothing length 1,000m). The TRAIL-produced elevational and DTW profiles with channel locations are shown in Fig 5.8, in comparison with the originally proposed routes. Also entered in Figure 5.8 are the upstream catchment areas (in ha) and the corresponding minimum culvert diameters (in cm) at each road –stream crossing location.

Table 5.5 Setting alternative levels of perceived risks and preferences pertaining to stream and wet are crossings, slope and terrain ruggedness, and road length for two proposed trail segments for the recreational traffic zone (RZ) and for three proposed road segments within the forest operations zone (FOZ).

Route alternatives	SA	WA	WAAF	Slope Threshold (%)	SL	CF	TR	TR Conformance	Vegetation Risk	Road Length
Road 1-1	4	4	n/a	10	6	2	n/a	n/a	n/a	2
Road 1-2	4	4	3	10	6	2	n/a	n/a	n/a	10
Road 1-3	1	1	n/a	10	1	1	n/a	n/a	n/a	n/a
Road 1-4	1	1	n/a	10	1	n/a	n/a	n/a	n/a	n/a
Road 1-5	6	1	2	10	0.3	2	Int	1	n/a	1
Road 2-1	1	1	n/a	10	1	1	Int	1	n/a	n/a
Road 2-2	1	1	n/a	10	1	1	n/a	n/a	n/a	n/a
Road 2-3	6	6	n/a	10	2	1	n/a	n/a	n/a	n/a
Road 2-4	6	6	3	10	4	2	n/a	n/a	n/a	n/a
Road 2-5	6	6	3	10	6	2	n/a	n/a	n/a	4
Road 2-6	4	1	3	10	2	2	n/a	n/a	n/a	6
Road 3-1	1	1	n/a	10	1	1	Int	1	n/a	n/a
Road 3-2	1	1	3	10	1	1	Int	1	n/a	n/a
Road 3-3	1	1	3	10	8	1	Int	1	n/a	n/a
Road 3-4	6	4	4	10	8	4	Int	4	n/a	n/a
Road 3-5	4	4	n/a	10	2	1	Int	1	n/a	n/a
Road 3-6	1	1	n/a	10	0.3	1	Int	1	n/a	n/a
Road 3-7	6	4	4	10	8	4	Int	4	n/a	10
Road 3-8	4	2	2	10	4	6	Int	4	n/a	10
Trail 1-1	8	10	n/a	25	10	7	Mod	8	10	1
Trail 1-2	8	10	n/a	25	10	7	Mod	8	0	1
Trail 1-3	10	8	2	25	8	8	Mod	8	5	1
Trail 1-4	8	10	n/a	15	10	7	Mod	8	10	1
Trail 1-5	8	10	n/a	15	10	7	Mod	8	0	1
Trail 1-6	10	8	2	15	8	8	Mod	8	5	1
Trail 2-1	8	10	n/a	25	10	7	Mod	8	10	1
Trail 2-2	8	10	n/a	25	10	7	Mod	8	0	1
Trail 2-3	10	8	2	25	8	8	Mod	8	5	1
Trail 2-4	8	10	n/a	15	10	7	Mod	8	10	1
Trail 2-5	8	10	n/a	15	10	7	Mod	8	0	1
Trail 2-6	10	8	2	15	8	8	Mod	8	5	1

Table 5.6 Summary of the results of the TRAIL analysis of LCP options under variable risk tolerances.

Name	Length (km)	Slope Above Threshold (m)	Length of route in Wet Areas (m)	Est. Stream Crossings	Total EarthWork (m^3)	Vegetation
Road 1-1	9.11	5	338	6	53542	-
Road 1-2	9.47	2	28	1	39394	-
Road 1-3	9.58	3	160	6	44770	-
Road 1-4	6.84	2	163	3	29419	-
Road 1-5	6.90	0	232	1	32622	-
Road 1 AP1	9.11	11	1806	12	58824	-
Road 2-1	3.14	8	180	3	15765	-
Road 2-2	3.07	4	80	3	22165	-
Road 2-3	3.81	25	42	2	23415	-
Road 2-4	3.87	24	20	3	24246	-
Road 2-5	3.83	6	26	2	22894	-
Road 2-6	3.00	18	232	4	17847	-
Road 2 AP	3.00	24	464	7	22969	-
Road 3-1	6.84	49	475	14	55790	-
Road 3-2	6.76	109	268	8	57986	-
Road 3-3	7.25	6	826	14	57803	-
Road 3-4	9.47	21	230	5	70438	-
Road 3-5	7.70	149	48	3	66501	-
Road 3-6	6.73	114	303	9	61642	-
Road 3-7	8.11	35	429	7	60634	-
Road 3-8	7.72	55	605	9	63554	-
Road 3 AP	7.17	199	1029	14	75617	-
Trail 1-1	2.24	5	26	1	-	1.2
Trail 1-2	1.98	4	24	1	-	4.3
Trail 1-3	1.56	3	41	1	-	3.1
Trail 1-4	2.11	17	30	1	-	1.2
Trail 1-5	1.43	21	20	1	-	3.2
Trail 1-6	1.98	10	206	1	-	1.1
Trail 1 AP	1.41	110	70	2	-	3
Trail 2-1	1.09	12	15	1	-	2
Trail 2-2	3.08	5	19	1	-	8.1
Trail 2-3	1.45	3	94	1	-	3.1
Trail 2-4	3.51	78	19	1	-	3.1
Trail 2-5	2.52	84	15	1	-	6.5
Trail 2-6	3.12	75	43	1	-	3.9
Trail 2 Ap	0.98	602	15	1	-	2.8

Table 5.7 Summary of road obstacles along the proposed route and their TRAIL identified optimal alternatives.

Route	Number of Stream Crossings		Drainage Area (ha)		Total Culvert Size (cm)		Meters of Wet-Area Interaction	
	AP	TRAIL	AP	TRAIL	AP	TRAIL	AP	TRAIL
Road 1	12	1	193	174	658	132	1806	28
Road 2	7	3	734	427	773	324	464	130
Road 3	14	7	4,341	4245	1494	1245	1030	430
Trail 1	2	1	267	259	308	242	70	41
Trail 2	1	1	227	239	230	234	15	15

Route	Cut & Fill (000's)a		Route Length (km)		Slope > 15% (m)			
	AP	TRAIL	AP	TRAIL	AP	TRAIL		
Road 1	59	39	9.11	9.47	35	5		
Road 2	24	23	2.3	3.3	64	17		
Road 3	76	61	7.17	7.12	199	35		
Trail 1	-	-	1.4	1.6	110	3		
Trail 2	-	-	0.98	1.1	600	84		

a - Cut & fill amounts do not include fill requirements for wet areas.

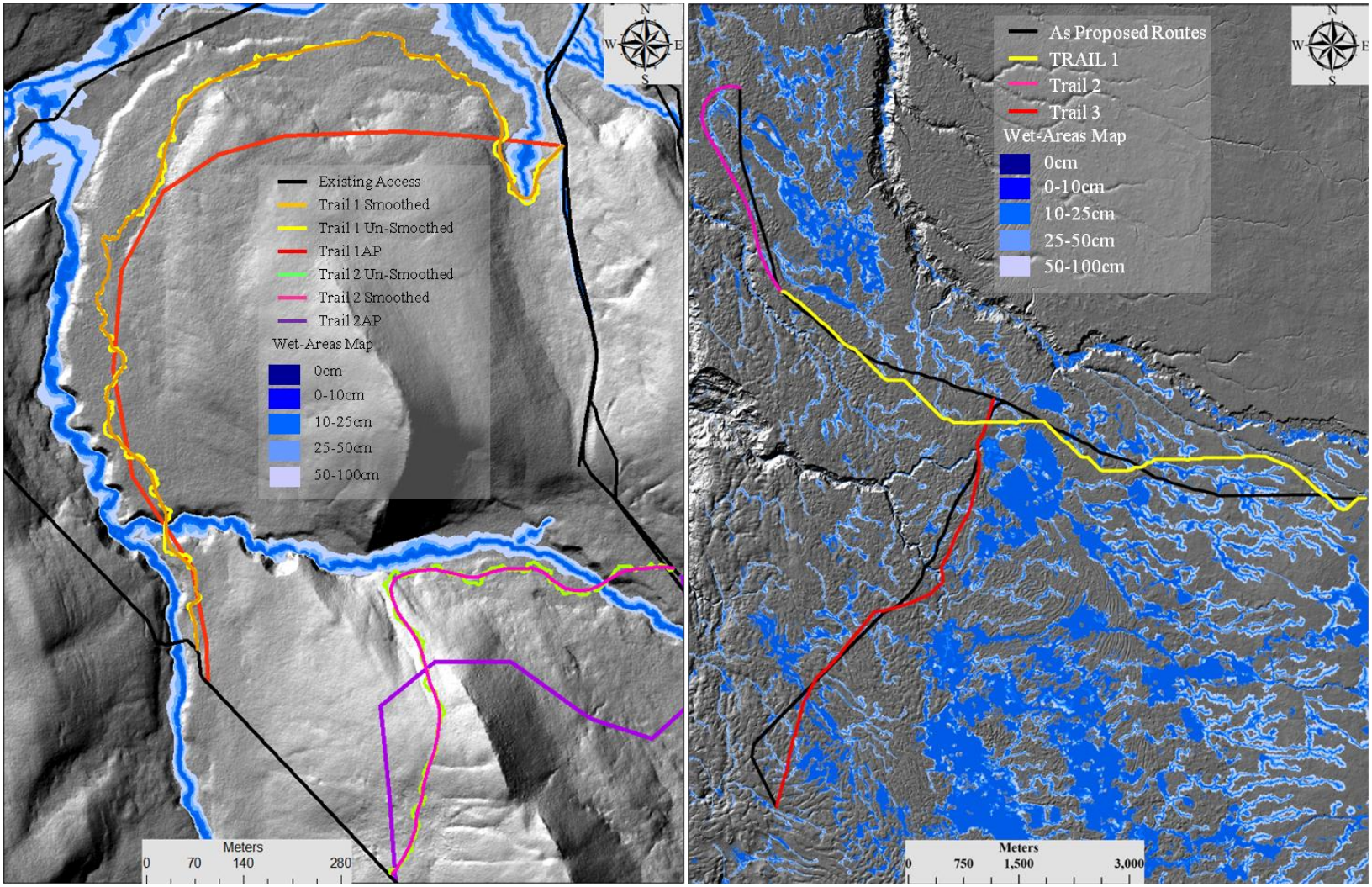

Figure 5.7 Left. Alternative route suggestions for a forest operations routing scenario on top of the LiDAR DEM hillshade and depth-to-water (WAM) map for the location. Routes were created utilizing available data layers, created data layers, and varying scales of user risk tolerance. Right. Alternative route suggestions for a recreational trail routing scenario on the LiDAR DEM hillshade and depth-to-water (WAM) map. Routes were created utilizing available data layers, created data layers, and varying scales of user risk tolerance.

Smoothing the LCP-delineated routes led to moderate increases in road length and reduced the length over steep slope for the trail segments within the hummocky RZ terrain, but increased the number of channels and the length of wet areas to be crossed within the fairly flat FOZ terrain (Table 8). Decreasing the raster resolution from 1 to 3, 9 and 15 m slightly increased the LCP generated segment lengths, and the overall cut & fill requirements, while the non-smoothed lateral deviations from roads and trails generated with the 1m trails remained within 8 to 16 m. The effect of decreased resolution on the length of steep slope crossing was variable (Table 9).

Table 5.8 Effect of smoothing length on the LCP segments.

Segment	Smoothing length (m)	Length (km)	Slope above threshold (m, 12%)	Length of route in Wet Areas (m)	Est. Cut & fill (m^3)	Est. Stream crossing
Road 1	0	9.5	0	30	5083	1
	10	9.5	0	31	5087	1
	100	9.4	2	53	5061	1
	1000	9.2	7	797	4973	6
Road 2	0	3.9	23	21	2370	2
	10	3.9	24	21	2366	2
	100	3.8	20	27	2371	2
	1000	3.7	22	111	2281	3
Road 3	0	8.1	28	549	4425	7
	10	8.1	28	546	4436	7
	100	8.0	34	505	4467	7
	1000	7.1	80	980	4190	12
Trail 1	0	2.1	69	17	177	1
	10	2.0	71	15	159	1
	100	1.8	52	30	143	1
	1000	1.8	53	31	142	2
Trail 2	0	1.1	427	10	97	1
	10	1.1	404	11	85	1
	100	0.9	360	12	75	1
	1000	0.9	347	22	73	1

Table 5.9 Average changes in trail locations with decreasing raster resolution.

Raster resolution, m	Lateral deviation, m	Segment length, %	Length of steep slope, %	Cut & fill requirements, %
3	8.1	5.0	16.0	10.0
9	13.3	8.0	29.0	13.0
15	16.5	9.0	21.0	14.0

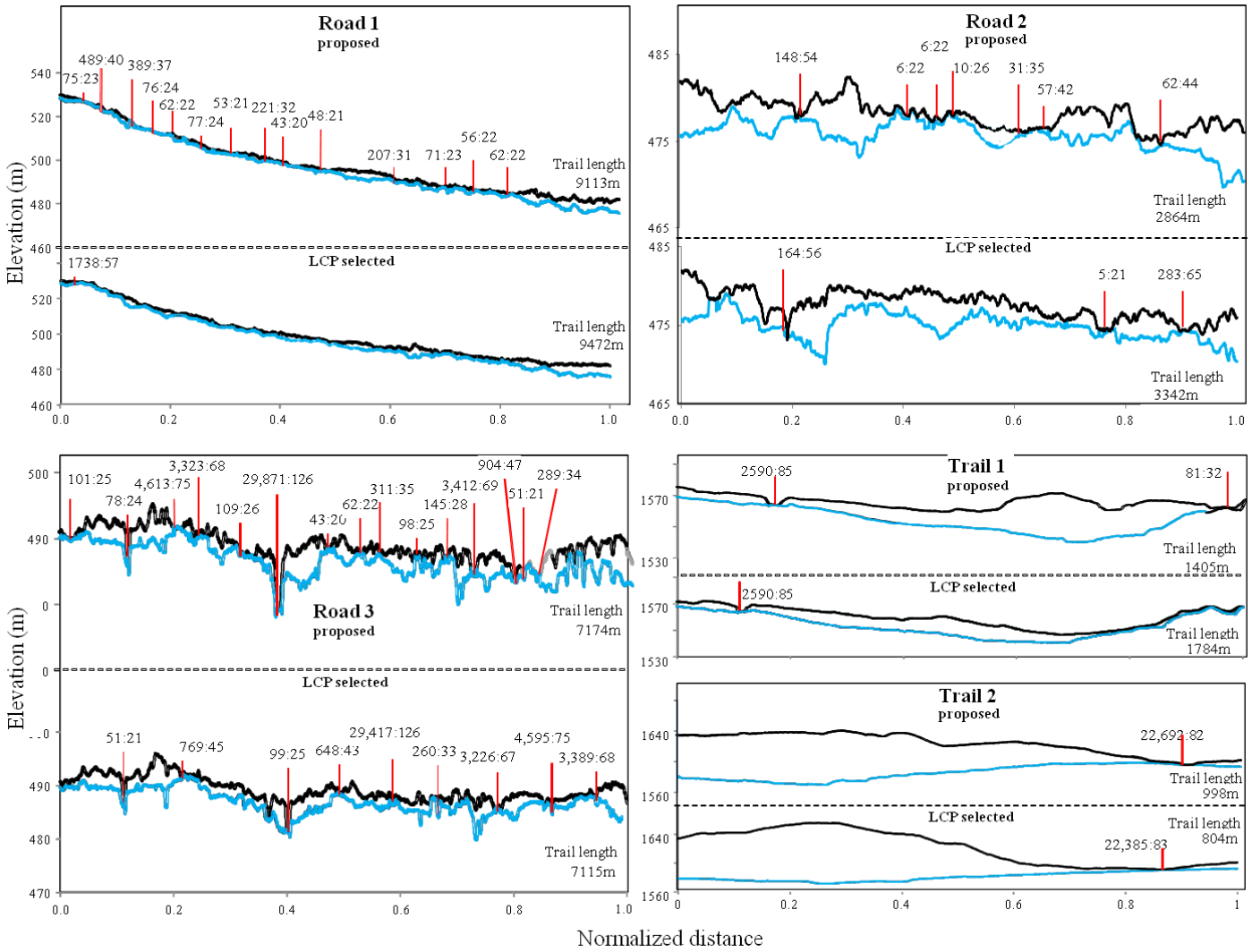

Figure 5.8 Originally proposed and TRAIL-generated road and trail profiles for the two study areas, by segments: Road 1, 2, 3 and Trail 1 and 2. Black lines: road and trail bed elevations; blue line: cartographically derived elevation of the water table; red markers with xxx:xx specifications: culvert locations with catchment area (ha) and minimum culvert diameter estimate (cm), respectively; x-axis refers to position along each segment, normalized by road length from A to B.

Using DEM-derived flow channels, wet-area and slope layers provide major advantages for the TRAIL evaluation and placement of OHV trails and forest access roads. As demonstrated, TRAIL-based advantages refer to finding routes that require substantially fewer stream, wet-area and steep slope crossings than proposed locations derived from traditional trail and route delineation methods. Raster resolution of the risk layers marginally affect results, however, flow-channel and wet-area delineations are best when originally derived from 1m bare-earth DEMs than from coarser DEMs (Murphy et al. 2009).

The above route selection criteria center on minimizing cost-producing flow-channel and wet-area crossings. Other trail-delineation motives such as (i) degrees of recreational trail challenge, (ii) scenic experiences, and (iii) "time in saddle" for hiking, biking, OHV and horse riding can also be enhanced. Figure 5.9 provides examples as to utilization of the TRAIL tool in various situations. In detail, Figure 5.9a shows TRAIL-selected OHV routes for low (flat), moderate, and intermediate to "extreme" trail ruggedness preferences. Figure 5.9b provides an example of directing trail users to higher ground away from flow channels and wet areas according to the weather, with the 4-ha threshold denoting the upslope area requirement for flow initiation during dry seasons, the 1-ha threshold denoting flow initiation following major precipitation events, and the 0.1 ha threshold applicable during spring melt seasons. For the latter condition, TRAIL selects shorter and steeper routes along ridge tops, to avoid traffic induced damage along slopes. Figure 5.9c contrasts the delineation of trails according to user preferences for woody versus open-space trails. An opening size, in this instance, of 1000m² or greater is completely avoided lending to TRAIL results within forested areas;

conversely, selecting dense forest as a negative feature on the landscape lends TRAIL to delineating routes through openings. These two opposing ideas can be merged to delineate routes avoiding open areas as well as densely forested areas. Figure 5.9d shows how TRAIL can be used to consider the avoidance or accommodation of traffic along already existing linear features (e.g. trails, roads, seismic lines) while in regard to other route creation criteria.

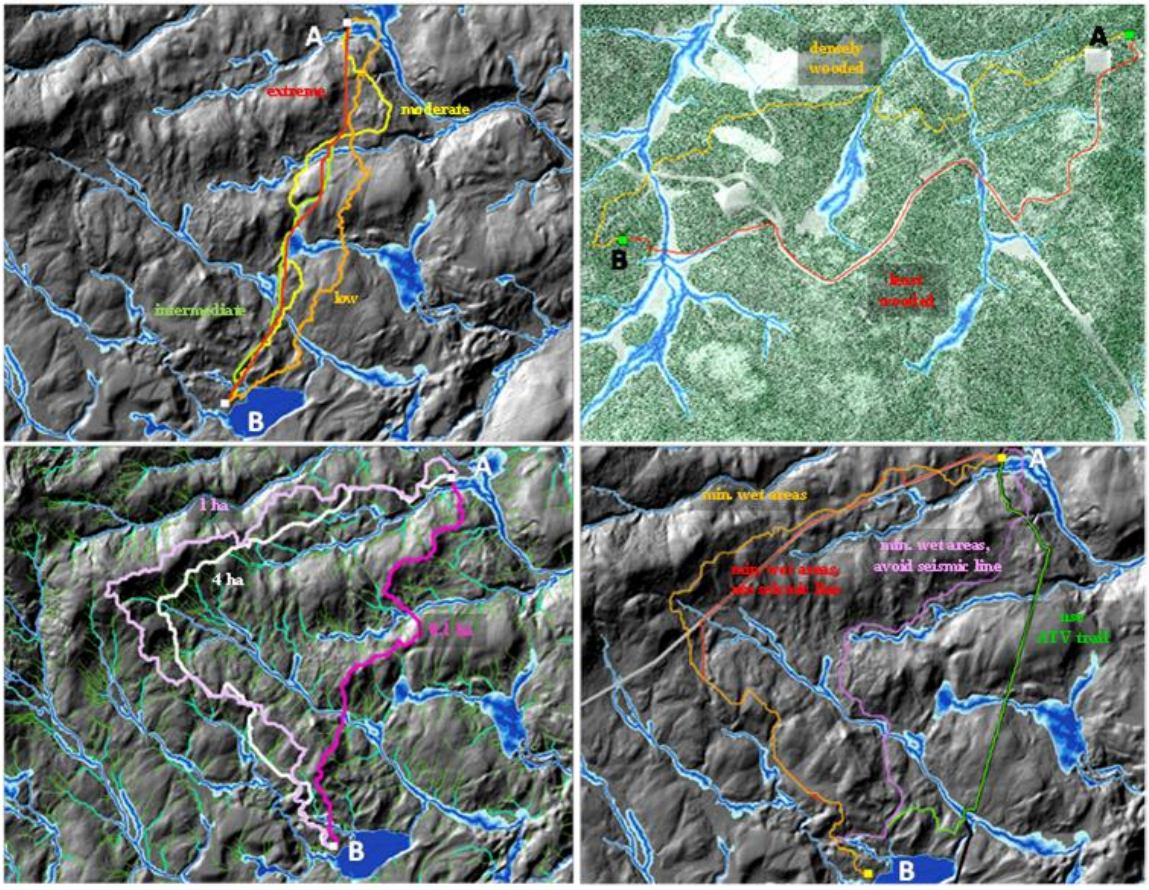

Figure 5.9 Trail selections between A and B according to (a) ruggedness , (b) avoiding wooded trails versus open spaces > 1000m^2, (c) avoiding soil wetness by flow initiation threshold (4, 1 and 0.1 ha), (d) using existing linear features (ATV trail, seismic lines) or not, and avoiding wet areas.

In relation to other currently available trail and road lay-out platforms Table (1), TRAIL offers a number of advantages:

1. it works in conjunction with the ESRI platform and its spatial analysis platforms, including LCP, and in conjunction with Microsoft Excel for road and trail profiling and tabular attribute summation;
2. it allows for expanding the list of data layers needed for integrative and informative trail and road risk weighing;
3. it allows for customizing the trail and road delineation according to stated or perceived user preferences and transport-mode specifications detailing expected footprint loads;
4. it facilitates trade-off communications and examinations between alternative road and trail suggestions;
5. the platform is not limited to trails and roads , but can also be used to locate best infrastructure locations for, e.g., drainage systems, power lines, pipelines and any other linear structures including wildlife corridors and wetland-to-wetland connectivities;
6. increasing field reconnaissance comprehensiveness while reducing related resource allocations.

TRAIL processing time may become a factor with increasing data-layer resolution. For that reason, it is recommended to clip the extent of the maps to the area of trail-specific interests, and – if necessary – resample the individual risk layers to a coarser resolution, say from 1 to 2 m, or more. The final trail selections are generally not highly sensitive to

this resampling, provided that the individual risk maps remain fairly insensitive to cell-based neighbourhood smoothing.

While the TRAIL tool is fairly comprehensive at this stage, additional work can be done in terms of, e.g., (i) enhancing the cut & fill determination to account for road smoothing as well as slant corrections, (ii) incorporating viewshed analyses, (iii) conducting further comparisons between TRAIL selected routes and already established routes from simple hiking and riding trails to forest logging roads, and (iv) dealing with weather-affected soil moisture and frost conditions as part of the LCP route delineation process.

5.8 Concluding Remarks

The TRAIL platform provides an innovative and economical approach to spatially locate and evaluate new, culturally, ecologically and economically desirable trails and roads while avoiding areas that may pose significant risks regarding trail stability, user health, and construction and maintenance costs. TRAIL also provides a means to compare already existing or proposed routes with optimal TRAIL route locations. As such, TRAIL offers the following conveniences to route planners:

1. providing a user-friendly interface to compile all the data layers deemed necessary for route selection and optimization based on user-perceived risks;
2. using the same interface to quantify risk perceptions from low to high;

3. producing data layers that guide route selection process through least-cost visualizations and comparisons of route profiles;
4. applying the platform across a variety of terrain types, with focus on route-affecting factors such as slope, soil wetness, vegetation cover, proximity to scenic locations, avoidance of ecologically or culturally sensitive locations, etc., and;
5. ready modifications of planned road and trail networks through re-locating route control points dealing with the beginning, end, and other target locations along existing or proposed roads and trails, such as camp grounds, scenic stops, etc.

5.9 Acknowledgments

We are grateful to the Alberta Sustainable Resource Development's Forestry and Land's Divisions for financial and in-kind support. We are also thankful for the continuing support from Alberta Tourism, Parks and Recreation, the Ghost-Waiparous Stewardship Committee, and several industrial forestry organizations in Alberta and New Brunswick. We also acknowledge Mr. Xiangfei Meng regarding his role during the initial NSERC-SFMN supported TRAIL development phase.

5.10 References

Adruansen, F., Chardon, J., DeBlust, G., Swinnen, E., Villalba, S., Gulinck, G. 2003. The application of ‘least-cost’ modeling as a functional landscape model. Land Urb Plan 54, pp 233-247.

Atkinson, D., Deadman, P. Dudycha, D., Traynor, S. 2005. Multi-criteria evaluation and least cost path analysis for an arctic all-weather road. App Geo 25, pp 287-307.

Berry, J.K., 2001. MapCalc educational materials, with MapCalc academic software by Red Hen Systems, Fort Collins, Colorado, USA, [Online, Accessed Oct. 2011] www.redhensystems.com

Boldstad, Paul. 2002. GIS fundamentals. White Bear Lake, Minnesota: Elder Press.

Buckley, R.. 2004. Ecotourism book series, volume 2: environmental impacts of ecotourism. CABI publishing.

Census Division, Alberta finance. 2010. Alberta population projection report (2010-2050) [Online, Accessed Jul. 2011]. Alberta Government. http://www.finance.alberta.ca/aboutalberta/population_reports/2010-2050-alberta-population-projections.pdf

Chung, W., Sessions, J. 2001. Designing a forest road network using heuristic optimization techniques. Proceedings of the 24th meeting of the Council on Forest Engineering, July 15-19, Snowshoe, West Virginia.

Collischonn, W., Pillar, J. 2000. A direction dependant least cost path algorithm for roads and canals. Int J Geo Inf Sc 14, pp 397-406.

Crawford, M. 2008. An analysis of terrain roughness: Generating a GIS application for prescribed burning. MSc. Range Science thesis. Texas Tech University.

Cromley, R., Hanink, D. 1999. Coupling land-use allocation models with raster GIS. J Geo Sys. 1, pp 137–53.

Dijkstra, E. 1959. A note on two problems in connexion with graphs. Numer Math I, pp 269-271.

Eckert, R., Wood, M., Blackburn, W., Petersen, F. 1979. Impacts of off road vehicles on infiltration and sediment production of two desert soils. J Rng Mngmt 32, pp 394-397.

Epstein, R., Sessions, J. 2001. PLANEX: A system to identify landing locations and access. 11th International Mountain Logging and Pacific Northwest Skyline Symposium, Seattle, Washington, USA.

Forman, R., Alexander, L. 1998. Roads and their major ecological effects. Annu Rev Ecol Syst 29, pp 207-231.

Heralt, L. 2002. Using the ROADENG system to design an optimum forest road variant aimed at the minimization of negative impacts on the natural environment. J For Sci 48, pp 361-365.

Johnson, K.N. 1986. FORPLAN version 1: An overview. Washington, D. C.: USDA Forest Service, Land Management Planning Systems Section, Washington, USA.

Kautz, R. Kawula, R., Hoctor, T. 2006. How much is enough? Landscape-scale conservation for the Florida Panther. Bio Cons 130, pp 118-133.

Keays Software. 2007. The Integrated Solution for Civil Engineering and Surveying Software [Online, Accessed Nov. 2011] http://www.keays.com.au/root.php?path=field&m0=1&m1=2

Lambert, J., Joshi N., Peterson, K., Wadie, S. 2007. Coordination and diversification of investments in multimodal transportation. Public Works Management and Policy. 11, pp 250-265.

Malczewski, J. 2004. GIS-based land-use suitability analysis: a critical overview. Prog Plan 62, pp 3–65.

Miller, W., Collins, M. G., Steiner, F. R., Cook, E. 1998. An approach for greenway suitability analysis. Landscp Urb Plan 42, pp 91–105.

Moreno, M., Levachkine, S., Torres, M., Quintero, R. 2003. Geomorphometric analysis of raster image data to detect terrain ruggedness and drainage density. Lecture Notes in Computer Science. 2905, pp 643-650.

Murphy, P., Ogilvie, J., Arp, P. 2009. Topographic modeling of soil moisture conditions: a comparison and verification of two models. Eur J Soil Sci *60, pp 94-109.*

Nonis, C., Varghese, K., Suresh, K. 2007. Investigation of an AHP based multi criteria weighting scheme for GIS routing of cross country pipeline projects. 24th Int Sym on Aut and Rob Constr, ISARC, Sept 23-28, India.

Ray N. (2005) PATHMATRIX: a GIS tool to compute effective distances among samples. Mol Eco Notes 5, pp 177-180.

Reutebuch, S. 1988. ROUTES: A computer program for preliminary route location. Pacific Northwest Research Station, Forest Service, Department of Agriculture, U.S.

Riley, S., DeGloria, S., Elliot, R. 1999. A terrain ruggedness index that quantifies topographic heterogeneity. Intermtn J Sci. 5, pp 23-27.

Rogers, L. 2005. Automating contour-based route projection for preliminary forest road designs using GIS. Master thesis pp 187, University of Washington.

Rooney, T. 2008. Distribution of ecologically invasive plants along off road vehicle trails in the Chequeamegon national forest, Wisconsin. The Mich Bot 44, pp 178-181.

Rothwell, R.L. 1978. Watershed management guidelines for logging road construction in Alberta. Information Report NOR-X-208. Northern Forest Research Centre. Canadian Forest Service. Edmonton, Alberta, Canada. pp 43.

Schiess, P. and O'Brien, L.M. 1995. The application of geographic information systems to forest operations: the integration of cable setting design into GIS. Second Brazilian Symposium on Timber Harvesting and Forest Transportation. Salvador, Bahia, Brazil.

Sessions, J., Akay, A., Murphy, G. 2006. Chapter 5: Road and harvesting planning and operations. Computer Applications in Sustainable Forest Management. Springer. Netherlands, pp 83-99.

Shah,V.B. and B.H. McRae. 2008. Circuitscape user guide. Santa Barbara: Univeristy of California.

Slaughter, C., Racine, C., Walker, D., Johnson, L., Abele, G.. 1990. Use of off road vehicles and mitigation effects in Alaska permafrost environments: a review. Environ Manage 14, pp 63-72.

Snyder, S., Whitmore, J., Schneider, I., Becker, D. 2008. Ecological criteria, participant preferences and location models: A GIS approach toward ATV trail planning. App Geo 28, pp 248-258.

Tucek, J. and Pacola, E. 1999. Algorithms for skidding distance modeling on a raster digital terrain model. Int J For Eng 10, pp 67-69

Vaught, J. 2008. Proceedings of the 7th Python in Science Conference. Pasadena, CA, August 19-24. pp 62-66.

Vega-Nieva, D., Murphy, P., Castonguay, M., Ogilvie, J., Arp, P. 2008. A modular terrain model for daily variations in machine-specific forest soil trafficability. *Can J S Sci 89, pp 93-109.*

Vianova. 2006. Introduction of products: The most complete infrastructure design system. Vianova Systems AS Company [Accessed Nov. 2011]. http://www.novapoint.com/index.asp?id=23421&it=13

Weaver T., and Dale, D. 1978. Trampling effects of hikers, motorcycles and horses in meadows and forests. J App Ecol 15, pp 451-457.

Webb, R., Wilshire, H.. 1983. Environmental effects of off road vehicles. New York. Springer. pp 534.

Wilshire, H., Nakata, J., Shipley, S. Prestegaard, K. 1978. Impacts of vehicles on natural terrain at seven sites in the San Francisco Bay area. Enviro Geo 2, pp 295-319.

Xiang, W. 1996. A GIS based method for trail alignment planning. Land Urb Plan, 35, pp 11-23.

Chapter 6 : Concluding Remarks

6.1 Thesis Summary

1. A literature review was conducted to provide background on the major concepts introduced. Special reference was given to soil trafficability parameters and their deduction, soil moisture modeling and GIS process towards improved linear feature location with particular interest focusing upon DTM collection methods;
2. A GIS tool was created that features a user friendly GUI and addresses most common factors that are in need of consideration when contemplating sustainable routing under cost saving necessities;
3. Field research was conducted to quantify the resistance of soil penetration including potential rutting induced by recreational vehicles such as ATV from ridge to depression.
4. The results of this quantification showed that the resistance to soil penetration was directly related to soil texture, bulk density, and moisture content, and indirectly to the DEM-derived depth-to-water index as follows:

   $\log_{10}$CI(10cm depth0 = 0.27(±0.04) + 0.283(±0.011) log10DTW - 0.00041(±0.00003) Elevation; R^2=0.47; RMSE=0.27.

5. The above relationship was used to model and map CI and ATV-specific rutting depths (10 passes) for both study areas. The maps so generated were generally consistent with the plot-specific CI determinations.
6. The trail damage survey within the study area indicated that the the severity of trail-induced soil disturbances: about 70% of the ATV-induced damage occurred in areas for which DTW < 5 m, as mapped.

6.2 Original Contributions

1. This thesis is the first to present and examine soil trafficability data in conjunction with LiDAR derived WAM and DEMs.
2. This thesis developed an interpretation of the cartographically derived DTW index in terms of soil resistance to penetration and potential machine/load rutting depth.
3. The methodology so established is consistent with literature studies and reports dealing with soil penetrability and soil trafficability.
4. This thesis introduces a new GIS-based least-cost trail delineation tool. This tool is useful for evaluating and optimizing existing road and trail segments, and for establishing new trail networks based on user preferences dealing with, e.g., minimizing trail costs and potential risks pertaining to trail failure (e.g. washouts, braiding) due to crossing wet areas and flow channels.

6.3 Suggestions for Further Work

1. Improve field protocol for soil trafficability testing: (i) use smaller diameter cone to capture the linearity between soil resistance to penetration above 3 Mpa; (ii) improve consistency in soil core aggregation; (iii) increase transect and sample size to deal with variations in soil substrate across the landscape.

2. Do soil moisture and CI determinations in direct relationship with actual depth to water

3. Relate field-determined soil moisture levels and CI to antecedent and current weather conditions.

4. Perform a rut depth study, to confirm model-predicted rutting depth with increasing number of vehicle passes, based on ground conditions that vary from coarse to fine textured and from dry to moist to wet.
5. Add additional features to the Trail TOOL: viewshed preferences, add engineering methods to improve the methods used for trail- and road-specific smoothing and cut & fill requirements; optimize trail locations based on costs instead of and/or in addition to user-perceived risks and preferences.
6. Conduct a soil disturbance comparison study between TRAIL and non-TRAIL developed trail segments.
7. To migrate the TRAIL tool to a VB.NET stand-alone platform. Doing so would remove the dependency of the tool to be contained within an ArcMap project;

APPENDIX A

THE TRAIL TOOL

USER MANUAL

1.0 Introduction

This document informs about the usage of a linear feature planning tool developed for ARCGIS 9.3. The processes and functions of TRAIL features are outlined within this document. The purpose of this tool is to assess the risks present on the landscape, through the assessment of user inputs and risk tolerances, and create a trail that mitigates this risk.

TRAIL route planning software will allow the user to:

1. assess the potential locations for new trails given various risks and risk tolerances
2. assess a current trail networks in terms of risky segments of trails and offer alternatives to these segments (remediation)
3. produce multiple alternatives to any one routing problem and assess legitimacy utilizing trade-off analysis
4. identify bottlenecks in risk on the landscape.

2.0 Requirements

The TRAIL tool requires the following:

1. ARCGIS 9.3 (ARCGIS minimum system requirements)
2. spatial analyst license of ARCGIS 9.3
3. recommended free disk space proportional to largest raster under analysis ('X' x 10)
4. digital elevation model (DEM)
5. start and end locations of a desired trail.

Without any one of these requirements, the tool will not operate. Please contact your ARCGIS license holder to attain proper licensing and products.

3.0 Definitions

Risk Map - Individually loaded or created rasters originating from user button clicks and tool processing.

Punishment grid – The combined, final risk map containing all risk maps and their associated penalty considerations

Penalty – Selectable, slide-bar created values that are applied to risk maps to create the punishment grid.

First/Last Return LiDAR Data – The LiDAR process involves multiple returns from laser pulses. The last return is typically the bare ground, the first typically the highest vegetation.

4.0 Abbreviations

TRAIL – Trail Routing, Analysis, and Investigative Layout
GUI – Graphic User Interface
DEM – Digital Elevation Model
LUZ – Limited Use Zone
FA – Flow Accumulation

LiDAR – LIght Detection And Ranging

5.0 Overview

Upon starting the ArcMap project containing the TRAIL tool, the TRAIL icon will be displayed in the toolbar at the top of the screen (Figure 1). The graphic user interface (GUI) is initiated upon pressing this icon (Figure 2). The TRAIL tools GUI contains 6 tabs:

- load data
- transportation
- rutting sensitivities
- qualities
- sensitivities
- routing options

5.1 Load data

The 'load data' tab is the initial tab of the TRAIL GUI. This tab prompts the user to:

6. select an analysis window and raster cell size
7. define output feature location
8. define input feature locations
9. execute feature creation routines
    g) create slope raster
    h) create terrain ruggedness raster
    i) create cut and fill raster
    j) create culvert sizing raster
    k) create vegetation heights/density rasters
    l) create/load flow accumulation raster
10. indicate longest vehicle length
11. Indicate the desired road width.

Critical for minimal operation are:

7. select an analysis window and raster cell size
8. define output feature location
9. load default raster
10. load DEM
11. when culvert sizing and/or WAM values are to be defined the stream layer is also critical.

NOTE: If a feature class or raster is empty (i.e. no features are present), the tool will crash. Ensure all loaded data has information stored within.

5.2 Transportation

The ‘transportation’ tab is designed to:

1. link user transportation type id’s to tools memory
2. allow for the remediation of current trail networks
3. utilize seismic lines in route design

This tab is optional and is not critical for tool operation.

5.3 Rutting sensitivities

The ‘rutting sensitivities’ tab is to be utilized when considering vehicular impacts upon soils. This section allows the user to:

1. input unique specifications detailing route user types
2. select pre-defined user types from a selection list
3. account for the amount of use expected for the route
4. select the aversion to rutting

This tab allows for the detailing of the landscape in terms of its soil trafficability by vehicle type. This tab is optional and is not critical for tool operation.

5.4 Sensitivities

The ‘sensitivities’ tab allows the user to begin assessing the major risks to routing problems. This tab enables:

6. Indicate aversion to crossing slopes of defined limit
7. indicate aversion to crossing stream channels
8. indicate aversion to wet area crossing
9. apply wet area avoidance protocols to distance routes from wet areas
10. indicate aversion to earth moving (cut and fill)
11. apply avoidance factors to user defined limited use zones (LUZs)

This tab is **NOT** optional. At a minimum, the slope ‘use/don’t use’ check box must be selected and slider set to ‘0’.

5.5 Qualities

The ‘qualities’ tab allows the user to account for the desired traits of the route to be created. This section allows the user to:

6. account for ‘cost’ of trail blazing
7. manage the size of forest clearings encountered and their frequency
8. create easy-difficult trail types (skill level) and place importance on the maintenance of specified trail type through terrain ruggedness level management
9. apply length of route considerations, leading to elongated-shortened routes while considering landscape risks
10. apply intelligent stream/WAM rasters utilizing flow accumulation

This tab is optional and is not critical for tool operation.

5.6 Routing Options

The ‘routing options’ tab is used to finalize data layers, create route alternatives, and create route information tables. The tab is broken into 4 separate buttons:

5. build sensitivity map
6. build route – containing:
    a) set road width
    b) load end point
    c) load start point
    d) begin route analysis
7. create route information table
8. exit

The ‘routing options’ tab allows the user to:

1. rasterize user inputs and risk tolerances into a single punishment grid
2. define beginning and end points
3. create tables detailing the properties of created trails
4. exit process without losing loaded data.

This tab is **NOT** optional. End condition produces a route and a route information table detailing specifics of trail-terrain interactions.

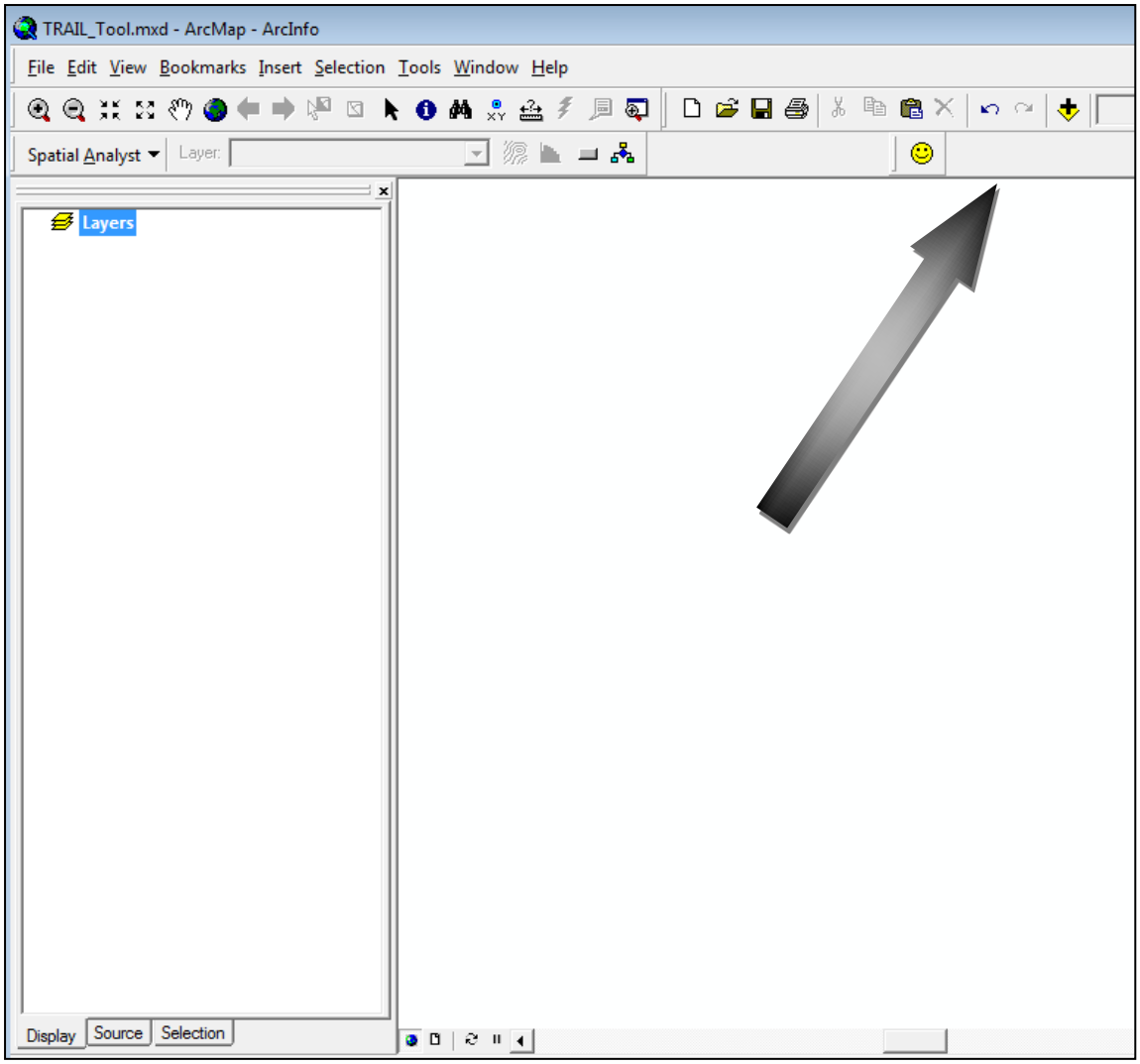

Figure 0.1 The TRAIL tool ArcMap project and location of icon containing tool functionality.

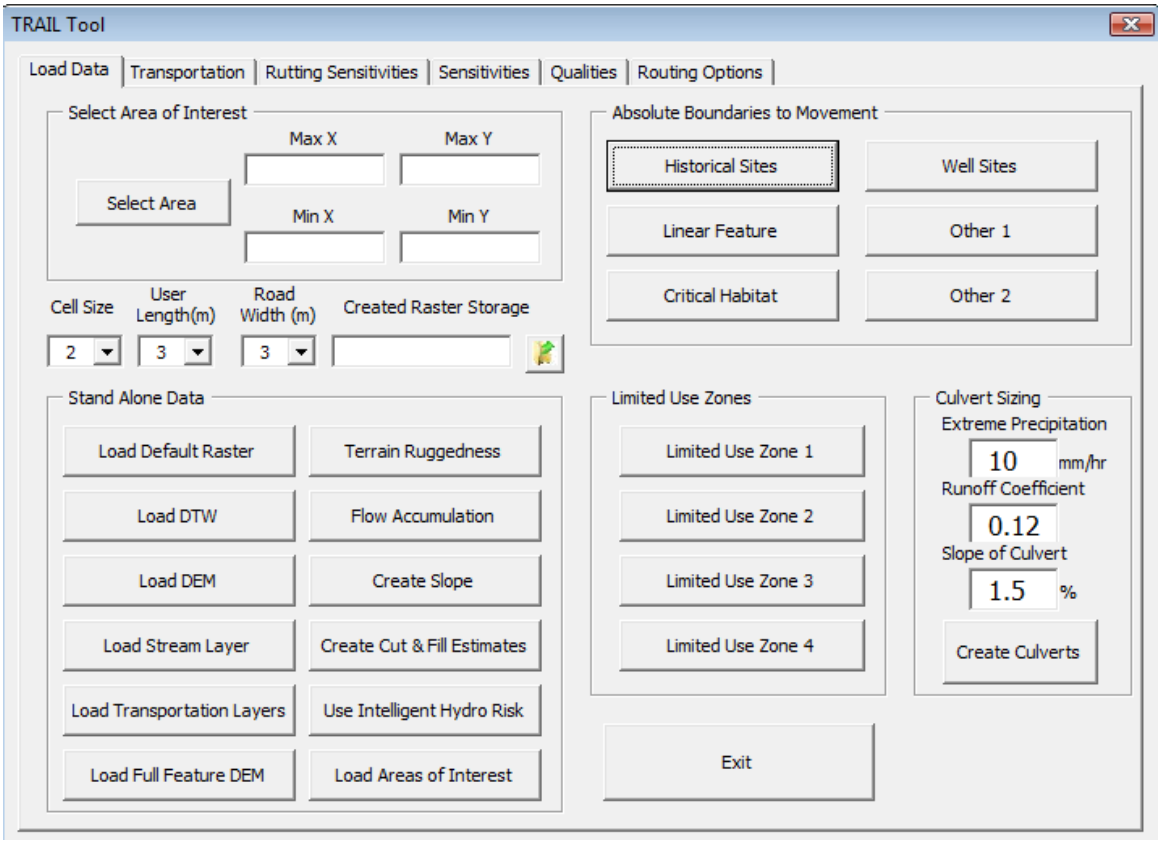

Figure 0.2 The leading tab of the TRAIL tools GUI. Users select operating area, define input feature locations on hard drive, run layer creation routines, and select analysis cell size, output location on hard drive, and vehicle lengths.

6.0 In detail

The independent zones within each tab are identified and explored. Inner functionality is flushed out for a better understanding of what each button does in the background. With a better understanding for how the tool interprets inputs, improved utilization of the tool will follow.

6.1 Penalty Value Assignment

Friction surface creation involves the contemplation of a number of problems before analysis can proceed. Raster source issues and the number of considerations to be analyzed have to be recognized in any solution and are addressed within the TRAIL tools code. Combine the fact that not all GIS layers are in the same value ranges (Miller et al., 1998), and that every user has a variable view on what constitutes risk, the creation of a usable, intuitive friction surface, becomes difficult.

Power functions and variable dependant scaling are proposed as the solution to appropriate value assignments. Power functions behave in a favorable manner when

scaling values from 0-2. Utilizing root powers to scaled values of 0-1 create decreasing values with increasing risk and utilizing basic powers with scaled values of 1-2 create increasing values with increasing risk. As the perception of risk increases, so does the difference between values representing various risk levels. Thus, variables that require thresholding (slope, WAM, etc.) can be scaled to 0-1 for favorable areas, and 1-2 for unfavorable. Values that do not require thresholding are scaled between 1-2. The only variables that are scaled in this manner are those that do not have positive areas available for travel (i.e. cut and fill, and rut depth).

Another advantage to this method is that LCP does not assume high risk values as barriers to movement. Risk is applied as a continuum of values on a non-linear track, preventing movement into the next level of risk through creating cost associated in doing so. The TRAIL tool utilizes this method and allows users to assign their perception of risk within a slidebar representing values of 0.1, 0.25, 0.33, 0.5, 1, 2, 4, 6, 8, and 10. These values are the power to which scaled variables are raised. All created and loaded data are scaled and penalized according to the method described above.

Miller, W., Collins, M. G., Steiner, F. R., and Cook, E. (1998). An approach for greenway suitability analysis. Landscape and Urban Planning, 42, 91–105.

6.2 Load Data

The initial tab of the TRAIL GUI is ‘load data’ and must be addressed first when beginning any routing exercise utilizing the TRAIL tool. This tab contains 6 sections aimed at bringing all data into one location and instigating the creation of various risk maps as needed. Following is a detailed look at each section outlining the functionality and inner workings behind each button.

6.2.1 Select area of interest

This feature has been incorporated into the TRAIL tool to reduce processing times in calculations. The larger the area, the more processing time that is required. Upon loading a geo-referenced layer to ArcMap, zoom into the area that contains, at minimum, the minimum bounding rectangle of where your start and end points will be. The zoomed in area is the only area that will be processed.

> **NOTE:** If your start or end point falls outside of this area, the tool will crash; if the area is not large enough, the tool will produce routes that follow the boundaries of the rectangle. Trial and error for containing the route may be necessary; however, reducing restrictions upon constraints applied to the trail will mitigate this effect. Generally, the larger the minimum bounding rectangle of the start and end points, the larger the ‘area of interest’ should be.

Once a suitable ‘area of interest’ fills the view, click the actionable button ‘select area’; the formerly empty text boxes, labeled max-min y and x, fill with the geo-referenced corner points of the view. Figure 3 visualizes this process.

Figure 0.3 Utilizing the ‘select area of interest’ section of the ‘load data’ tab visualized.

6.2.2 Analysis settings

This section of the GUI applies to all further sections, thus has not been included as a stand-alone section within the tab. As detailed by Figure 4, analysis ‘cell size’, 'user length', 'road width' and ‘created feature storage’ is required to be entered.

‘Cell size’ has been included as an option in order to reduce processing times. Starting at larger cell size values to begin assessment of routes is a valuable method of saving time in analysis. As trends or information begin to emerge through multiple scenario analysis, results at a higher level of detail can be attained for preferred routes by reducing the cell size to original values.

‘User length’ is an optional setting. The default is 3 meters. This setting affects the neighborhood analysis window of kernel based processes such as ‘cut and fill’, ‘slope’, or ‘terrain ruggedness’. The larger the trail user, the larger of an area required in analysis.

'Set road width' allows the user to define the width of the desired route in meters. The default is 3 meters. This setting affects the neighborhood analysis window of kernel based processes such as ‘cut and fill’, ‘slope’, or ‘terrain ruggedness’. The larger the trail user, the larger of an area required in analysis.

‘Created feature storage’ is a required setting which informs the tool on where to place created information. The folder that is chosen is required to be empty. Once files are created in this folder they **CAN BE OVERWRITTEN**, allowing for seamless movement between analysis areas. However, for any one analysis area it is recommended that it have its own folder. This will assist in organization, but will require more hard disk space.

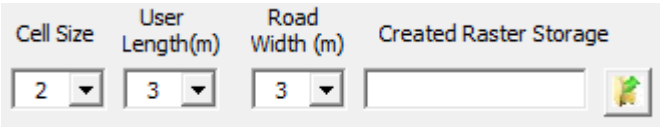

Figure 0.4 Analysis settings for all created and loaded information into the TRAIL tool. For each new analysis area, a new, empty, folder is required to be created and pointed to.

6.2.3 Stand alone data

This section of the lead tab of the TRAIL GUI contains the location where users are to define locations of pre-existing rasters/layers and create new information pertinent to the project. The left hand side of Figure 5 are existing data sources that are in need of definition (a definition layer); whereas the right side are the creatable layers (a creatable layer), outside of ‘load areas of interest’, which is a definition layer.

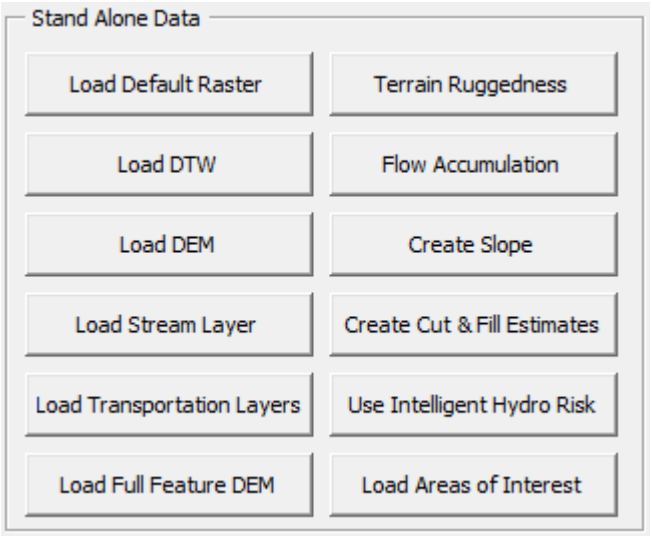

Figure 0.5 The leading tab of the TRAIL GUI where users direct the tool to data locations and create new data through loaded actionable buttons.

6.2.3.1 Load default raster. The 'load default raster' button has been designed to ensure the correct spatial referencing characteristics are locked up in memory. The information contained in this dataset follows through to all outputs. While it is not necessary to have all other loaded data layers with spatial referencing, it is always advisable. This raster is a component of each raster creation to ensure spatial misalignments do not occur.

6.2.3.2 Load DTW. The 'load DTW' button triggers a load data call up window where the user points to the location of the depth-to-water map (DTW; wet area map (WAM)). Values of 0 in the DTW map are removed from the final DTW raster and are accounted for by the stream layer if one is loaded. This assures no double counting of stream features. If a stream layer is not loaded, the DTW raster maintains its 0 values. Wet areas are defined within the tool as any area within the 0 – 50 centimeter value range of the DTW.

6.2.3.3 Load DEM. The 'load DEM' button triggers a load data call up window where the user points to the location of the digital elevation model. This raster is used in multiple instances throughout the tool.

6.2.3.4 Load stream layer. The 'load stream layer' button triggers a load data call up window where the user points to the location of the DTW produced stream layer. All streams are assigned a value of 2; other areas are assigned a value of 0.

6.2.3.5 Load transportation layers. The 'load transportation layers' button triggers a pop-up window which is displayed in Figure 6. This interface categorizes layers available for transportation into 3 classes: roads, trails, and seismic lines. If your database contains more than one shapefile for any one of these classes, they must be merged. Within each button, the user is asked to specify which field contains the reference values for type of feature; i.e. 'primary highway' = 0, 'tertiary forest road' = 6.

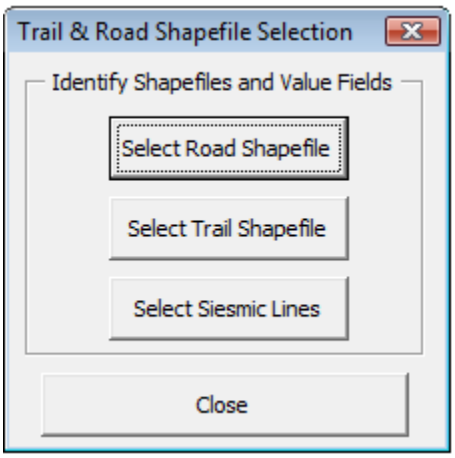

Figure 0.6 The load transportation pop-up allowing for the locating of any layers that have linear features available for transport.

6.2.3.6 Load full feature DEM. This feature is typically only usable while using LiDAR models of terrain. The 'load full feature DEM' button triggers a load data call up window where the user points to the location of the full feature digital elevation model. Once loaded, a vegetation raster is created estimating the heights and density of the "first return" LiDAR data. In this work, full feature LiDAR data (FFLD) can be used to assist in representing vegetation heights and relative abundance for predicting related movement issues.

Extracting vegetation heights from the data is the primary step. This is accomplished through subtracting the Bare Earth DEM (BEDEM) from the FFLD (Figure 7). Vegetation heights are then grouped into classes (Table 1). Relative abundance of vegetation are derived by classifying heights as either present (0.5 meters plus) or not present (0 to 0.5 meters) and summing the numbers on a 3 by 3 kernel grid system (0 - 9 values, Figure 8).

Based upon the self-thinning rule (Reineke (1933), it is assumed tree spacing increases with increasing tree height. This premise logically aids in the creation of a movement constraint matrix for vegetation (Figure 9). Utilizing this matrix will result in the creation of a raster that will effectively identify easily-non accessible areas (Figure 10).

The classification of openings is made possible through utilization of the presence and non-presence raster. Locations with no presence of vegetation are grouped and assigned an area. Once users proceed to the 'routing options' tab with the 'opening avoidance' check box active within the 'qualities' tab, the tool prompts for the definition of the maximum size of an opening to allow routing around. Areas larger than this threshold are avoided.

> **Note:** All values are deduced from the *first return* from LiDAR data. This means only the dominant canopy is considered. Understory beneath the canopy is not a part of this calculation and should be considered when inspecting actual routing.
>
> **Note:** LiDAR data is a snapshot in time of the conditions at that moment. Vegetation growth is variable while LiDAR data is static. Without updating LiDAR information, vegetation estimates will continually decrease in accuracy with time from original LiDAR capture date.

Reineke, L.H. (1933). Perfecting a stand-density index for even-aged forests. Journal of Agricultural Research 46, 627–638.

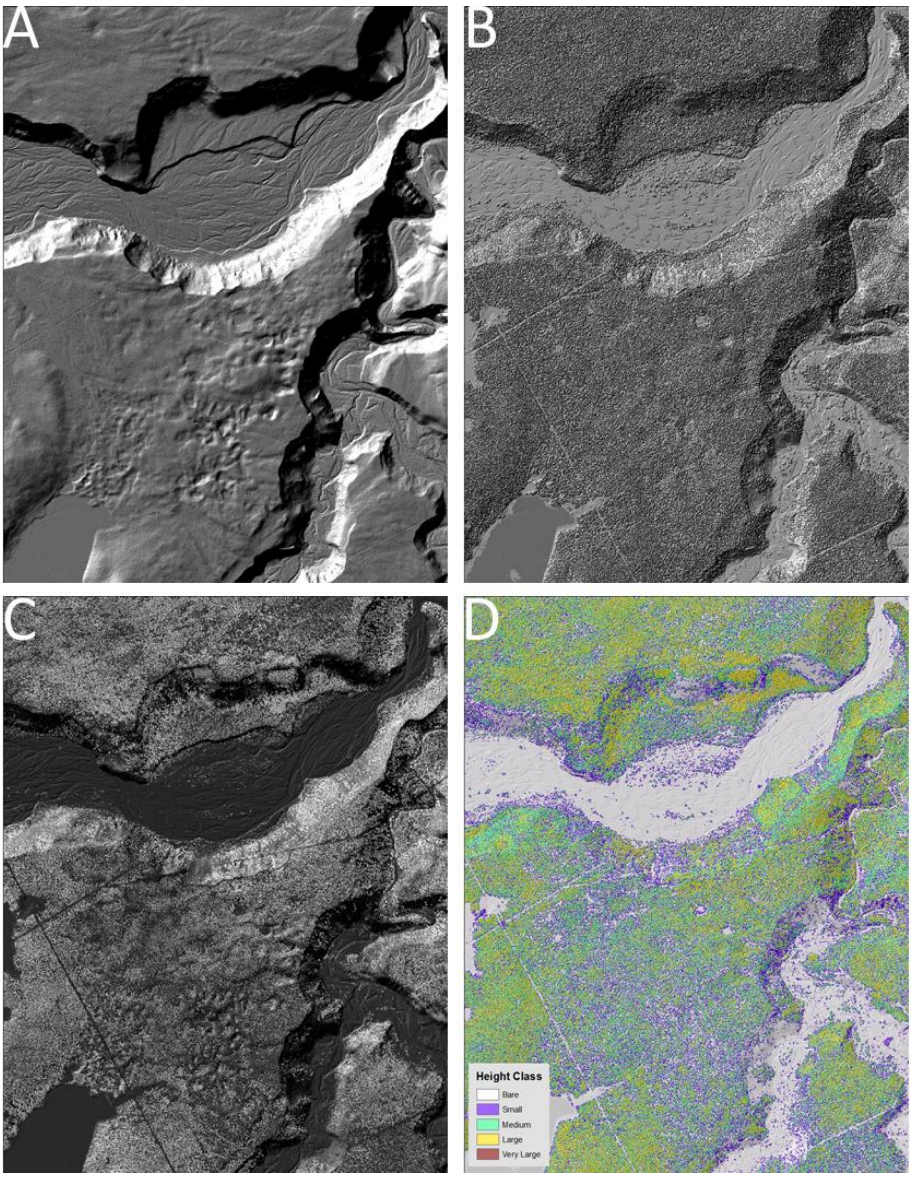

Figure 0.7 The rasters involved with height classification. a) BEDEM, b) FFDEM, c) Vegetation heights, d) Height classes.

Table0.1 Height class break down for penalty assessment.

Height Class	Height (m)	Value
Bare	0 to 0.2	1000
Small	0.2 to 4	2000
Medium	4 to 10	3000
Large	10 to 20	4000
Very Large	20 plus	5000

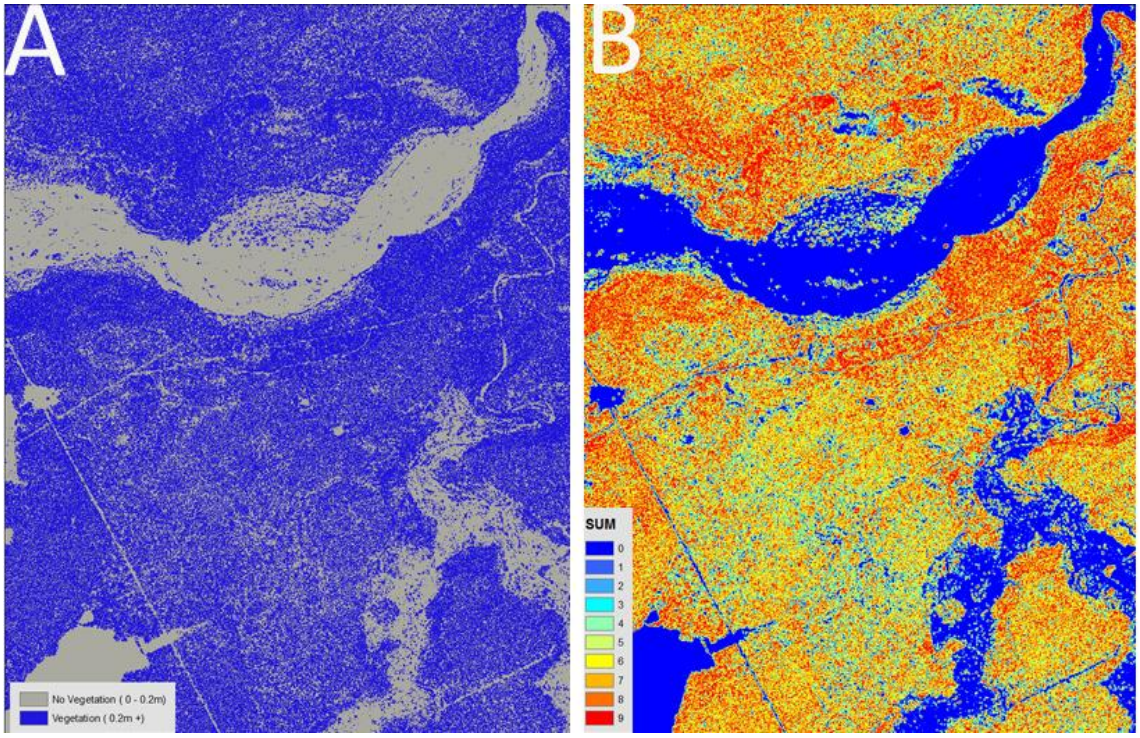

Figure 0.8 Method of determining vegetation abundance. a) Presence and non-presence of vegetation, b) 3 by 3 kernel sum of presence and non-presence (value range of 0-9).

Figure 0.9 The method of combining created density and height estimates into a single movement penalty for vegetation.

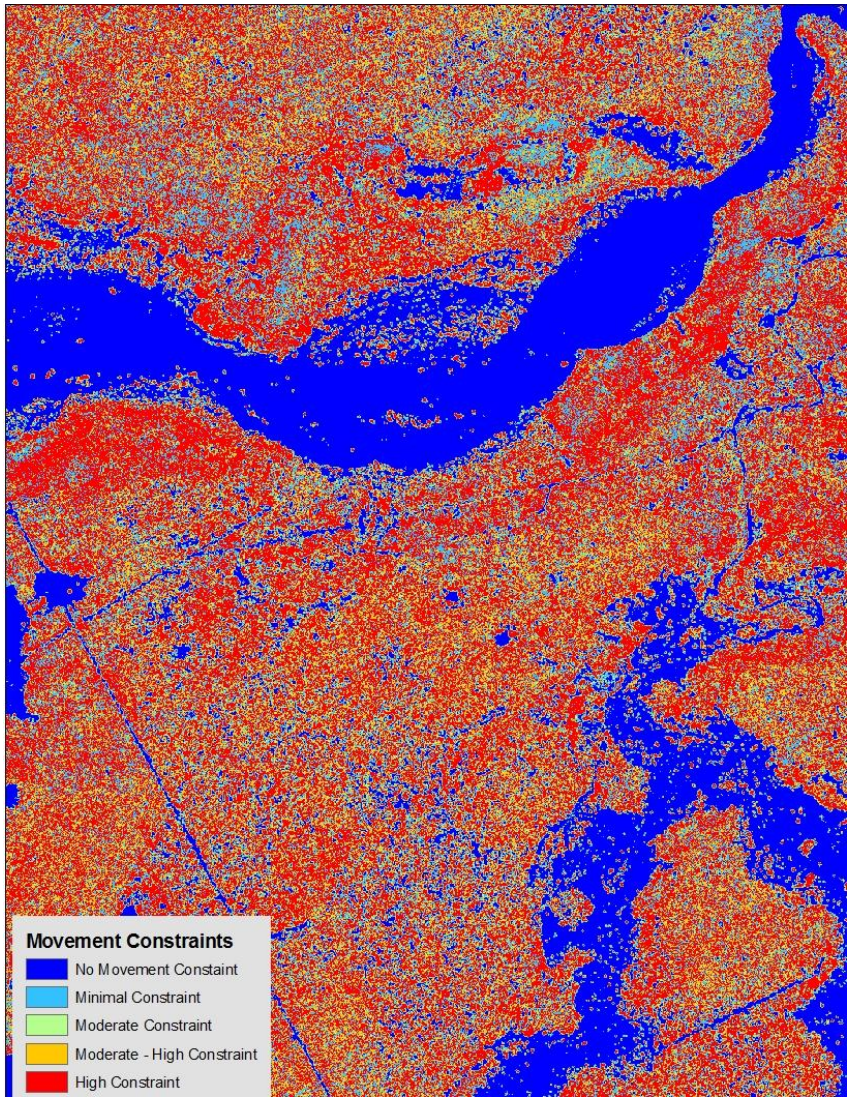

Figure 0.10 Vegetation movement constraint raster.

6.2.3.7 Create slope. This action button triggers the tool to search for the DEM and create a slope raster; if the DEM is not loaded the tool will instruct you to load it before continuing. Slope is calculated utilizing accepted ESRI methods.

6.2.3.8 Terrain ruggedness. This action button triggers the tool to search for the DEM and create a ruggedness raster; if the DEM is not loaded the tool will instruct you to load it before continuing. Terrain ruggedness is the relative evenness of the ground as viewed from ground level. The perception of ruggedness can change based on user size, skill level, and desire, and is required to be accounted for within the creation of a raster representing terrain ruggedness.

User size is accounted for within the 'user length' setting within the 'analysis settings' section of the 'load data' tab; the user length by 3 times the cell size defines the neighborhood of the kernel processes involved within the script. The terrain ruggedness

level and the desired maintenance of that level (how important it is to stay on the selected level of ruggedness) is set within the ‘qualities’ tab of the GUI.

The terrain ruggedness index (TRI), as theorized by Riley *et al.* (1999) and others, is based upon the absolute difference in elevation of the surrounding pixels within a 3x3 pixel block. Figure 11 (a-d) displays the formulation of this method (c) for a test area within a mountainous area versus a hillshaded DEM (a), a classified slope raster (b), and an alternative method of ruggedness prediction created for this work (d). Upon inspection, TRI over estimates ruggedness of hill slopes, under estimates rough areas, and mimics the classified slope map (regression analysis with 97% conformance).The TRI method of ruggedness prediction inherently implies steepness creates ruggedness. The ruggedness level map (d, RLM) is produced utilizing the absolute difference of the slope values within the ‘user size’ neighborhood kernel; removing the dependence upon similar high or low elevational differences and focuses upon the change from those similarities.

Riley, S., DeGloria, S., Elliot, R. 1999. A terrain ruggedness index that quantifies topographic heterogeneity. Intermountain journal of sciences. Vol. 5, No, 1-4, 23-27.

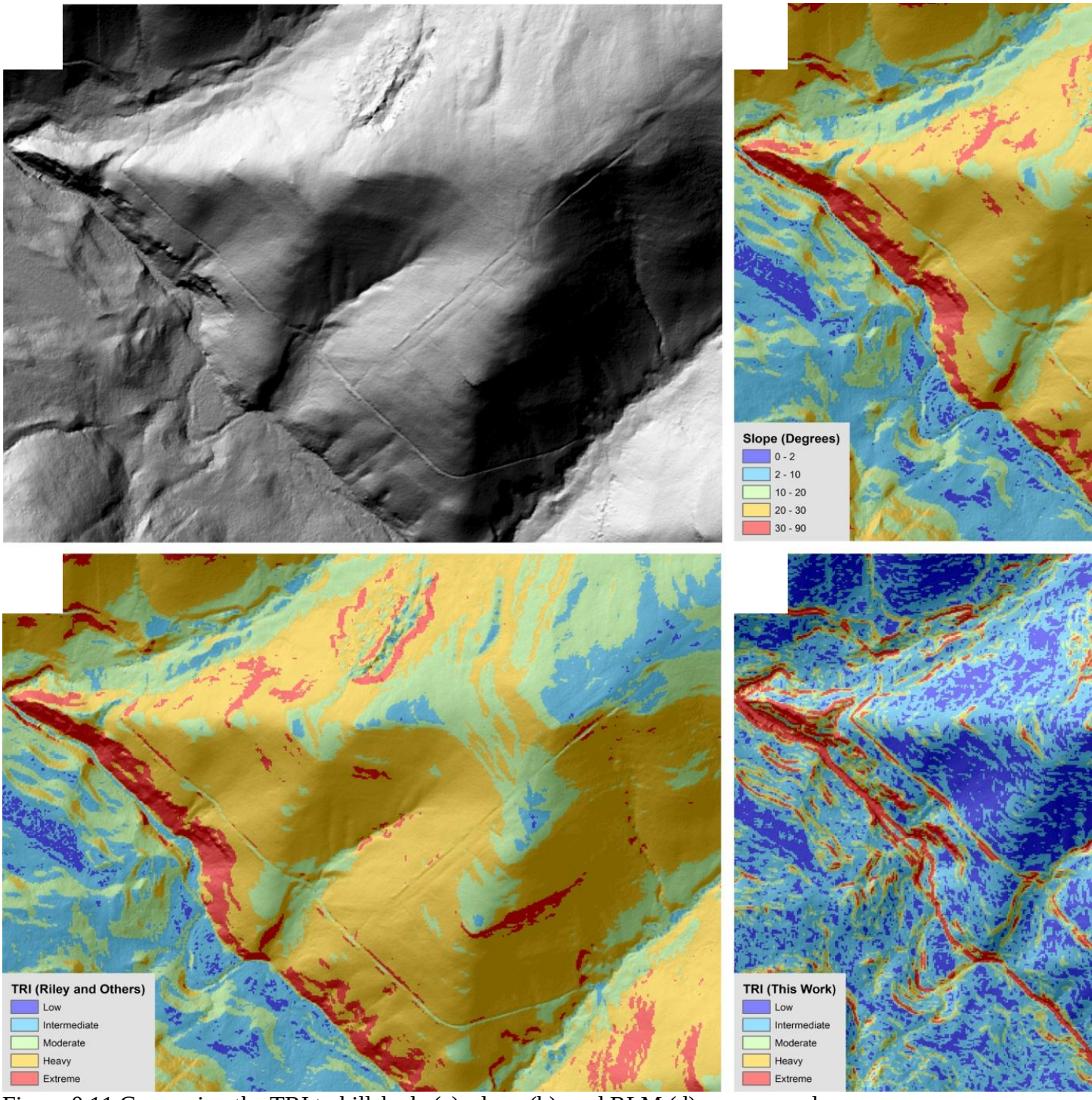

Figure 0.11 Comparing the TRI to hillshade (a), slope (b), and RLM (d) maps reveals the ambiguity of the TRI and the prevalence of the RLM for estimating the level of ruggedness on a landscape. A neighborhood window of 3x3 was used in creating both (c) and (d).

6.2.3.9 Flow accumulation. The TRAIL tool provides a platform for creating or loading flow accumulation. This platform is accessible once the 'flow accumulation' button has been triggered and is viewable in Figure 12.

Flow accumulation (FA) values are critically important to making accurate assessments to culvert sizes and to the creation of an intelligent hydrological feature penalty. When creating a flow accumulation grid it is vital to make one much larger than the area of operations. If you are loading an existing FA raster ensure it is from a larger dataset then the location of your area of operations. If you are using this tool to create the flow accumulation grid, the following steps are recommended:

1. Load the default TRAIL tool
2. Identify your area of operations and expand so that an area at least 10 times the size of your location is in the ArcMap view. Watersheds of all streams within your area of operations need to be in view for accuracy; the more of a watershed cut-off, the less accurate results will be.
3. Select an appropriate cell size for processing. If your DEM has 1m resolution use 1m; if 5m, use 5.
4. Load default, DEM, and stream layers.
5. Do not load any other data; proceed directly to the flow accumulation button.
6. Run the 'create new' FA button. Time varies with size, but usually hours are required.
7. Save this raster in a back-up location for re-use.
8. Reset the tool to default and start over with the correct size of the area of operations.

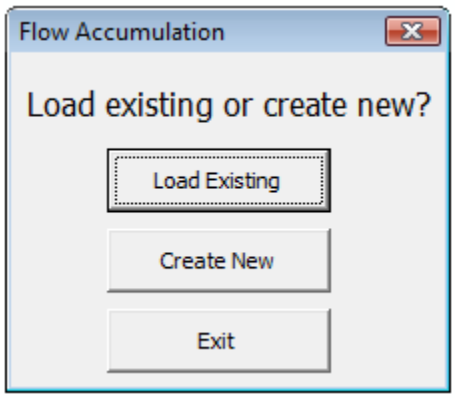

Figure 0.12 The platform for creating or loading a flow accumulation raster to the TRAIL tool.

NOTE: This process is highly dependent upon the continuation of flow channels; the crossing of a flow channel across DEM raster tiles, if processed separately, will yield incorrect FA values. FA calculations only utilize data that is loaded to predict drainage areas; if a stream continues from one tile into the tile you are working with, the FA value of that stream at that point is 0 when in fact, it is likely much larger than this. Again, ensure when processing DEMs for FA that all watersheds of

concern are contained within the same DEM and in view of the ‘area of operations’.

6.2.3.10 Create cut & fill estimates. This action button triggers the tool to search for the DEM and create a cut and fill raster (C&F); if the DEM is not loaded the tool will instruct you to load it before continuing. C&F relies on the assumption that the larger you are the more road bed smoothing required and vice versa. C&F is direction dependant; estimates are utilized for preliminary inclusion of C&F into risk maps.

The amount of C&F material is estimated by averaging the elevation values within the kernel and subtracting this output from the original DEM. These values are then multiplied by the square of the cell size to create the cell C&F amount. The cell C&F raster is summed across the pre-specified neighborhood kernel to yield the initial estimate of C&F material. Finalized C&F amounts are created through buffering of the created route by the road width and summing the cell C&F raster values within the created buffer instead of summing within a moving neighborhood window.

6.2.3.11 Use intelligent hydro risk. This button triggers the tool to search for the FA raster to assign a range of penalty values to streams and wet areas. In principle, this option assigns features high up in a watershed lower penalty values then those incurred lower in a watershed, effectively saying wet areas and stream channels high in a watershed are less costly to crossing then further down in a watershed. Figure 13 illustrates this process.

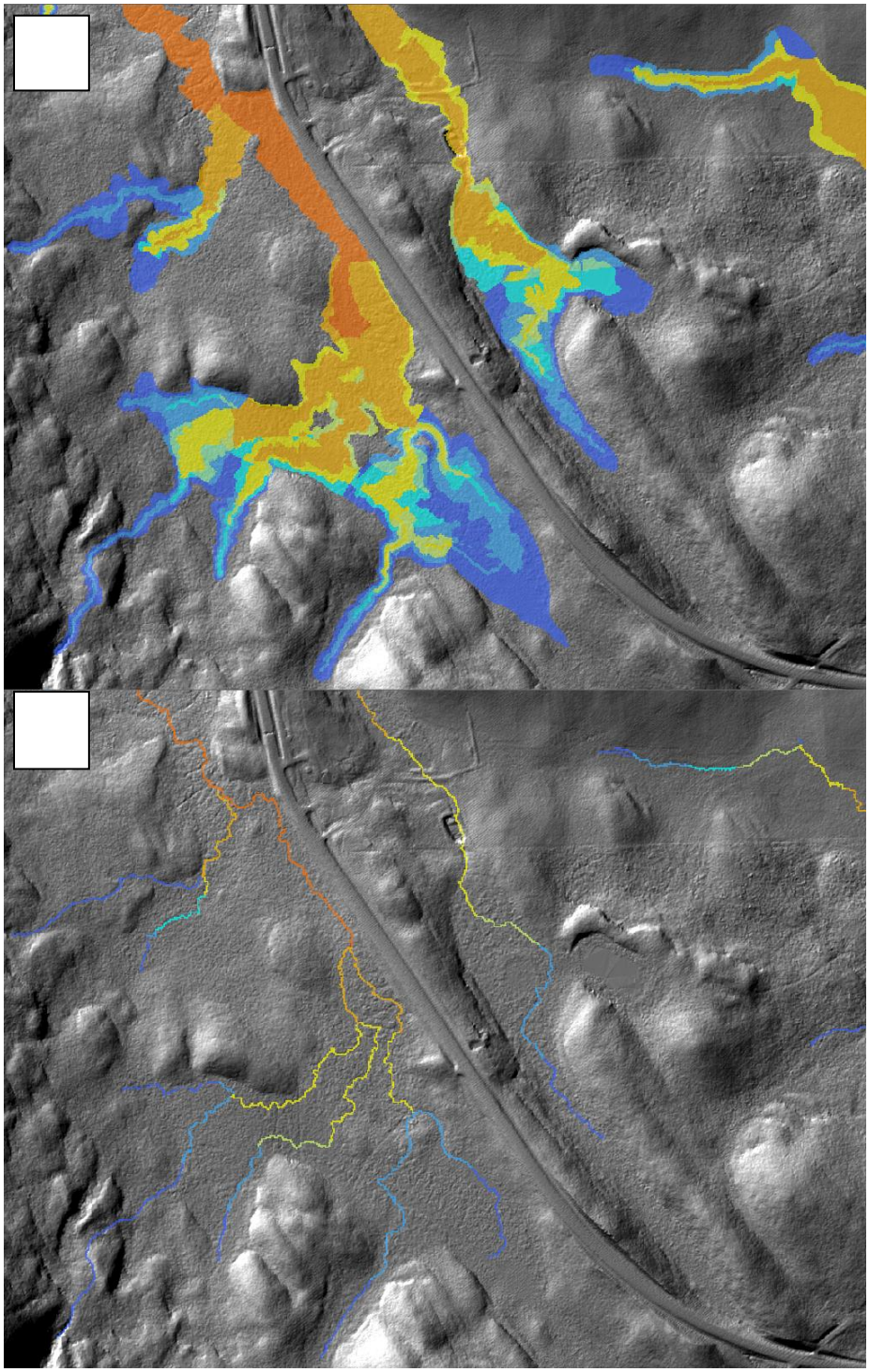

Figure 0.13 Result of the ‘use intelligent hydro risk button’. Utilizing FA and loaded WAM/DTW (a) and stream layers (b), the tool assigns risk to these areas as a function of their relative position on the landscape.

6.2.3.12 Load areas of interest. The ‘load areas of interest’ button triggers a load data call up window where the user points to the location of areas that are preferred to be accessed, but not critical to trail construction. Only one raster/shapefile may be loaded, thus for multiple location analysis, files must be merged into 1 single file. For locations that are critical for access, utilize these locations as a start or end points and analyze.

6.2.4 Absolute boundaries to movement

Each button within this segment of the TRAIL tool triggers a load data window entailing the loading of data towards the removal of segments from within the area of operations. Some locations may be completely un-traversable such as, but not limited to: unique areas, historical sites, and critical habitat. The tool loads the selected datasets (raster or shapefiles) and creates NODATA holes within the punishment grid. NODATA holes are impassable, and require the tool to critically avoid. This may lead to infeasibilities.

6.2.5 Limited use zones

Each button within this segment of the TRAIL tool triggers a load data window entailing the outlining of zones that are accessible under extreme prejudice. Figure 14 details the concept of the limited use zone (LUZ) penalty assignment criteria. Upon triggering a LUZ button, the user is tasked with identifying a layer and the distance from feature where no penalty for proximity is to occur. The area that is loaded is assigned maximum penalty (not absolute barrier values) with decreasing values to the distance specified.

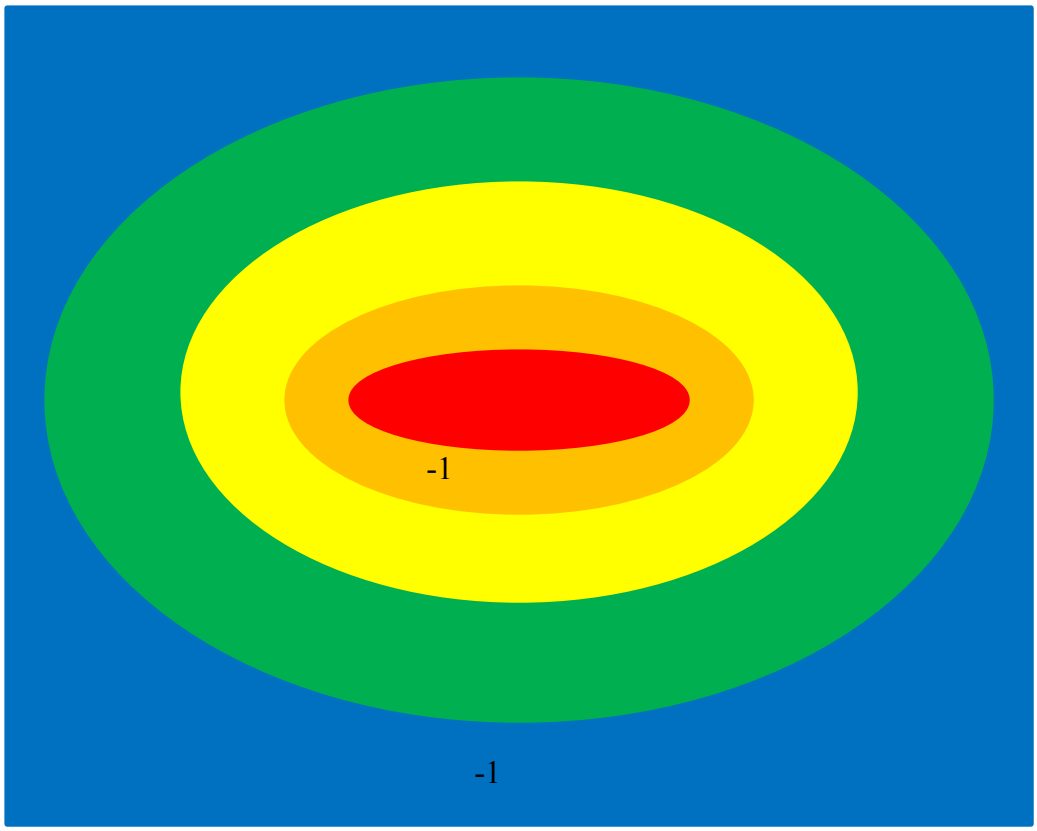

Figure 0.14 An example of how the LUZ penalty system works. User loaded data is essentially buffered and assigned increasingly larger values the closer to the core one gets.

> **NOTE:** It is advisable that all like feature types are merged into one final LUZ layer per type (i.e. polygon, point, or polyline).

6.2.6 Culvert sizing

The 'culvert sizing' segment of the TRAIL tool contains functionality to calculate culvert sizing along all stream channels given (i) extreme precipitation, (ii) the runoff coefficient, (iii) the slope for the installed culvert, and (iv) flow accumulation. Figure 15 displays the culvert sizing segment of the TRAIL tool. The information within the text boxes are utilized as part of equations for creating the culvert sizing utilizing scientific methods developed by the ConDOT (2000), UW-M (2007) systems and Rothwell (1978) employed Manning equation (1889). Flow accumulation is used as a major part of the calculation.

6.2.6.1 Extreme precipitation. This text field is to be filled with the 50 or 100 year maximum precipitation amount that has fallen in 1 hour, in millimeters. The rate can be changed to gauge effect upon culvert size requirements.

6.2.6.2 Runoff coefficient. The runoff coefficient is the percent of precipitation that does not penetrate the surface and contributes to 'flash' increases to a flow channels width

and flow rate. Every surface has a different runoff calibration, however, without detailed soil maps for an area, detailed accounting of this variable is difficult. Utilizing Table 2 as a guide for typical values for 3 terrain types, average values can be assigned.

6.2.6.3 Slope of culvert. This text box allows for the accounting of slope angle in placement of culverts. Generally, values range from 1 to 2%. These values will affect the flow rate of water through the culvert, effecting culvert width requirements.

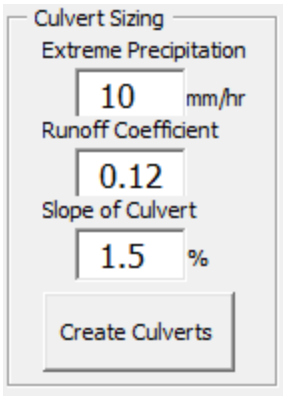

Figure 0.15 The 'culvert sizing' segment of the TRAIL tool with the pop-up window used to create a culvert sizing grid based upon flow accumulation and definable parameters.

Table0.2 Determining runoff coefficients based on slope percent (Frevert et al. 1955)

Slope (%)	Open Sandy Loam	Clay and Silt Loam	Tight Clay
0-5	0.10	0.30	0.40
5-10	0.25	0.35	0.50
10-30	0.30	0.50	0.60

ConDOT. 2000. Chapter 11.5-1 Storm Drainage System: Hydrology. Department Of Transportation, Connecticut, United States of American

Frevert, R. K., Schwab, G. O., Edminster, T. W. and Barnes, K. K. 1955. Soil and Water Conservation Engineering. John Wiley and Sons, New York, New York, Pp. 479

Rothwell, R.L., Schmab, G.O. Deminster, T.W. and Barnes, K.K. 1955. Soil and Water Conservation Engineering. John Wiley and Sons, Inc. New York

UW-M. 2007. Hydraulic principles: Chapter 3 Runoff coefficient. Biological Systems Engineering, University of Wisconsin-Madison
http://209.85.165.104/search?q=cache:dMxUztufvP8J:bse.wisc.edu/courses/472/Lecture_Notes_03_Ch3.doc+runoff+coefficient&hl=en&ct=clnk&cd=7

6.3 Transportation

The ‘transportation’ tab contains functionality to inform the TRAIL tool as to what values in the selected field (from the ‘load transportation layers’ button in the ‘load data’ tab) represent listed features (Figure 16).

6.3.1 Value matching (with value weighting)

Shapefile values for feature type are set into the text box to the right of the feature category label and then selected to be utilized or not within the ‘use/don’t use’ check box. The values within brackets next to the feature category label (i.e. primary highway (0.1)) are the penalty value scales used when creating a usable transportation penalty raster. Bracketed values are assigned to the final transportation penalty raster.

6.3.2 Qualifiers for linear feature extraction

The functionality contained within this segment of the ‘transportation’ tab allows for the consideration of risk to current linear features and the inclusion or exclusion of seismic line features. Remediation potential of current features is assessed; areas of hydrological risk are excluded and re-connected based upon least risk assessments by the tool (end nodes of excluded areas may not be directly re-connected if it is least ‘risky’ to rejoin at a point further down the feature). Hydrological risk areas are those where DTW (WAM) values are 0.5m or less; stream channels are as well accounted for. Seismic lines may be selected for use if loaded. The ‘utilize seismic lines’ check box allows for the inclusion and exclusion of these features.

The 'create usable features' button, once clicked, uses all information placed into this tab to formulate the transportation penalty raster that moves to the next processing step.

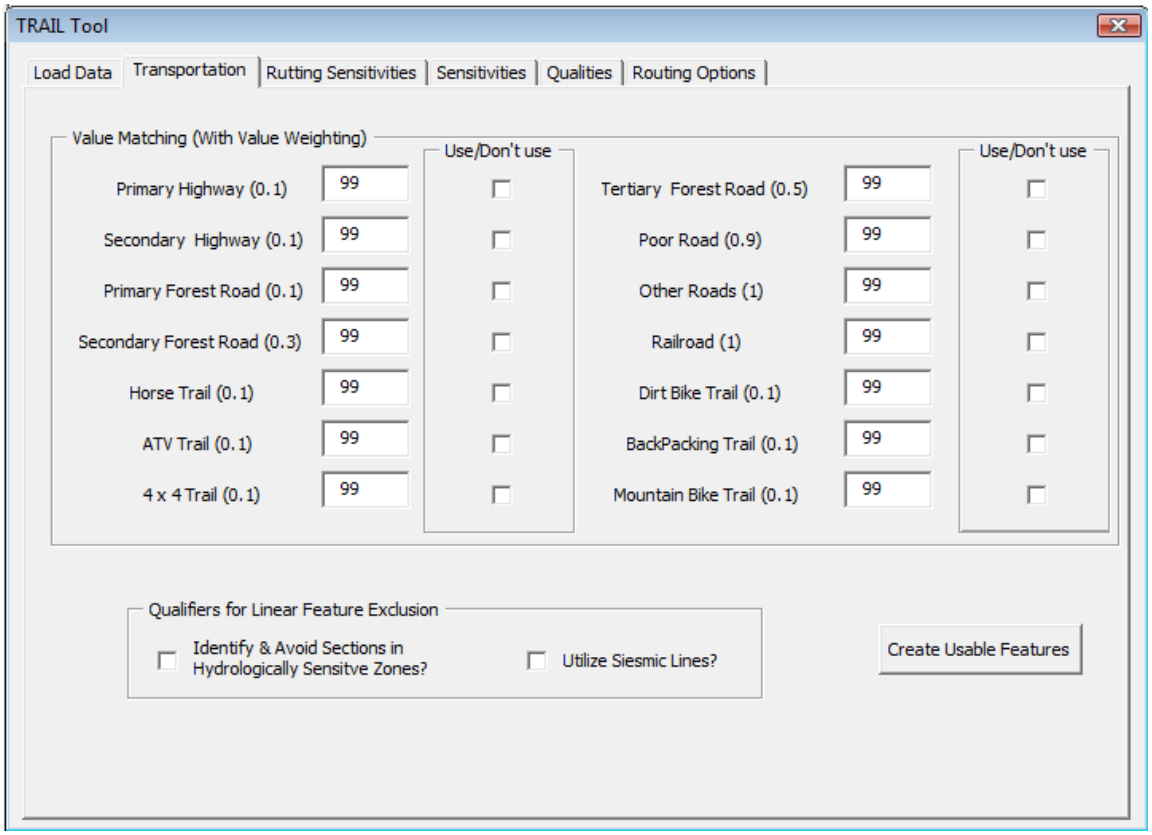

Figure 0.16 The transportation tab of the TRAIL tool.

6.4 Rutting Sensitivities

The 'rutting sensitivities' tab is designed to include the consideration of impacts to soils when creating routes. This tab contemplates type of user on route and resultant soil mechanics to the application of the user to the soil. For complete information on the science behind the calculations, please refer to Vega *et al* (2008) and Campbell *et al.* (2012). Figure 17 displays the 'rutting sensitivities' tab which contains the functionality required to prime the predictive rut depth algorithms found within these articles.

6.4.1 Vehicle inputs

This section requires the loading of information towards trafficability deductions. All requirements refer to tire type (tire width, section height, and radius), loads (number of tires, weight), tire inflation pressures, and the number of passes that is to be on the landscape. Users can save these specs for future utilization using the 'save specs' button. Specs may be loaded to populate the text boxes utilizing previously saved specs using the 'load specs' button.

The 'create usable features' button, once clicked, uses all information placed into this tab to formulate the rutting penalty raster that moves to the next processing step. All text boxes must be complete for this section to operate optimally. The DTW/WAM raster is

required for calculations. For a complete run down of slide bar penalty assignment principles, refer to the 'penalty value assignment' section of this document.

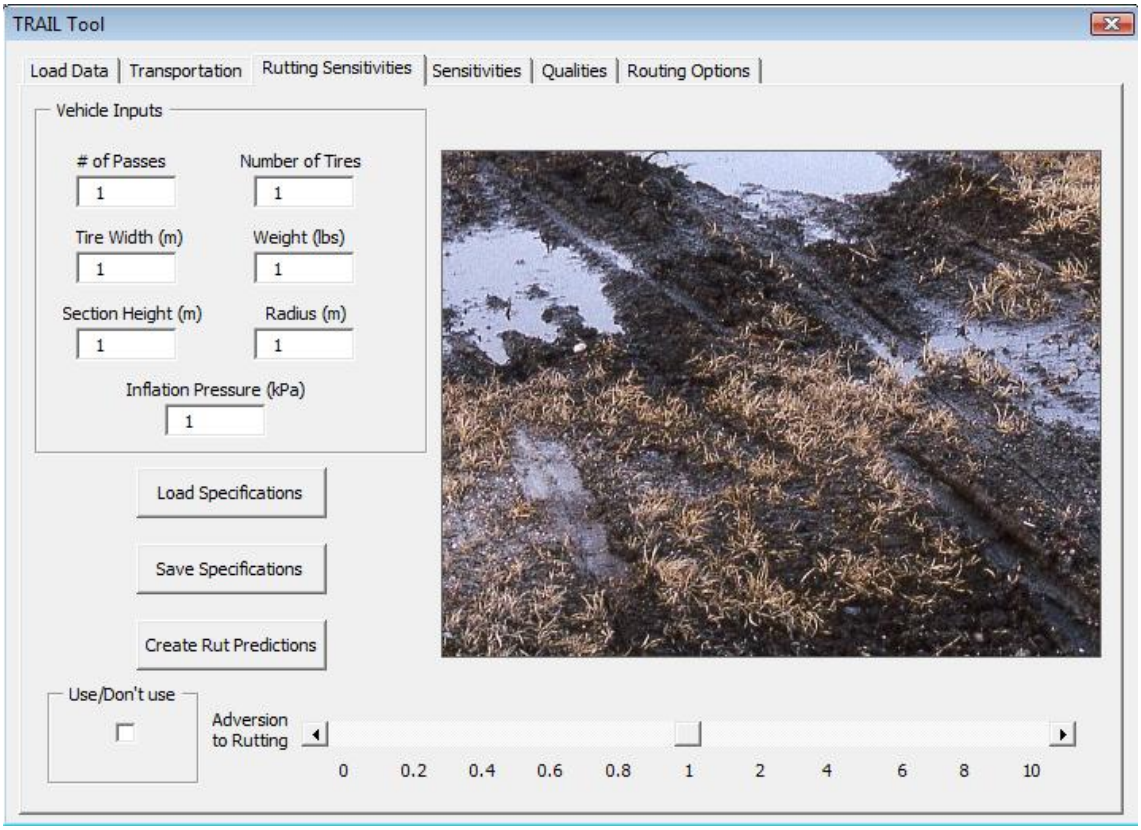

Figure 17 The rutting sensitivities tab of the TRAIL tool. Vehicle type and ground conditions are loaded and created to yield a soil trafficability map based upon soil moisture condition and load applied.

Vega-Nieva, D., Murphy, P., Castonguay, M., Ogilvie, J., Arp, P.. 2008. A modular terrain model for daily variations in machine-specific forest soil trafficability. Canadian Journal of Soil Sciences. 89(1); 93-109.

6.5 Sensitivities

The 'sensitivities' tab of the TRAIL tool allows for the final consideration of risks on the landscape (Figure 18). Through methods outlined in the 'penalty value assignment' section, slope, stream crossings and a host of other considerations can be effectively managed.

The 'wet area avoidance factor' slide bar is an additional constraint to add to wet area avoidance. This slide bar effectively forces routes further and further away from wet areas as the avoidance factor increases in size. In concept, this method turns areas surrounding wet areas into limited use zones, creating higher penalties for getting closer to these areas.

Note: At all times, the stream penalty value assignment must be equal to or greater than the wet areas penalty as to avoid following stream channels as reduced areas of risk as compared to the surrounding wet area.

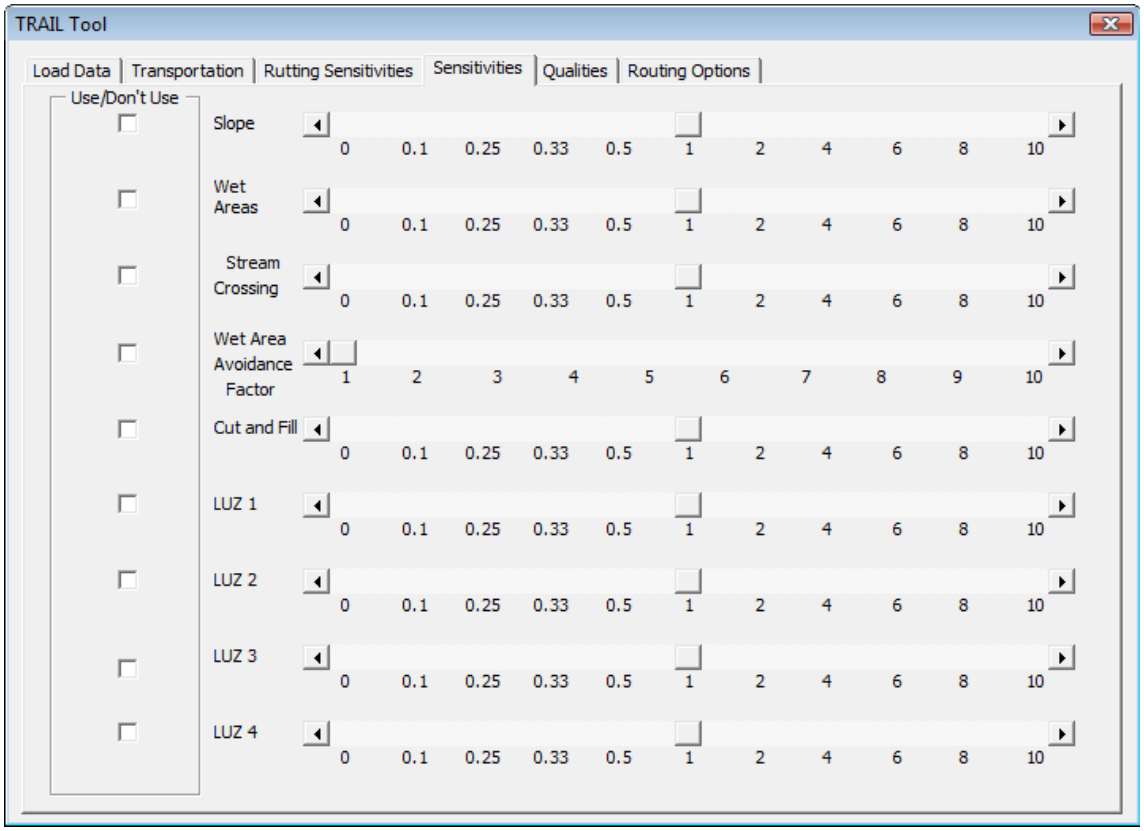

Figure 18 The sensitivities tab of the TRAIL tool. Users define their aversion to specific risks.

6.6 Qualities

This tab of the TRAIL tool sets various traits for the created route (Figure 19). The 'qualities' tab defines the aversion to trail blazing, openings, and route length while considering ruggedness level requirements. Outside of the ruggedness slide bars, all follow the penalty raster creation method as defined within the 'penalty value assignment' section. The 'ruggedness preference' and 'desire for ruggedness level' slide bars allow the user to select the type of route to create. Assigning a desired ruggedness level to maintain, and specifying the importance of maintaining it, can ensure a route conscientious of user skill level or can apply additional constraints to earthwork volumes.

6.5.1 Hydrological penalty intelligence

The intelligent hydrological risk assignment check boxes activate the rasters created within the ‘use intelligent hydro risk’ button of the ‘load data’ tab for use. If these check

boxes are activated without this button activated, it is ignored in calculations. With the check boxes active and with rasters created, the tool will assign hydrological features (wet areas as well as streams) high up in a watershed lower penalty values then those incurred lower in a watershed.

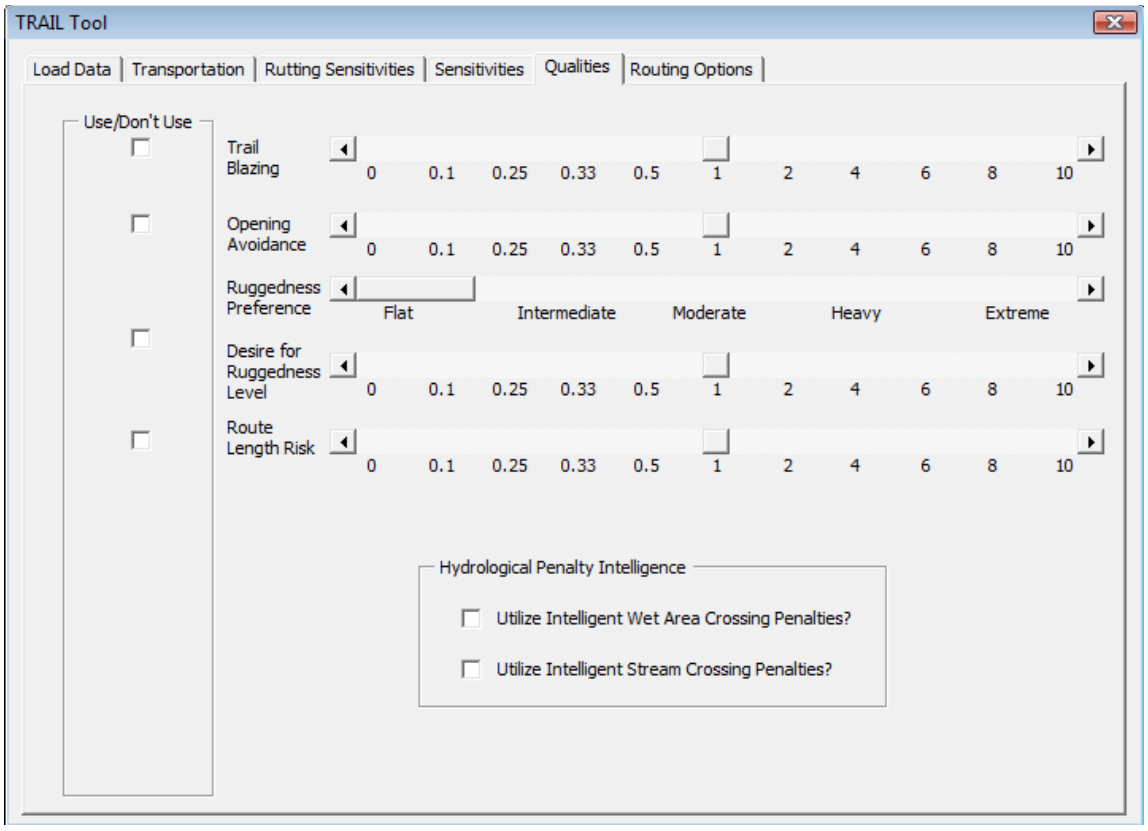

Figure 19 The qualities tab of the TRAIL tool. Users select aversion levels to various risks and define their desired ruggedness level.

6.7 Routing Options

It is within the 'routing options' tab of the TRAIL GUI that users enter into the final steps of creating routes for a tradeoff analysis (Figure 20).

6.7.1 Build sensitivity (punishment) map

The ‘build sensitivity map’ button triggers the tool to begin the rasterization of user inputs and risk tolerances. This button is pressed every time change has been made to the slide bars.

The user is prompted by way of a pop-up dialog to define slope threshold. This value is used to distinguish between appropriate slope values for routing considerations. Through penalty scaling and user risk factoring methods employed by the tool, areas above the defined threshold are not necessarily avoided. These areas are penalized accordingly to provoke LCP to avoid these areas, but once these areas are needed to be crossed, the value assignment method employed encourages LCP to take the least change in risk to the end of these zones. This method of non-direction based analysis is the most appropriate value assignment method without instigating computationally intensive directionally based algorithms.

If the 'opening avoidance' check box has been engaged, a pop-up window containing a text box for the definition of the largest size of opening to allow routing to continue through appears when beginning route analysis . Values to be specified are in m^2. This feature ensures the consideration of potential braiding problems through the avoidance of open areas route users may find.

6.7.2 Build route

The ‘build route’ button is executed under one of two pre-conditions: i) either the ‘build sensitivity map’ button has just completed; or ii), a sensitivity map has been created and is to be loaded and utilized again without adjustment allowing the user to assess multiple beginning and end points under the same risk assessment. The 'build route' button triggers a 'control point selection' pop-up box where users may select their beginning and end points, load or create their final sensitivity map, and create a least cost route (Figure 21).

6.7.2.1 Load start point. Users are tasked to load a point shapefile to identify the beginning location of the desired route. Currently, this must be a single location, as well as a single point.

6.7.2.2 Load end point. Users are tasked to load a point shapefile to identify the end location of the desired route. Currently, this must be a single location, as well as a single point.

6.7.2.3 Load penalty raster. Users are asked through a pop-up dialog as to whether utilize a punishment grid that was just created or to load a previously created raster. Users should ensure every finalized punishment grid is saved and the slidebar settings for it are known. This will allow you to test all further created routes against previously created punishment grids.

6.7.2.4 Begin route analysis. Upon execution of this button, the tool initiates the LCP process upon the user defined control points utilizing the user created/loaded punishment grid.

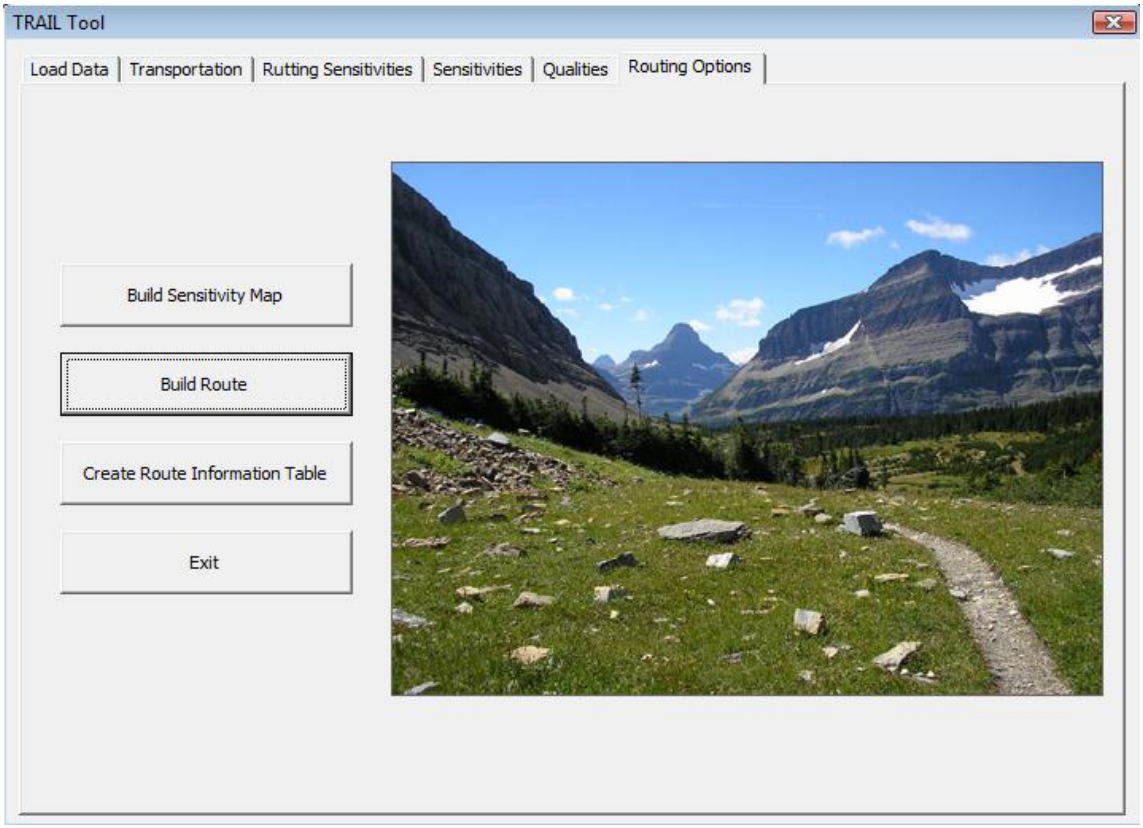

Figure 20 The routing options tab of the TRAIL tool.

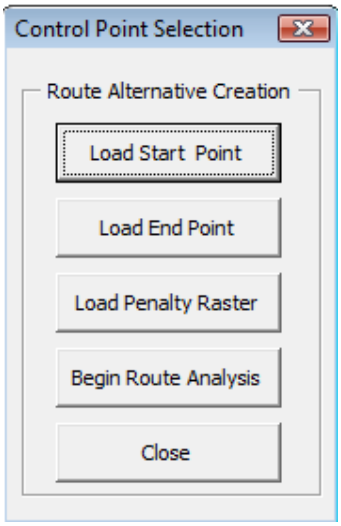

Figure 21 The control point selection pop-up dialog executed under the 'build route' button of the 'routing options' tab.

6.7.3 Create route information table

Currently, the LCP method used within the TRAIL tool does not employ a large neighborhood spreading function as suggested by Saha *et al.* (2005) and others, or employ a directional dependant algorithm. Lacking these two suggestions does not allow for LCP to analyze the desired route width for best path. Attempts to effectively address this issue without employing these computationally intensive processes included summation of the entire friction surface with a route width neighborhood and the averaging of the friction surface with a route width neighborhood. Both methods incurred near exact matches to original, non-modified LCP results. Currently, only the values under the created path are used in estimates of wet area and cut & fill interactions.

Upon executing this button the tool asks to use the current route which is still in memory or if the user would like to load a different linear feature to analyze. This tool feature is employed to allow for the examination of any route with a loaded punishment grid.

The data that is derived for the information table includes the potential to assess risk values along proposed routes, including:

i. slope above threshold (m)
ii. stream crossings (n)
iii. wet area crossings (m)
iv. C&F volumes (m^3)
v. culvert sizing's (cm)
vi. route length (m)

Saha, A., Arora, M., Gupta, R., Virdi, M., Csaplovics, E. 2005. GIS-based route planning ing landslide-prone areas. Int. J. geo. Inf. Sc. 19(10), 1149-1175.

7.0 Interpretation of Results

Currently, the interpretation of results has to proceed through Microsoft Excel. The created route information tables within ArcMap are opened within Excel and pasted into a pre-designed Excel worksheet. Only select the raw numbers (select all the raw data at once), no field names are required in the paste. Right click on the Excel worksheet box G2 and paste; data should populate each column with a heading. In the Excel boxes C4 and C9 select the slope value that was used within the TRAIL tool and create a name for the route. Follow this procedure for each created route that is required to be compared against each other utilizing the 10 route tabs available in the spreadsheet. As you load data, the 'tables' and 'Figures' tabs populate with the information required for beginning the tradeoff analysis of routes (Figure 22). With these tables and graphs, a dialog may begin on the potential positives and negatives of each loaded or created route.

8.0 Summary

This document was constructed to aid trail planners in the development of sustainable trail networks while considering the various concerns of planning. Through the user friendly GUI and a platform for tradeoff analysis, trail planning can proceed swiftly and knowledgably to meet the requirements of the various user groups.

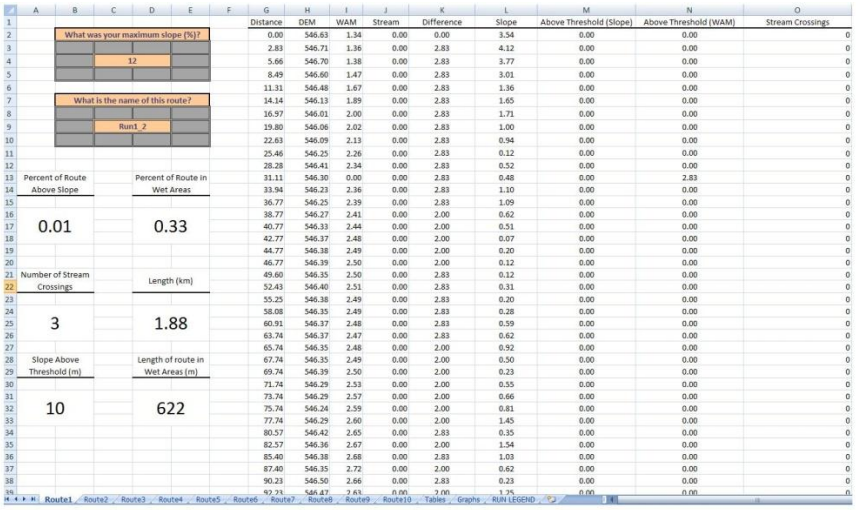

						Distance	DEM	WAM	Stream	Difference	Slope	Above Threshold (Slope)	Above Threshold (WAM)	Stream Crossings
	What was your maximum slope (%)?					0.00	546.63	1.34	0.00	0.00	3.54	0.00	0.00	0
						2.83	546.71	1.36	0.00	2.83	4.12	0.00	0.00	0
		12				5.66	546.70	1.38	0.00	2.83	3.77	0.00	0.00	0
						8.49	546.60	1.47	0.00	2.83	3.01	0.00	0.00	0
						11.31	546.48	1.67	0.00	2.83	1.36	0.00	0.00	0
	What is the name of this route?					14.14	546.13	1.89	0.00	2.83	1.65	0.00	0.00	0
						16.97	546.01	2.00	0.00	2.83	1.71	0.00	0.00	0
		Run1_2				19.80	546.06	2.02	0.00	2.83	1.00	0.00	0.00	0
						22.63	546.09	2.13	0.00	2.83	0.94	0.00	0.00	0
						25.46	546.25	2.26	0.00	2.83	0.12	0.00	0.00	0
						28.28	546.41	2.34	0.00	2.83	0.52	0.00	0.00	0
	Percent of Route Above Slope		Percent of Route in Wet Areas			31.11	546.30	0.00	0.00	2.83	0.48	0.00	2.83	0
						33.94	546.23	2.36	0.00	2.83	1.10	0.00	0.00	0
						36.77	546.25	2.39	0.00	2.83	1.09	0.00	0.00	0
	0.01		0.33			38.77	546.27	2.41	0.00	2.00	0.62	0.00	0.00	0
						40.77	546.33	2.44	0.00	2.00	0.51	0.00	0.00	0
						42.77	546.37	2.48	0.00	2.00	0.07	0.00	0.00	0
						44.77	546.38	2.49	0.00	2.00	0.20	0.00	0.00	0
						46.77	546.39	2.50	0.00	2.00	0.12	0.00	0.00	0
	Number of Stream Crossings		Length (km)			49.60	546.35	2.50	0.00	2.83	0.12	0.00	0.00	0
						52.43	546.40	2.51	0.00	2.83	0.31	0.00	0.00	0
						55.25	546.38	2.49	0.00	2.83	0.20	0.00	0.00	0
						58.08	546.35	2.49	0.00	2.83	0.28	0.00	0.00	0
	3		1.88			60.91	546.37	2.48	0.00	2.83	0.59	0.00	0.00	0
						63.74	546.37	2.47	0.00	2.83	0.62	0.00	0.00	0
						65.74	546.35	2.48	0.00	2.00	0.92	0.00	0.00	0
	Slope Above Threshold (m)		Length of route in Wet Areas (m)			67.74	546.35	2.49	0.00	2.00	0.50	0.00	0.00	0
						69.74	546.39	2.50	0.00	2.00	0.23	0.00	0.00	0
						71.74	546.29	2.53	0.00	2.00	0.55	0.00	0.00	0
	10		622			73.74	546.29	2.57	0.00	2.00	0.66	0.00	0.00	0
						75.74	546.24	2.59	0.00	2.00	0.81	0.00	0.00	0
						77.74	546.29	2.60	0.00	2.00	1.45	0.00	0.00	0
						80.57	546.42	2.65	0.00	2.83	0.35	0.00	0.00	0
						82.57	546.36	2.67	0.00	2.00	1.54	0.00	0.00	0
						85.40	546.38	2.68	0.00	2.83	1.03	0.00	0.00	0
						87.40	546.35	2.72	0.00	2.00	0.62	0.00	0.00	0
						90.23	546.50	2.66	0.00	2.83	0.23	0.00	0.00	0
						92.23	546.47	2.63	0.00	2.00	1.25	0.00	0.00	0

Route1 | Route2 | Route3 | Route4 | Route5 | Route6 | Route7 | Route8 | Route9 | Route10 | Tables | Graphs | RUN LEGEND

Name	Length (km)	Slope Above Threshold (m)	Length of route in Wet Areas (m)	Est. Stream Crossings	Percent of Route Above Slope Threshold	Percent of Route in Wet Areas
Run1_2	1.88	9.66	622.02	3.00	0.51%	33.01%
Run1_25M	1.87	6.83	848.51	5.00	0.37%	45.39%
Run1_20	1.89	26.63	420.51	5.00	1.41%	22.26%
Run1_205M	1.89	24.14	495.05	5.00	1.28%	26.18%
Run2_20	2.64	30.97	158.77	2.00	1.17%	6.01%
Run2_205M	2.33	34.28	235.62	3.00	1.47%	10.13%
Run3_205M	2.15	41.31	258.93	3.00	1.92%	12.06%
Run4_205M	2.16	43.11	278.45	3.00	1.99%	12.88%
Run5_205M	1.94	24.49	309.13	5.00	1.26%	15.92%
DMI_P1	2.00	13.66	702.70	5.00	0.68%	35.10%

Route1 | Route2 | Route3 | Route4 | Route5 | Route6 | Route7 | Route8 | Route9 | Route10 | Tables | Graphs | RUN LEGEND

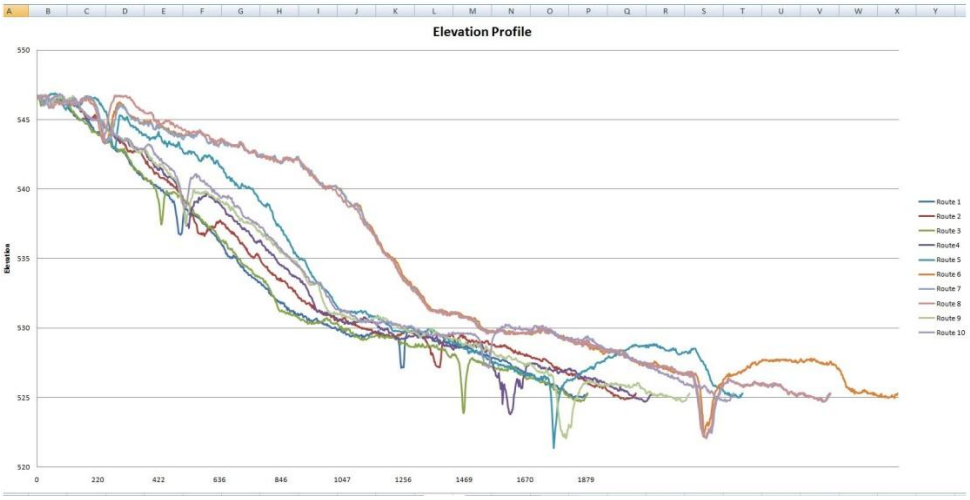

Apr-2009 - Gatineau, QC - SFMN Organizers and Attendees - SFMN Symposium- Envisioning Tomorrow's Forests: Knowledge Networking for Sustainability - Field Verification of LiDAR Derived Wet Area Mapping (200)

May-2009 - Moose Factory, ON - SFMN Organizers and Attendees/ People from the First Nations Settlement - Moose Cree First Nations Workshop - Wet Area Mapping for Improved Terrain Knowledge: Trafficability (30)

Jun-2009 - Edmonton, AB - AB Energy Employees - ASRD Workshop- Alberta's New Wet Areas Mapping Initiative - New Tools That Incorporate WAM to Improve the Way We Move Across the Land (15)

Jun-2009 - Edmonton, AB - AB Environment Employees - ASRD Workshop- Alberta's New Wet Areas Mapping Initiative - New Tools That Incorporate WAM to Improve the Way We Move Across the Land (25)

Jun-2009 - Edmonton, AB - AB Parks and Recreation Employees - ASRD Workshop- Alberta's New Wet Areas Mapping Initiative - Utilizing WAM and New GIS Tools for the Placement of New and the Remediation of Old Trails (40)

Jun-2009 - Hinton, AB - ASRD Employees - ASRD Workshop- Alberta's New Wet Areas Mapping Initiative - New Tools That Incorporate WAM to Improve the Way We Move Across the Land (10)

Jun-2009 - Edson, AB - AB Government Land Use Framework Development Committee - ASRD / SFMN Workshop- Alberta's New Wet Areas Mapping Initiative - Defining Footprint: Can WAM Help to Improve the Current Definition? (20)

Jun-2009 - Peace River, AB - DMI Employees - Presenting LiDAR WAM Data and Discussing Thesis Ideas - Avenues for Study: WAM and Terrain Trafficability (5)

July-2009 - Oromocto, NB - Military Mobility Sectors (Geomatics, Meteorology, Command) - CFB Gagetown Trafficability Workshop - The New Trails Tool: Examples as Related to Military Operations (30)

Aug-2009 - Fredericton, NB - J.D. Irving Employees - Black Book Forest Products Group Meeting - Terrain Trafficability: Utilizing WAM and GIS Tools to Improve Road and Trail Locations (6)

Sep-2009 - Peace River, AB - Gov/ Forest Sector/ Energy Sector/ Recreation Sector/ Consultants/ Local Interest Groups - ASRD / SFMN KETE Workshop- Alberta's New Wet Areas Mapping Initiative - Trails for Sustainability: Incorporating Wet Area Mapping into the Calculation of Footprint (60)

Sep-2009 - Grand Prairie, AB - Gov/ Forest Sector/ Energy Sector/ Recreation Sector/ Consultants/ Local Interest Groups - ASRD / SFMN KETE Workshop- Alberta's New Wet Areas Mapping Initiative - Trails for Sustainability: Incorporating Wet Area Mapping into the Calculation of Footprint (100)

Sep-2009 - Rocky Mountain House, AB - Gov/ Forest Sector/ Energy Sector/ Recreation Sector/ Consultants/ Local Interest Groups - ASRD / SFMN KETE Workshop- Alberta's

New Wet Areas Mapping Initiative - Trails for Sustainability: Incorporating Wet Area Mapping into the Calculation of Footprint (50)

Sep-2009 - Chain Lakes, AB - Gov/ Forest Sector/ Energy Sector/ Recreation Sector/ Consultants/ Local Interest Groups - ASRD / SFMN KETE Workshop- Alberta's New Wet Areas Mapping Initiative - Trails for Sustainability: Incorporating Wet Area Mapping into the Calculation of Footprint (50)

Sep-2009 - Edmonton, AB - Gov/ Forest Sector/ Energy Sector/ Recreation Sector/ Consultants/ Local Interest Groups - ASRD / SFMN KETE Workshop- Alberta's New Wet Areas Mapping Initiative - Trails for Sustainability: Incorporating Wet Area Mapping into the Calculation of Footprint (125)

Oct-2009 - Fredericton, NB - Various Under Graduate and Graduate Level Students and Faculty - Killarny Lake Trafficability: 4020 Student Project - GIS Tools for Increased Knowledge of Terrain Trafficability (20)

Nov-2009 - Fredericton, NB - J.D. Irving Employees - Past and Future Research Discussions - Monthly Changes in Terrain Trafficability (6)

Dec-2009 - Boyle,AB - AlPac Employees - SFMN Workshop: KETE- AlPac - Tools for Reducing our Footprint: Utilizing WAM and GIS Tools to Improve Trafficability Awareness (30)

Dec-2009 - Calgary, AB - ASRD Employees/ Recreational User Groups - Building Partnerships - Tools for Reducing our Footprint: WAM and its Value in Predicting Locations for New Trails (20)

Jan-2010 - Fredericton, NB - J.D. Irving Employees - Results and New Opportunities in Research - Monthly Changes in Terrain Trafficability (as incorporated into Dr. Arp's presentation) (20)

May-2010 - Fredericton, NB - J.D. Irving Employees - Results and New Opportunities in Research - Gis-based landscape risk assessment for trafficability purposes (13)

May-2010 - Edmonton, AB - MITACS/CORS members - MITACS/CORS annual meeting - GIS-based recreation trail planning (10)

May-2010 - Edmonton, AB - Alberta Parks/Lands/Forestry - Masters work review and opportunities for new WAMing areas - GIS-based trail planning: a cross departmental effort to land management (12)

June-2010 - Fredericton, NB - Graduate students; advisory commitiee - Masters proposal presentation - Modeling and assessing recreational trafficability conditions within the Ghost River Forest Land Use Zone, Alberta (15)

Oct-2010 - Rocky Mnt House, AB - AB Government, Public, Bighorn Backcountry standing committee - Knowledge exchange to recreational user groups and local government. Remote - Tools For Sustainability: High Resolution Planning Tools to Minimize Trail Impacts and Costs (30)

Oct-2011 - Venezuela - Venezuela Government, Conference attendees and presenters - IV Jornadas Nacionales de Geomatica - WAM: Tools for Sustainability Utilizing LiDAR DEMs (60)

Nov-2012 - Calgary, AB - ASRD Employees/ Recreational User Groups - Information Update and Tool Presentation - The TRAIL Tool (10)